



ADDIS ABABA UNIVERSITY
ADDIS ABABA INSTITUTE OF TECHNOLOGY
SCHOOL OF CHEMICAL AND BIO ENGINEERING

**PRODUCTION AND OPTIMIZATION OF BIOETHANOL FROM AGRO-
INDUSTRIAL WASTE-BREWER`S SPENT GRAIN**

A Thesis submitted to the school of Chemical and Bio-Engineering Addis Ababa Institute of Technology in partial fulfillment of the requirement for degree of Master of Science in Chemical Engineering under Process Stream.

By: - Mintesinot Dessalegn

Addis Ababa, Ethiopia

June 2018

ADDIS ABABA UNIVERSITY
INSTITUTE OF TECHNOLOGY
SCHOOL OF CHEMICAL AND BIO ENGINEERING

This is to certify that the thesis prepared by Mintesinot Dessalegn, entitled: Production and optimization of bioethanol from agro-industrial waste-BSG and submitted in partial fulfilment of the requirement for the degree of Master of Science (Chemical and Bio Engineering) complies with the regulations of the University and meets the accepted standards with respect to originality and quality.

Signed by the Examining committee:

| | Signature | Date |
|---------------------------------|-----------|-------|
| Advisor: - | | |
| Dr. Eng. Hundessa Dessalegn | _____ | _____ |
| Internal examiner | | |
| Prof. Eduardo Ojito Cespedes | _____ | _____ |
| Extrenal examiner | | |
| Dr. Ing. Zebene Kiflie | _____ | _____ |
| School or center of Chairperson | _____ | _____ |

DECLARATION

I declare that this thesis entitled “Production and optimization of bioethanol from agro-industrial waste-brewer`s spent grain” has not been submitted in any form for another degree, diploma or an award at any university or other institution of the tertiary education. Whenever contributions of others are involved, every effort is made to indicate this clearly, with due reference to the literature and discussions. Information taken from published and unpublished work of others has been acknowledged in the text and a list of references is given. The work was under the guidance of Dr.Eng. Hundessa Dessalegn (Assistant Professor) instructor in Addis Ababa University, School of Chemical and Bio Engineering.

Name: Mintesinot Dessalegn

Signature: _____

Date: _____

ACKNOWLEDGMENTS

First of all and for most, I would like to thank almighty God for being with me all the time and given me health, strength and uncountable gifts during this thesis work and in my entire life for His glory and His name.

Moreover, I would like to express my deepest appreciation and heartfelt thanks to my former instructor and now this thesis advisor Dr. Eng. Hundessa Dessalegn (assistant professor, lecturer in School of Chemical and Bio-Engineering, chairperson of process stream and president of Ethiopian Society of Chemical Engineers), for his sustainable and appreciable guidance, advising, providing information, skill, experience, editing final document and most of all being as friend and visiting my lab setup and work by fine-tuning starting from the idea of the title through proposal development until the successful completion of my thesis work.

I also like to express my gratitude to the laboratory technicians of AAiT, School of Chemical and Bio-Engineering in general and Mr. Hintsasilasse Seifu in particular for their/his time and professional helps during my laboratory work.

My deepest gratitude also goes to my classmates of process stream in particular and to the graduating class of school of chemical and bio-engineering, and school of chemical and bio-engineering dean office in general for providing financial support under the Ministry of Education.

I would like to express my deepest and heartfelt appreciation and love for my beloved wife and also classmate, Mrs. Meseret Ethiopia, for her being with me in my weak side, for her motivation, patience, love, and help during my experimental work.

At last but not at least my deepest appreciation and heartfelt thank goes to my families, especially my mother, Mrs. Zinash Osebo, she is my role model for being strong man and all the successful roads I had passed, her fingerprints were there.

ABSTRACT

This work basically focuses on the production and optimization of bioethanol from brewer`s spent grain-lignocellulose, which is a by-product from breweries. The proximate analysis for brewer`s spent grain was conducted and found that BSG contains: moisture content of 12.08%, extractives and ash 2-4%, cellulose 34.62%, hemicellulose 18.84%, lignin 11.23% and the balance protein and fiber, high composition of cellulose which was used to produce fermentable sugar. Hydrolysis was conducted in two stages. First stage hydrolysis was conducted at moderate process conditions: temperature of 130⁰C, retention time of 20min, and acid concentration of 1% and liquid to solid ratio of 10v/w; a second stage hydrolysis was conducted at extreme conditions of process parameters due to the high crystallinity of cellulose. The process parameters: temperature, time, and acid concentration were held at 140-150⁰C, 20-30min, and 2-3%, respectively by holding liquid to solid ratio of 10v/w and particle size of 2mm-1mm constant. Two levels randomized with one block full factorial design with three replicate for three factors was conducted and total number of runs were $2^3 \times 3 = 24 + 6 = 30$ with 6 center points. By using analysis of variance the statistical data were generated and results that show the effect of process parameters on the yield of total reduced sugars produced during hydrolysis process were analyzed and found a maximum yield of 57.8% at a temperature, time and acid conc. of 150⁰C, 20min and 3%, respectively. After collecting reduced sugars from the hydrolysis stages, fermentation was conducted at a temperature range of (30, 32, 34, 36 and 38)⁰C and pH of 4.5, 5, 5.5, 4.8 and 5.2, by holding concentration of substrate to yeast strain 10 v/v and fermentation time of 72hr constant. Power law assumption was considered for fermentation and the optimum fermentation temperature and pH were identified as 32⁰C and 5, respectively. Thermodynamic and kinetic analysis was conducted for the fermentation step and 2.4×10^{11} and 16.133KJ of frequency factor and activation energy were found, respectively. Water-ethanol mixture and other heavy compounds were separated in the distillation column and recovered ethanol was characterized.

Keywords: - brewer`s spent grain, bioethanol, kinetics, cellulose, hydrolysis

| CONTENTS | Page no. |
|--|---------------------|
| ACKNOWLEDGMENTS | i |
| ABSTRACT | ii |
| CONTENTS | iii |
| LIST OF FIGURES | ix |
| LIST OF TABLES | xii |
| NOTATIONS | xiv |
| ACRONYMS | xv |
| Chapter One | 1 |
| 1. INTRODUCTION | 1 |
| 1.1. Background | 1 |
| 1.2. Problem statement | 3 |
| 1.3. Objectives | 4 |
| 1.3.1. General objective | 4 |
| 1.3.2. Specific objective | 4 |
| 1.4. Significance and Scope of the Study | 5 |
| 1.4.1. Significance of the study | 5 |
| 1.4.2. Scope of the study | 6 |

| | |
|---|----|
| Chapter Two | 7 |
| 2. LITERATURE REVIEW | 7 |
| 2.1. Bioethanol Production | 7 |
| 2.2. World bioethanol production | 8 |
| 2.2.1. First-Generation biofuels | 9 |
| 2.2.2. Second-Generation biofuels | 9 |
| 2.3. Bioethanol production in Ethiopia | 10 |
| 2.4. Feed stock for bioethanol production | 11 |
| 2.5. Lignocellulosic feedstocks for ethanol production | 12 |
| 2.6. Brewer`s spent grain | 15 |
| 2.7. Sustainable utilization of BSG | 16 |
| 2.7.1. Animal nutrition and feed formulation | 17 |
| 2.7.2. Bioethanol production | 17 |
| 2.7.3. Lactic acid production | 18 |
| 2.7.4. Xylitol and pullulan production | 18 |
| 2.8. Processing technologies for converting BSG to EtOH | 19 |
| 2.8.1. Pretreatment | 20 |
| 2.8.1.1. Physical pretreatment | 21 |
| 2.8.1.2. Chemical pretreatment | 21 |

| | |
|--|----|
| 2.8.1.3. Physic-Chemical pretreatment | 24 |
| 2.8.1.4. Biological pretreatment | 26 |
| 2.8.2. Hydrolysis | 27 |
| 2.8.2.1. Acid hydrolysis | 28 |
| 2.8.2.2. Enzymatic hydrolysis | 30 |
| 2.8.2.3. Alkaline hydrolysis | 31 |
| 2.8.3. Fermentation | 31 |
| 2.8.4. Distillation | 33 |
| 2.9. Benefits and Impacts of cellulosic biomass conversion to EtOH | 34 |
| 2.9.1. Greenhouse gas reduction | 34 |
| 2.9.2. Strategic benefits | 34 |
| 2.9.3. Solid waste disposal | 35 |
| 2.9.4. International fuel market | 35 |
| 2.9.5. Sustainable production of organic fuels and chemicals | 35 |
| 2.9.6. Competition with food | 36 |
| 2.10. Physical and Chemical characteristics of ethanol | 36 |

| | |
|--|----|
| Chapter Three | 38 |
| 3. MATERIALS AND METHODS | 38 |
| 3.1. Materials, Chemicals and Equipment | 38 |
| 3.2. Methods | 39 |
| 3.2.1. Proximate analysis and mechanical pretreatment of BSG | 39 |
| 3.2.2. Hydrolysis (first and second stages) | 41 |
| 3.2.2.1. First stage hydrolysis | 41 |
| 3.2.2.2. Second stage hydrolysis | 42 |
| 3.2.2.3. Characterizing reducing sugar using FTIR | 43 |
| 3.2.3. Preparation of yeast cultures for fermentation | 44 |
| 3.2.4. Filtration | 45 |
| 3.2.5. Design of experiment | 45 |
| 3.2.6. Fermentation | 46 |
| 3.2.6.1. Thermodynamic analysis | 46 |
| 3.2.6.2. Kinetic analysis | 47 |
| 3.2.7. Distillation of water-ethanol mixture | 48 |
| 3.2.8. Characterization of ethanol | 48 |
| 3.2.8.1. Determination of density | 48 |
| 3.2.8.2. Determination of kinematic viscosity | 49 |

| | |
|--|-----------|
| 3.2.8.3. Determination of functional groups in ethanol | 49 |
| 3.3. Process description, process flow diagram and experimental setup for the bioethanol production from BSG | 49 |
| 3.3.1. Process description | 49 |
| 3.3.2. Process flow diagram | 50 |
| 3.3.3. Experimental setup | 51 |
| Chapter Four | 54 |
| 4. RESULTS AND DISCUSSION | 54 |
| 4.1. Proximate analysis of BSG | 54 |
| 4.2. Hydrolysis | 57 |
| 4.2.1. First stage hydrolysis | 57 |
| 4.2.2. Titration using a DNS method | 58 |
| 4.2.3. Second stage hydrolysis | 62 |
| 4.2.3.1. Development of regression Model equation | 69 |
| 4.2.3.2. Model Adequacy Checking | 70 |
| 4.2.4. Individual effect of process parameters on the yield of total reduced sugar | 73 |
| 4.2.5. Interaction effect of process parameters on the yield of total reduced sugar | 76 |
| 4.2.6. Optimization | 82 |
| 4.3. Fermentation | 84 |
| 4.3.1. Thermodynamic analysis | 84 |
| 4.3.2. Kinetic analysis | 85 |

| | |
|--|-----|
| 4.4. Distillation of water-ethanol mixture | 98 |
| 4.5. Characterization of ethanol | 98 |
| 4.5.1. Determination of density | 98 |
| 4.5.2. Determination of kinematic viscosity | 99 |
| 4.5.3. FTIR functional group analysis | 99 |
| Chapter Five | 101 |
| 5. CONCLUSIONS AND RECOMMENDATIONS | 101 |
| 5.1. Conclusion | 101 |
| 5.2. Recommendation | 103 |
| REFERENCES | 104 |
| APPENDICES | 112 |
| Appendix A: Thermodynamic Analysis | 112 |
| Appendix B: Thermodynamic property table for selected substances | 115 |
| Appendix C: Infrared Spectroscopy Table with respective wavelength range for Functional Group Analysis | 116 |
| Appendix D: Diagnostics Case Statistics | 118 |
| Appendix E: Laboratory Equipment and Experimental samples | 120 |

LIST OF FIGURES

| Figure no. | Title of figure | Page no. |
|------------|---|----------|
| 2.1 | Processing stages to produce ethanol from different feed stocks. | 11 |
| 2.2 | Energy and GHG emissions impact | 13 |
| 2.3 | Structure of single cellulose molecule | 14 |
| 2.4 | BSG technical flow diagram | 19 |
| 3.1 | Sugar showing aldehyde functional group in open chain form | 44 |
| 3.2 | Process flow diagram for production of bioethanol from BSG | 50 |
| 3.3 | Preparation and pretreatment stage of BSG | 51 |
| 3.4 | Hydrolysis and Titration stage of BSG hydrolysate | 52 |
| 3.5 | Fermentation stage and distillation of water-ethanol mixture stage | 53 |
| 4.1 | Proximate analysis of composition of BSG | 57 |
| 4.2 | Standard curve for standard glucose solution | 61 |
| 4.3 | Half Normal plot of design parameters of the experiment | 62 |
| 4.4 | Studentized Residuals versus Predicted Values of yield of total reduced sugar | 66 |
| 4.5 | Studentized Residuals versus Run numbers for yield of total reduced sugar | 71 |
| 4.6 | Normal probability plot of residuals versus studentized residuals | 72 |
| 4.7 | Effect of temperature on the yield of total reduced sugar | 73 |

| | | |
|------|--|----|
| 4.8 | Effect of retention time on the yield of total reduced sugar | 74 |
| 4.9 | Effect of phosphoric acid conc. on the yield of total reduced sugar | 75 |
| 4.10 | Interaction of reaction temperature and retention time on yield of total reduced sugar | 76 |
| 4.11 | Interaction of temperature and acid conc. on the yield of total reduced sugar | 77 |
| 4.12 | Interaction of retention time and acid conc. on the yield of total reduced sugar | 78 |
| 4.13 | Response surface plot of the interaction effect of temperature and retention time on yield of the total reduced sugar. | 79 |
| 4.14 | Response surface plot of the interaction effect of acid conc. and temperature on the yield of total reduced sugar | 80 |
| 4.15 | A cube graph of yield of total reduced sugar with the three factor combination | 81 |
| 4.16 | $\ln \frac{dC_A}{dt}$ versus $\ln C_A$ at a temperature of 30 ⁰ C and pH of 4.5 | 82 |
| 4.17 | $\ln \frac{dC_A}{dt}$ versus $\ln C_A$ at a temperature of 32 ⁰ C and pH of 5 | 84 |
| 4.18 | $\ln \frac{dC_A}{dt}$ versus $\ln C_A$ at a temperature of 34 ⁰ C and pH of 5.5 | 87 |
| 4.19 | $\ln \frac{dC_A}{dt}$ versus $\ln C_A$ at a temperature of 36 ⁰ C and pH of 4.8 | 89 |
| 4.20 | $\ln \frac{dC_A}{dt}$ versus $\ln C_A$ at a temperature of 38 ⁰ C and pH of 5.2 | 91 |
| 4.21 | $\ln K$ versus $\frac{1}{T}$ plot | 93 |
| 4.22 | Simple distillation setup to recovery ethanol from water-ethanol mixture | 95 |
| 4.23 | Fourier Transform Infrared spectra of ethanol produced from BSG | 96 |

| | | |
|------|--|-----|
| 4.24 | Simple distillation setup | 98 |
| 4.25 | FTIR spectra of recovered ethanol from BSG | 100 |

LIST OF TABLES

| Table no. | Title of Table | Page no. |
|-----------|---|----------|
| 2.1 | Worldwide Ethanol Production: 2009-2015 (billions of gallons) | 10 |
| 2.2 | Composition of lignocellulose in common agricultural and waste residue in dry basis | 12 |
| 2.3 | Summary for Chemical composition of BSG by component on average basis | 16 |
| 2.4 | Physical and Chemical property of Ethanol | 37 |
| 3.1 | Factors and respective operating values for second- stage hydrolysis | 42 |
| 4.1 | Moisture Content of BSG at 105 ⁰ C a triplicate sample | 55 |
| 4.2 | Concentration versus Absorbance for the Standard glucose solution | 60 |
| 4.3 | Experimental analysis of total reduced sugar concentration and yield from absorbance | 64 |
| 4.4 | ANOVA for Selected Factorial Model Analysis of variance table | 67 |
| 4.5 | The regression Coefficient estimate of the process variable and corresponding 95% CI Low and High | 69 |
| 4.6 | Solution output from categorical optimization for maximum yield of total reduced sugar | 83 |
| 4.7 | Summary of thermodynamic analysis from Appendix A | 85 |
| 4.8 | Generated concentration at a fermentation temperature of 30 ⁰ C and pH of 4.5 | 86 |
| 4.9 | Generated concentration at a fermentation temperature of 32 ⁰ C and pH of 5 | 88 |
| 4.10 | Generated concentration at a fermentation temperature of 34 ⁰ C and pH of 5.5 | 90 |
| 4.11 | Generated concentration at a fermentation temperature of 36 ⁰ C and pH of 4.8 | 92 |

-
- | | | |
|------|--|----|
| 4.12 | Generated concentration at a fermentation temperature of 38 ⁰ C and pH of 5.2 | 94 |
| 4.13 | Kinetic summary for decomposition of glucose in to ethanol and carbon dioxide | 95 |

NOTATIONS

| Symbol | Definition | Unit |
|--------------------|--------------------------------|---------|
| Abs | Absorbance | % |
| b | Intercept from standard curve | % |
| C_A | Concentration of reactant | g/ml |
| ΔG | Gibbs free energy | KJ |
| ΔH^0_{rxn} | Change in enthalpy of reaction | KJ |
| K_{equ} | Equilibrium constant | |
| K | Reaction rate constant | |
| m | Slope from standard curve | ml/g |
| n | Order of reaction | |
| M | Mass of biomass | g |
| R | Universal gas constant | J/mol.K |
| ΔS | Change in entropy | J/K |
| V | Volume of liquid | ml |
| Y | Yield of total reduced sugar | % |

ACRONYMS

| | |
|-------|---|
| AAiT | Addis Ababa Institute of Technology |
| AAU | Addis Ababa University |
| AFEX | Ammonia fiber explosion |
| ANOVA | Analysis of variance |
| AOAC | Association of official analytical chemists |
| ASTM | American Society for Testing and Materials |
| BSG | Brewer`s spent grain |
| DF | Degree of freedom |
| DNS | Dinitrosalicylic acid |
| EtOH | Ethanol |
| FAO | Food and Agriculture Organization |
| FTIR | Fourier transform infrared spectroscopy |
| HMF | Hydroxymethyl furfural |
| RTIL | Room temperature Ionic Liquids |
| TRS | Total reduced sugar |
| VIF | Variance inflation factor |

Chapter One

1. INTRODUCTION

1.1. Background

Biofuel is one of the best alternative fuels in order to trounce the energy crisis. Now a days the energy crisis seeing everywhere around the world which then leads to increasing electric energy`s as compared to its supply which is very less (Da Silva and Chandel, 2012). Any immense bottle neck or increase in the energy resources supply to a country`s economy is called as energy crisis. It is the need of the time that we should focus to inspect new energy resources because for about 40 years our present oil reserves will last at most and before then will decline significantly (Mata et al., 2015). This perhaps because some fear by realizing that our present energy resources are declining and causing environmental problems and leads to devastating results for the global life quality and global economy as well (Liguori et al., 2015).

With the global increasing demand for energy, energy shortage will be a global problem. Bioethanol is considered as an important renewable to partly replace fossil-derived fuel (Kang,et al., 2014). The development and production of alternative fuels such as bioethanol, is seen as a viable option to reduce our dependence on fossil fuels and help alleviate their impact on the environment by reducing the greenhouse gas (GHG) emissions and the global warming (Coman and Andreea, 2015).

Bioethanol as a fuel has been known over hundreds of years. In 1860 Nicholas August Otto from Germany employed ethanol as a fuel in his internal combustion engine (Wilkinson, et al., 2017). From beginning of nineteenth century up to 1960 mixed ethanol with gasoline was used widely for transportation in many European countries such as Germany, France, Italy, Sweden, and England as well as Brazil and U.S.A (Thiago et al., 2014).

It is a type of fuel which drives its energy from the carbon fixation biologically. The fuels included in biofuels are derived from the solid biomass, conversion of biomass, various biogases and liquid fuels as well (Wilkinson et al., 2017). Biofuels are driven by the factors like need for

increasing energy security and hikes and gaining the scientific and public attention. Ethanol can be made by any organic material which contains sugar, starch, or cellulose (Mata et al., 2015). According to new technologies ethanol is producing from the cellulose from the woody fibers from the crops, grasses, and trees residues. Ethanol is an environmental friendly fuel (Moreira et al., 2013). It is biodegradable and water soluble as well. In comparison with gasoline, if a fuel spill occurs, its effects are less severe environmentally. Ethanol can cause lower emissions of CO when using as a fuel additive because ethanol contains oxygen (Caetano and Moura, 2013).

The utilization of lignocellulosic biomass is one of the most promising alternatives for the liquid biofuel to be used directly in the vehicle engine or as raw material for the production of other biofuels, with environmental, societal, and economic benefits (Awolu and Ibileke, 2011). Bioethanol production from lignocellulosic biomass is complex due to its structural properties and requires the utilization of the carbohydrate fractions, i.e. cellulose and hemicelluloses (Maache-rezzoug et al., 2009). Brewer`s spent grain (BSG), the barley malt residue obtained after wort filtration, is the main by-product from brewer`s representing 85% of total waste (Thiago et al., 2014).

BSG is available at low or no cost all through the year, but its main application is limited to animal feed. Nevertheless, it is lignocellulosic biomass that can be better used, since it is rich source of oligo- and polysaccharides as well as polyphenols (Acacio et al., 2014). BSG is a material that presents in its composition sugars polymerized in to cellulose and hemicellulose. Bioethanol production from brewer`s spent grain is considered a second generation biofuel process since it has no direct conflict with human food, as it happens with the first generation biofuels produced from agricultural crops, such as corn and sugarcane for bioethanol production, or soybean oil, or corn oil, for biodiesel production (Mata et al., 2015). The production process involves several steps basically four major ones: - the biomass pretreatment, hydrolysis of carbohydrates, fermentation of simple sugars into ethanol, and distillation for product recovery (Caetano et al., 2013).

1.2. Problem Statement

The commercial production of fuel ethanol in the world relies mainly on the fermentation of sugar and starch, but production of ethanol from such “first generation” (from corn and sugar) feedstock is often viewed as competing with food production and increasing prices of food. So that productions of bioethanol or biofuel from agricultural wastes such as brewer`s spent grain negotiate the debate of “food versus energy” controversy. Therefore this study is intended to solve such type of problem and to convert this low value by-product into a value-added product, bioethanol.

These days, brewer companies are diversifying in world and also in Ethiopia, so that there is available source of brewer`s spent grain which is produced after separation of aqueous solution at the end of mashing in to extract (wort) and insoluble fraction called spent grain, which is source of lignocellulose, but these high lignocellulosic biomass traditionally has been used as animal feed for low cost or dumped in to landfill. As BSG constitutes a large amount of brewer`s waste, 85% of total waste, 31% of original malt weight and 20kg per 100 liter beer produced, and in Ethiopia, the total BSG produced per day after wort separation is more than 290 million tons from around 14 brewing factories; the high composition of carbohydrates, cellulose and hemicellulose presence (50-60%), and high BSG production volume from breweries shows researchers a direction to employ and extract carbohydrates for value added products, bioethanol. The storage of BSG for long period, more than 7-10 days, is difficult environmentally since it creates bad odor by making favorable conditions for microorganisms due to high moisture content, it is difficult for farmers to transport and after using for animal feed, it creates bad odor (Mata et al., 2015). As the BSG is dried its protein and fat content will deteriorate due to the microorganism activity so that it will not be used for animal feed after losing its protein and fat content but is best to use it for other value-added products, bioethanol.

There is great political and social pressure to reduce the environmental pollution arising from industrial activities. Almost all developed and underdeveloped countries are trying to adapt to this reality by modifying their processes so that their residues can be recycled and/or reused. Consequently, most large companies no longer consider residues as waste, but as a raw material for other processes. The development of the infrastructure coupled with the national income has

exacerbated the demand for fuel. In addition to transport, fuel is important for industry, agriculture, households, and social service. Ethiopia imports fuel on average at the expense of 2million USD per annum and this covers 77% of the total export earnings, the demand for the fuel will increases when the economic growth of the nation increases.

1.3. Objectives

1.3.1. General Objective

The general objective of this work is the production and optimization of bioethanol from agro-industrial lignocellulosic biomass—brewer`s spent grain.

1.3.2. Specific objectives

The following specific objectives were achieved during the production and optimization of bioethanol from BSG.

- ❖ To carry out the proximate analysis of brewer`s spent grain (cellulose, hemicellulose and lignin) composition.
- ❖ To conduct and optimize hydrolysis stages by varying process parameters (temperature, residence time, and acid concentration).
- ❖ To carry out thermodynamic and kinetic analysis for fermentation of reduced sugar to ethanol.
- ❖ To recover ethanol from water-ethanol mixture using distillation and characterization of ethanol.

1.4. Significance and Scope of the Study

1.4.1. Significance of Study

Agro-industrial wastes or byproducts represent a large portion of biomass which does not compete with food production. Considering the large amount of agro-industrial wastes discarded the development of technological platform for a value-added product has yet to be established on a large scale (Vince, 2010).

Along with technical development, from the economic perspective, the renewable resources are gradually replacing the fossil resources as raw material. However, this is also used as a reality for the generation of energy, considering of number of chemicals, increasingly produced from agricultural merchandises in place of petroleum.

Using this low cost by-product to produce value-added products like bioethanol is essential for the environment and as well for the reduction of dependence on petroleum producing country for fuel. It creates the employment opportunity and increases gross income to the nation by saving energy, time, and transportation cost which is paid for fuel producing nations.

Ethiopia has high labor force, land potential and suitable climate for the development of bioethanol from BSG, which is not yet been implemented in any area around the country. The brewing company is diversifying in the country so that there is plenty of an available raw material which is discarded or used for no or low cost for animal feed.

1.4.2. Scope of the study

This paper focuses on the production and optimization of bioethanol from lignocellulosic biomass, brewer`s spent grain, which is a byproduct from brewing process. The methodologies that were used in this work were proximate analysis of BSG, pretreatment, dilute-acid hydrolysis, fermentation, and distillation. The statistical data was generated from laboratory experiments and by using analysis of variance (ANOVA) to analyze the effect of process parameters on the yield of total reduced sugar from second stage hydrolysis process and to draw a generalizing conclusion for each parameter on the optimum yield of total reduced sugar. The yield of total reduced sugar in the hydrolysate was analyzed by using a DNS method through determination of concentration via absorbance. The thermodynamic and kinetic analysis were conducted for the fermentation process in order to find an optimum fermentation temperature, thermodynamic parameters, and rate constant of reaction and order of reaction for total reduced sugar conversion to bioethanol. The water-ethanol mixture separation process was conducted using a distillation unit and the final product; ethanol was characterized using, refractive index to determine the density by measuring the specific gravity, vibro-viscometer to determine its viscosity and FTIR to determine the functional groups found in ethanol.

Chapter Two

2. LITERATURE REVIEW

2.1. Bioethanol production

Ethanol or ethyl alcohol has been used by man since the dawn of history. In 2006 the worldwide bioethanol production was estimated to be about 40 Mt (70% of which coming from USA and Brazil), with a steady increasing demand as requested, for instance, by the guidelines defined by Kyoto Protocol. The production of ethanol has two routes: synthetic and biological. The synthetic ethanol production is commonly carried out by a catalytic hydration of ethylene in vapor phase. The ethanol produced by this process is used as a solvent (60%) and chemical intermediate (40%) (Gencheva et al., 2012). Fermentative ethanol production accounts 93% of the total ethanol production in the world. *Saccharomyces cerevisiae* is the most popular microorganism used for ethanol production due to its high ethanol yield and high tolerance to rather high ethanol concentration. The ethanol produced is mostly used as fuel (92%), industrial solvents and chemicals (4%) and beverages (4%) (Vince, 2010).

Bioethanol also has low toxicity, volatility and photochemical reactivity, resulting in less smog production as compared with conventional fossil fuels (Idrees et al., 2013).

Thus, the implementation of processes to hydrolyze the lignocellulosic materials is necessary in order to maximize yield while reducing costs. Already many industrial plants exist for the production of bioethanol in countries across the world, with Brazil currently being the world leader next to USA in the industry due to limited internal fuel resources and the fuel crisis of the 1970's (Akanksha et al., 2014).

While bioethanol and biodiesel are the most typical biofuel types, the two top producers of ethanol in the world by far are the United States and Brazil. United States being the major producer among the two representing using corn as the main feedstock accounting for the vast majority of the input whereas Brazil are the second major uses sugarcane as major feedstock for ethanol production (Novy et al., 2015).

Regarding the socio-economic and environmental issues, after a detail study on the short and long-term socio-economic, and environmental impacts of growing crops like corn, sugarcane and oil palm for transport biofuels, sometimes it is concluded that even though these activities contribute to mitigate the price rise of fossil fuels and energy security they may contribute to increase food price (Muigai, 2012).

Bioethanol is an alcohol produced by fermenting sugar components of a plant material (renewable materials) (Awolu and Ibileke, 2011). Ethanol (ethyl alcohol, bioethanol) is the most employed liquid biofuel either as a fuel or as a gasoline enhancer (Sa, 2013). Bioethanol can be used to replace conventional gasoline in today cars with little or none modifications of vehicle engines (Caetano et al., 2013). It is made mostly from sugar and starch crops such as sugar cane and corn among others. In the “first generation” technology bioethanol is produced by converting sugars directly (“first generation” technology) from crops like sugar cane or sugar beets, indirectly through starch from corn, potatoes, wheat, or cassava in to ethanol via fermentation followed by distillation (Awolu and Ibileke, 2011).

In the “second generation” technology ethanol is produced through cellulose from biomass (A. K. Chandel et al., 2011). Lignocellulosic biomass typically contains 50-80% (dry basis) carbohydrates that are polymers of 5C and 6C sugar units. Long-term economic and environmental concerns have resulted in a great amount of research in the past couple of decades on renewable sources of liquid fuels to replace fossil fuels (P. Kumar et al., 2009).

2.2. World Bioethanol Production

Reasons for engaging in biofuels production include diversifying energy sources, alleviating dependence on importing fossil energy and reducing emissions of greenhouse gas (GHG).

Bioethanol production could be classified based on the type of feedstock used in to two (Pejin et al., 2016):

- 1) First-generation biofuels and
- 2) Second-generation biofuels

2.2.1. First-generation biofuels

Food crops such as: starch, sugar and vegetable oil as well as animal fats, are the main feedstock for first-generation biofuels. The most popular first-generation biofuels are biodiesel (produced mainly from canola, soybean and barley) and bioethanol (produced mainly from corn, wheat and sugarcane) followed by other types of vegetable oil and biogas (Kuila and Sharma, 2016).

There are many factors, which simultaneously constrain and strengthen the global growth of biofuels market. These include potential negative impacts on food commodities, the availability of natural resources, government subsidies, national commitments to mitigate climate change, oil prices and other political/environmental factors (Mata et al., 2015). Several sustainability issues surround the increasing demand for first-generation biofuels and biomaterials. One is the increasing pressure to make land-use changes in favor of biomass feedstock production.

This can be a challenge in two ways (Rojas-chamorro et al., 2017):

- Direct land-use change- for example, by removing forests to make way for agricultural production. This issue can be managed by utilizing a standard that requires production to take place on land that has not been converted when compared to a reference year.
- Indirect Land-Use Change (ILUC). Typically caused by supply and demand. This issue can be addressed by defining how additional biomaterials can be produced without affecting land use and food security.

2.2.2. Second-generation biofuels

Lignocellulosic biomass derived ethanol is often referred as a second-generation biofuels, have evolved independently from biomass sources of lignocellulose. Lignocellulosic biomass, otherwise termed as cellulosic biomass, is the only sustainable feedstock for bio refineries to meet the ever increasing energy demand (Sun and Cheng, 2002).

These second-generation biofuels are relatively immature so they should have good potential for cost reduction and increased production efficiency levels as more experience is gained. Depending partly on future oil prices, they are therefore likely to become a part of the solution to the challenge of shifting the transport sector towards more sustainable energy sources at some

stage in medium term. Cellulosic biomass conversion into biofuels and chemicals has several advantages including greenhouse gas emissions, near carbon neutrality, lesser dependence on fossil fuels, and improvement in nation`s energy security. Cellulosic ethanol, i.e. ethanol from forestry or agricultural waste is considered a way to prevent displacement of crops to feed humans. The joint study sees cellulosic ethanol as a viable alternative for reducing oil dependences while protecting food crops (Mata et al., 2015). The world ethanol production from 2009-2015 in billions of gallons was given below in table 2.1.

Table 2.1 Worldwide Ethanol Production: 2009-2015 (billions of gallons)

| World Ethanol Production | 2009 | 2010 | 2011 | 2012 | 2013 | 2014 | 2015 |
|--------------------------|------|------|-------|-------|-------|-------|-------|
| USA | 6.49 | 9.23 | 10.94 | 13.00 | 13.90 | 13.92 | 13.93 |
| Brazil | 5.02 | 6.47 | 6.58 | 6.92 | 6.97 | 6.98 | 6.98 |
| Europe | 0.57 | 0.73 | 1.04 | 1.21 | 1.27 | 1.29 | 1.31 |
| China | 0.49 | 0.50 | 0.54 | 0.54 | 0.55 | 0.58 | 0.59 |
| Canada | 0.21 | 0.24 | 0.29 | 0.36 | 0.46 | 0.48 | 0.49 |
| Asia(except China) | 0.13 | 0.16 | 0.53 | 0.24 | 0.33 | 0.35 | 0.37 |
| Other Countries | 0.15 | 0.21 | 0.39 | 0.74 | 0.76 | 0.78 | 0.79 |

Source: (“World Energy Resources Bioenergy | 2016,” 2016).

2.3. Bioethanol production in Ethiopia

The potential for producing fuel alcohol from molasses and other raw materials, including trees such as eucalyptus, it is quite large in Ethiopia. In fact, if considered seriously, production of bioethanol from biomass is considered to have double folds; i.e., solving the fuel problem and cleaning the environment (Mata et al., 2015).

The production of ethanol (ethyl alcohol) in Ethiopia in factories traces back to the beginning of 20th century, even though the number of firms involved in the sub-sector is still very limited. Ethanol production in Ethiopia is linked with sugar factories. At present, the main supply line in the domestic market is dominated by two sugar factories (Metahara and Fincha) and other alcohol factors namely; Akaki, Balezaf, Mechanisa, Desta, Eagles and Sebata with the combination of their annual production capacity at around 11.1 billion liters in 2016. In the near

future, Wonji/Shoa, Tendaho, Kuraz, and other new sugar factories under construction are expected to start producing ethanol. But exploiting lignocellulosic biomass for the production of ethanol is not yet implemented, though there is a plenty of lignocellulosic biomass found in the country; BSG, corn cobs, bagasse, agricultural residues and so on (Aliyu et al.,)

2.4. Feedstocks for bioethanol Production

Ethyl alcohol (ethanol) may be produced from any fermentable sugar by yeast under suitable conditions. The feed stocks are classified in to three principal classes (Dussán et al., 2014):

- i) The saccharine materials such as sugarcane and sugar beet molasses, and fruit juices.
- ii) The starchy materials, which include the cereals (corn, barely, sorghum, and the like) and potatoes.
- iii) Cellulose materials, such as wood and lignocellulosic wastes.

Feedstocks and processing methods for bioethanol production were shown in figure 2.1 below.

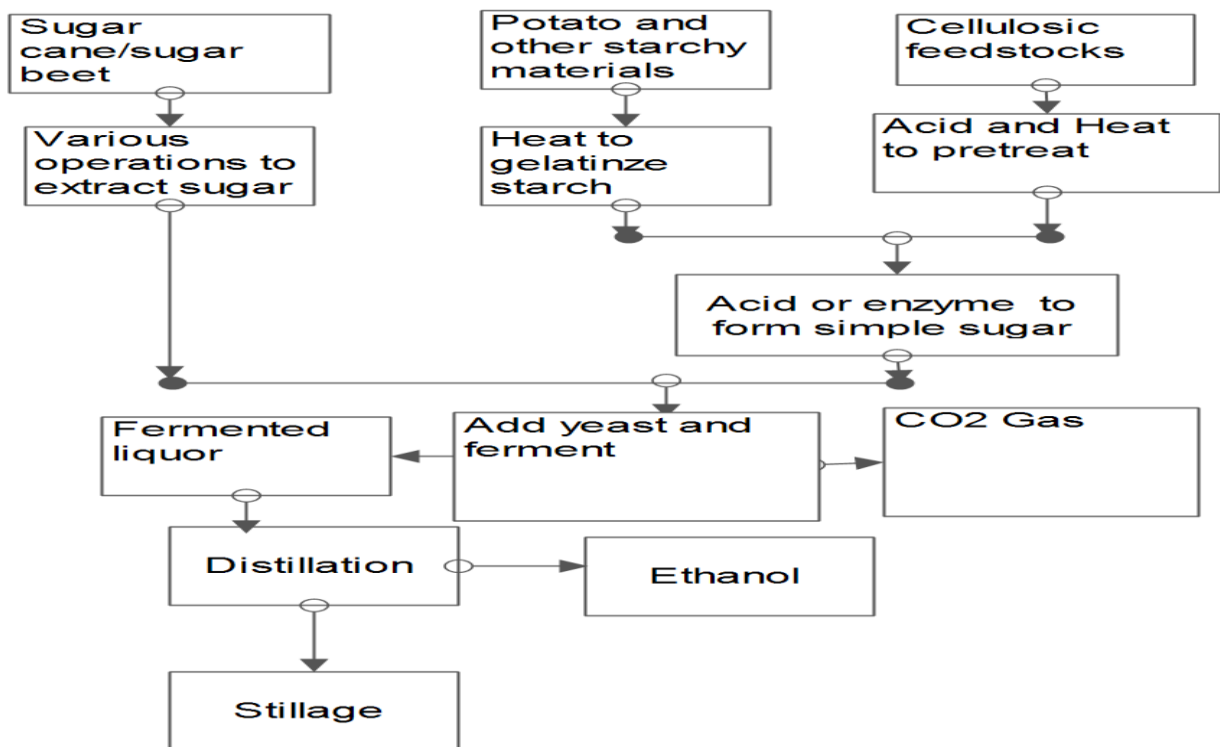


Fig. 2.1 Processing stages to produce ethanol from different feed stocks

2.5. Lignocellulosic feedstocks for Ethanol production

Bioethanol is a liquid produced by distillation of fermented sugar obtained from various locally available resources such as agriculture and forestry residue, dedicated starchy crops, woody and herbaceous crops and organic portion of municipal wastes (Chan-u-tit et al., 2013). Ethanol produced from lignocellulose and agro-industrial wastes can be seen as the most promising ones with the great advantages of bioenergy not competing with food resources and yet a broader spectrum of feedstocks used when compared to traditional processes (Raposo et al., 2009).

Table 2.2 below summarizes the composition of lignocellulose encountered in the most common sources of biomass.

Table 2.2 Composition of lignocellulose in common agricultural and waste residue in dry basis(Harmsen & Huijgen, 2010).

| Lignocellulosic Feedstocks | Cellulose | Hemicellulose | Lignin |
|----------------------------------|-----------|---------------|---------|
| Hardwoods Stems | 40-55 | 24-40 | 18-25 |
| Softwoods Stems | 45-50 | 25-35 | 25-35 |
| Nut Shells | 25-30 | 25-30 | 30-40 |
| Grasses | 25-40 | 35-50 | 10-30 |
| Paper | 30-41 | 20-30 | 15-20 |
| Wheat Straw | 30 | 50 | 15 |
| Spent Barley Grain | 35-45 | 20 | 10 |
| Cotton Seed Hairs | 25-35 | 50-70 | 0 |
| Newspaper | 40-55 | 25-40 | 18-30 |
| Waste Papers from Chemical pulps | 35-40 | 10-20 | 5-10 |
| Swine Waste | 16-25 | 30 | 20 |
| Solid Cattle Manure | 1.6-4.7 | 1.4-3.3 | 2.7-5.7 |
| Coastal Bermuda grass | 25 | 35.7 | 6.4 |
| Sorted Refuse | 30 | 20 | 25 |

Source: Reshamwala et al., (1995), Cheung and Anderson (1997) and Boothathy, (1998)

The composition of lignocellulose highly depends on its source. There is a significant variation of the lignin, hemicellulose and cellulose content of lignocellulose depending on whether it is derived from hardwood or softwood or grasses (Da Silva and Chandel, 2012).

The greatest benefit of bioethanol lies in its potential to decrease greenhouse gas emissions through partial substitution of gasoline as a transport fuel, this could support countries to attain their commitments under the Kyoto protocol and mitigate the effects of climate as it is shown in figure 2.2 below (Limayem and Ricke, 2012).

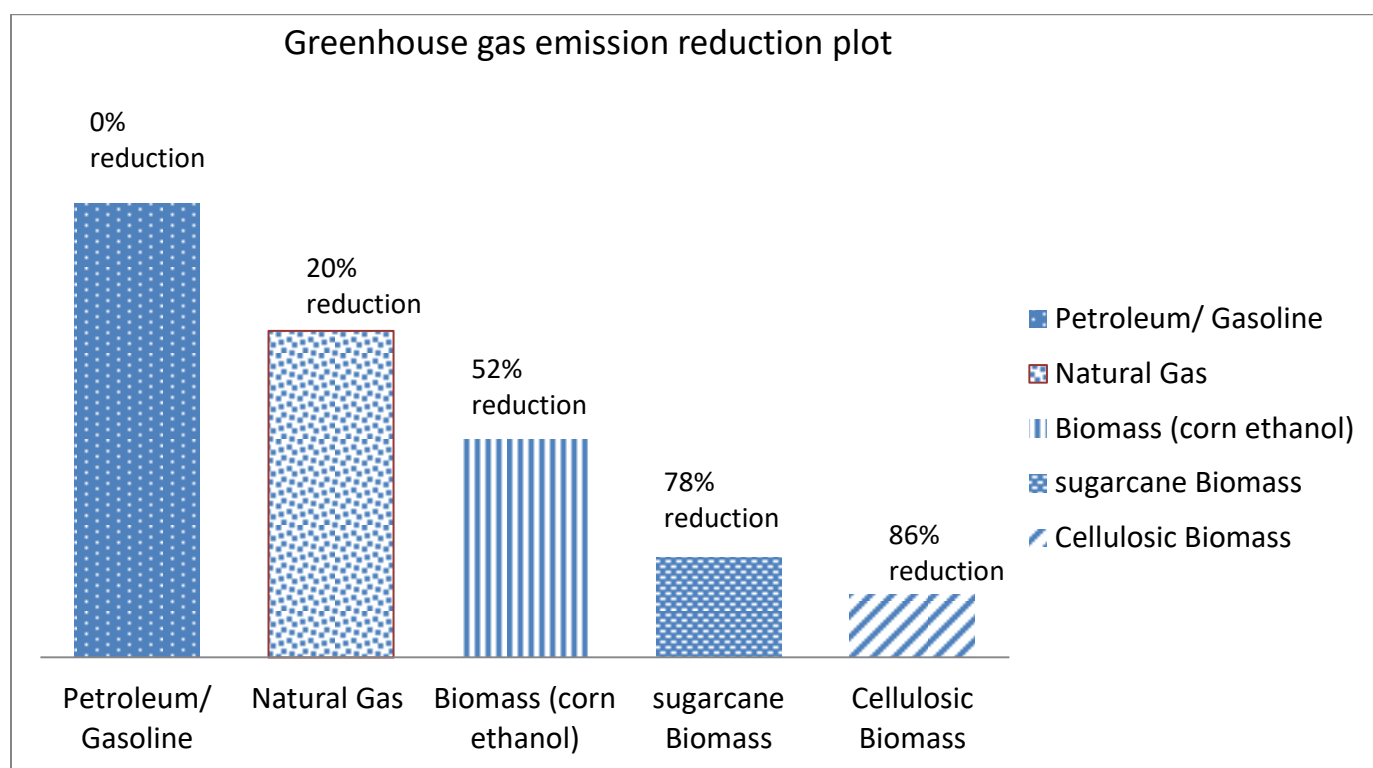


Fig. 2.2 Energy and GHG emissions impact Source: ((Chan-u-tit et al., 2013)

Lignocelluloses are the most abundant structural material that comprises much of the mass of a plant basically composed of cellulose, hemicellulose and lignin (A. A. K. Chandel et al., 2011).

Cellulose is the main structural constituent in plant cell walls and is found in an organized fibrous structure (P. Kumar et al., 2009).

Cellulose is more commonly considered as a polymer of glucose because cellobiose consists of two molecules of glucose and the chemical formula of cellulose is $(C_6H_{10}O_5)_n$ and the structure of one chain of the polymer is shown in figure 2.3 below (Orji et al., 2016).

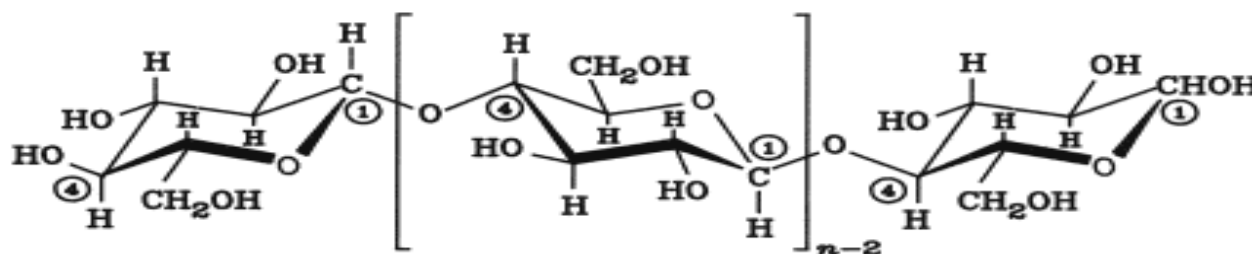


Fig. 2.3 Structure of single cellulose molecule

The structure of cellulose is a linear polymer consisting of D-glucose subunits linked to each other by β -(1,4)-glycosidic bond. Cellobiose is the repeat unit established through this linkage, and it constitutes cellulose chain and the long chain cellulose polymers are linked together by hydrogen and Van der Waals bonds, which cause the cellulose to be packed in to a microfibrils, which are building blocks fibrils and in turn builds the cellulose fiber (Limayem and Ricke, 2012). The number of glucose units in one cellulose molecule (i.e., degree of polymerization) is at least 9,000-10,000 and possibly as high as 15,000 (Dussán and Silva, 2014). Cellulose is a relatively hygroscopic material absorbing 8-14% water under normal atmospheric condition ($20^{\circ}C$, 60% relative humidity), nevertheless, it is insoluble in water, where it swells and cellulose is also insoluble in dilute acids at a temperature range of $140 - 150^{\circ}C$; the solubility of the polymer strongly related to the degree of hydrolysis achieved (Sun and Cheng, 2002). As a result, factors that affect the hydrolysis rate of the cellulose also affect its solubility that takes place, however, with the molecule being in a different form than native one. At higher temperatures it become soluble, as the energy provided is enough to break the hydrogen bonds that hold the crystalline structure of the cellulose molecule (Machado et al., 2016).

Hemicellulose is a polymer that is composed of several different sugars like, D-glucose, D-galactose, D-mannose, D-xylose, L-arabinose, L-rhamnose and is sometimes referred to by the sugars they contain, for example, galactoglucomannan, arabinoglucoronoxylan, arabinogalactan, etc (Novy et al., 2015). The degree of polymerization of hemicellulose is lower than cellulose, achieving an average of about 100-200 and due to the combination of several and for presenting

majority part of amorphous structure, the hemicellulose is more soluble and easily degradable in water than cellulose (Dussán et al., 2014).

The most common type of polymers that belongs to the hemicellulose family of polysaccharide is xylan. The molecule of xylan involves 1,4- linkages of xylopyranosyl units with α -(4-O)-methyl-D-glucuronopyranosyl units attached to anhydroxylose units. The result is a branched polymer chain that is composed of five carbon sugar monomers, xylose, and a six carbon sugar monomers such as glucose. Important aspects of the structure and composition of hemicellulose are the lack of crystalline structure, mainly due to highly branched structure, and the presence of acetyl groups connected to polymer chain (Machado et al., 2016).

Lignin is a very complex molecule comprised of phenylpropane linked in a three-dimensional structure (Lenihan et al., 2012). Among the lignocellulosic biomass (residues), the great interest has been focused on brewer`s spent grain, BSG due to its lower composition in lignin (L. Liguori et al., 2015).

Extractives and Ash any numbers of different compounds (resins, phenolics, and other chemicals) in biomass that are not an integral part the cellular structure are called extractives. These compounds can be extracted from biomass by means of polar or non-polar solvents including hot or cold water, benzene, ether, methanol, or other solvents that do not degrade the biomass structure. Minerals include: calcium, magnesium, potassium and other materials, that will leave as ash when biomass is burned (A. Ktenioudaki et al., 2012).

2.6. Brewer`s spent grain

BSG is the higher amount of waste resulting in brewing factories obtained after wort filtration (A. Dávila and A. Cardona, 2016). Brewers spent grain (BSG) is a high tonnage co-product of the brewing industry and is a lignocellulosic material which could potentially be used to produce bioethanol. It contains a substantial proportion of sugars, present in bound form as complex carbohydrates (Wilkinson and Cook, 2015). Due to its high moisture and fermentable sugars content, BSG is unsuitable material and is liable to deteriorate rapidly due to microbial activity. Three methods of preserving the spent grain: freezing-drying, oven drying, and freezing were

evaluated. Preservation by oven drying or by freezing-drying reduces the volume of the product and does not alter its chemical composition while freezing is inappropriate because large volumes must be stored and alterations in the arabinose content may occur (Fărcaș et al., 2014). The brewer`s spent grain chemical composition varies depending on the barley variety, harvest time and on the brewing process conditions (Mata et al., 2015). On the dry weight basis, brewer`s spent grain contains about 50-70% polysaccharides consisting of 30-38 % cellulose, 16-22 % hemicellulose, 10-13 % lignin, 11-14% moisture content, 2-4% ash and extractives and 18-22 % or more proteins and fiber and the balance ashes and extractives (Muthusamy et al., 2014). The summary from above findings was given in table 2.3 below on average basis.

Table 2.3 Summary for Chemical composition of BSG by component on average basis

| Component | Percentage (%) |
|---------------------|----------------|
| Cellulose | 34 |
| Hemicellulose | 19 |
| Lignin | 11.5 |
| Ash and Extractives | 2-4 |
| Moisture Content | 12.5 |
| Protein and Fiber | 20 |

Challenges associated with using BSG as a feedstock includes the existence of a complex outer layer, making it difficult to separate and convert, and high moisture content making it susceptible to microbial growth and spoilage within a seven day period. The moisture issue can be stabilized post production in the brewing process, deterioration of the feedstock through microbial activity can further reduce yields in the conversion process (Buffington, 2014).

2.7. Sustainable utilization of BSG

Lignocellulosic substrates being cheap and readily available, have recently gained considerable interest because of their possible use in secondary fermentation processes. However, the utilization of BSG is limited especially in developing countries and new ways of making use of

this residue would be beneficial for the process economy. The following uses in various fields been reported (Aliyu and Bala, 2013).

2.7.1. Animal nutrition and feed formulations

The utilization of this abundantly available raw material has found a place in animal nutrition, which not only reduces the cost of feeding but also creates an outlet for this material. Thus, brewery spent grains have been utilized as feed for animals for many years, the presence of hemicellulose, cellulose and lignin, and also the amount of readily available substance such as sugars and amino acids aid its utilization as feed for ruminants. However, its higher moisture content of BSG together with polysaccharide and protein makes it particularly susceptible for microbial growth and subsequent spoilage in a short period of time on average seven days (Nigam, 2017).

2.7.2. Bioethanol Production

Bioethanol can be produced from starch and sugar based crops as well as lignocellulosic biomass. Most of the starch and sugar-based crops (molasses, sweet sorghum, maize starch, sugarcane, rice, wheat, sorghum, etc) compete with human food production as well as have high production prices that restrict their industrial production. But with the increasing demand for ethanol, there is a search for the cheaper and abundant substrate and development of an efficient and less expensive technology so that ethanol can be made available and more cheaply (Ktenioudaki et al., 2012). The composition of BSG as described above containing primarily residual compounds such as; hemicellulose, cellulose and lignin makes it a good feedstock for ethanol production. Current advances for the conversion of residues like BSG to ethanol requires chemical or enzymatic hydrolysis to produce majorly fermentable sugars, followed by microbial fermentation. Thus, large amounts of enzymes required for enzymatic conversion of cellulose to fermentable sugars impact severely on the cost effectiveness of this technology (Aboltins and Palabinskis, 2015).

In Ethiopia, currently, from fourteen brewing companies the total BSG produced per annum is around 290 million tons by projecting the result from the known value. The following information on the BSG annual product was obtained from some volunteer brewing companies around Addis Ababa and Harar, Ethiopia; Heineken brewery around 25 million tons, BGI around 35 million tons, Harar brewery around 27 million tons, and Meta brewery around 36 million tons which was obtained through direct phone interview with the managers; this shows us a direction to utilize the raw material for bioethanol production.

2.7.3. Lactic acid production

Lactic acid (2-hydroxy propanoic acid) has found many applications in connection with foods, fermentations, pharmaceuticals, and the chemical industries. Recently, however, there has been an increasing demand in lactic acid production because it can be used as a precursor of polylactic acid (PLA) production. However, the realization of this potential is dependent on whether lactic acid can be produced at a low cost which is comparative on a global scale. One of the major challenges in the large-scale lactic acid production is the cost of raw material. The use of expensive carbon sources such as glucose, sucrose, or starch is not economical because lactic acid is a relatively cheap product (Aliyu and Bala, 2013).

2.7.4. Xylitol and pullulan production

Xylitol is a rare sugar that exists in low amount in nature. It acts an excellent sweetener with some health benefits especially in its ability to combat dental caries, to treat illness such as diabetes, disorders in lipid metabolism and parenteral and renal lesions and to prevent lung infection. Several agro-industrial residues can be used to produce xylitol, but BSG has advantage because it requires no preliminary detoxification steps, but overall production is favored by high initial xylose concentrations, oxygen limitation, high inoculum density and appropriate medium supplementation. As such, production of xylitol from brewer`s spent grain by yeasts is a potential option to upgrade this residue (Ktenioudaki et al., 2012). The technical flow diagram in figure 2.4 below shows that BSG has diverse advantages from its reduced sugar, glucose.

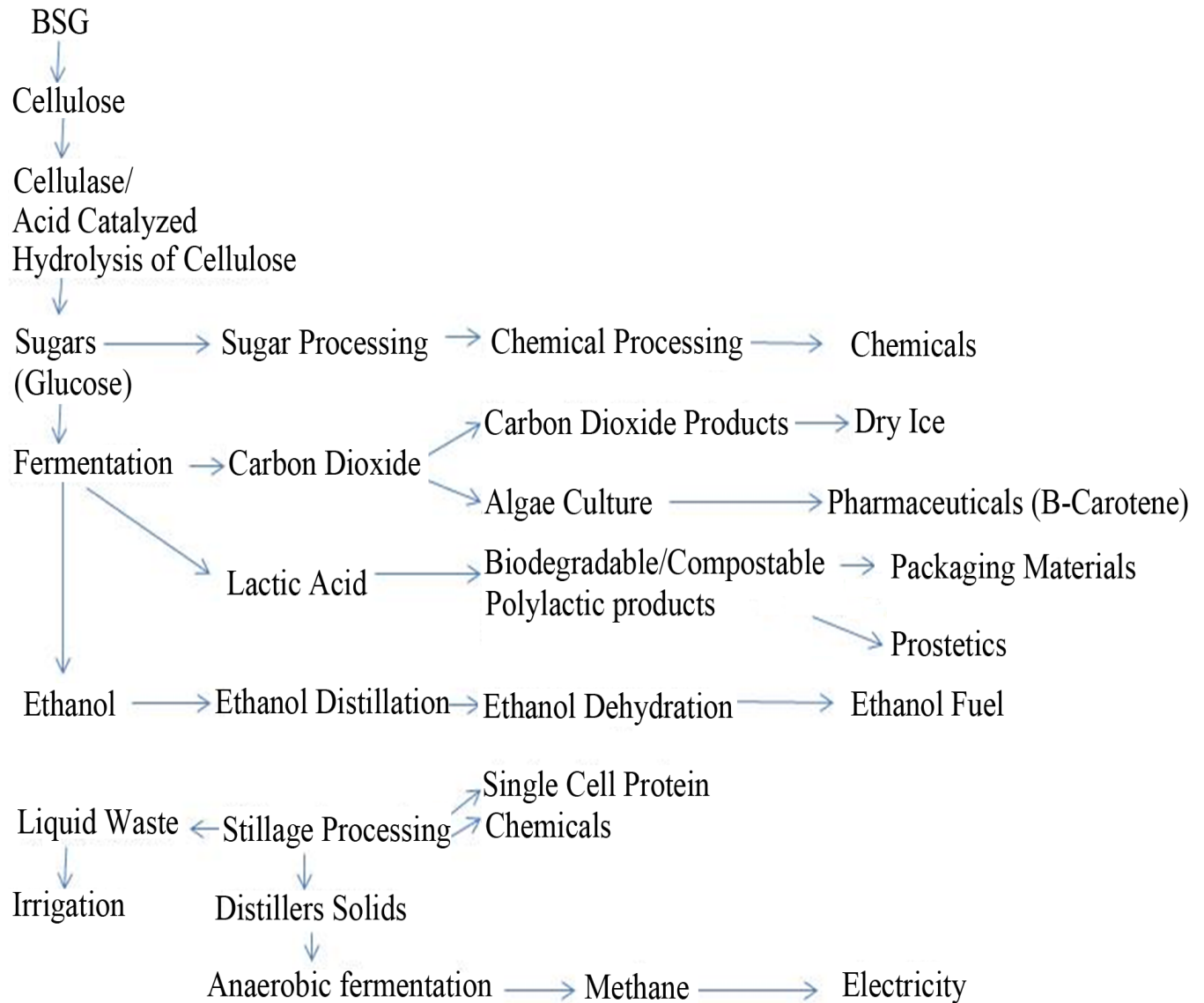


Fig. 2.4 BSG technical flow diagram, (adapted from Van Wyk, 2011)

2.8. Processing technologies for converting BSG to EtOH

There are different processing steps to convert lignocellulosic biomass (BSG) into a value-added product, bioethanol. The basic four steps are: pretreatment, hydrolysis, fermentation and distillation (Vince, 2010). The nature of the feedstocks puts certain constraints on the technology required for the manufacture of ethanol. For example, molasses or sugar solutions can be

fermented directly by yeast, using traditional and well-established technology. However, cellulose feedstock such as wood or bagasse or any lignocellulosic biomass must be hydrolyzed in to component molecules and sugars before fermentation by one or more specifically selected microorganisms (Roberto, 2005).

2.8.1. Pretreatment

Pretreatment methods are classified in different groups: physical such as milling or grinding, physicochemical like steam pretreatment or auto-hydrolysis, hydro-thermolysis or wet oxidation, chemical such as alkali or dilute acid or oxidizing agent or organic solvents, ionic liquid, biological, electrical and combination of them (Dehnavi, 2009).

Pretreatment of upstream portions include mainly physical, (i.e., BSG size reduction) and thermochemical processes that involve the disruption of the recalcitrant material of the biomass (Limayem and Ricke, 2012). The purpose of pretreatment is increasing porosity of as well as removing lignin (Muigai, 2012). The purely physical processes of pretreatment can be summarized by an intense mechanical grinding in order to increase the accessible surfaces to enzymes, thus supporting further hydrolysis and reducing polymerization degree of cellulose (Maache-rezzoug et al., 2009).

The features of successful pretreatment include the breaking down of the lignocellulosic complex, decreasing the cellulose crystallinity, preserving the hemicellulose sugars, limiting the formation of degradation products that prevent hydrolysis and fermentation, minimizing energy and chemicals in the conversion process, achieving a high value lignin co-product, and minimizing hazardous and toxic wastes (Gencheva et al., 2012).

A large number of pretreatment methods have been proposed generally on a wide variety of lignocellulosic biomasses for bioethanol production since different feedstocks have different physical-chemical characteristics. These pretreatment methods are usually divided in to physical, chemical: acid pretreatment and alkali pretreatment, physic-chemical such as steam explosion, and biological pretreatment (Zheng and Rehmman, 2014).

2.8.1.1. Physical pretreatment

Mechanical comminution

Waste materials can be comminuted by a combination of chipping, grinding and milling to reduce cellulose crystallinity. The size of material is usually 10-8mm after chipping and 0.2-2mm after milling. Vibratory ball mill has been found to be more effective in breaking down the cellulose crystallinity brewer`s spent grain and improving the digestibility of biomass and the power requirement of mechanical comminution of agricultural materials depends on the final particle size and characteristics of the biomass (Trajano and Wyman, 2013).

Pyrolysis

Pyrolysis has also been used for pretreatment of lignocellulosic materials. When the materials are treated at temperatures greater than 300⁰C, cellulose rapidly decomposes to produce gaseous products and residual char (Da Silva and Chandel, 2012).

According to (Zheng and Rehmann, 2014), the decomposition is much slower and less volatile products are formed at lower temperature. Mild acid hydrolysis (1N H₂SO₄, 97⁰C, 2.5h) of the residues from pyrolysis pretreatment has resulted in lesser conversion of cellulose to reduced sugar more dominantly, glucose and the process is enhanced with the presence of oxygen, but the process is energy intensive and might result in hazardous fumes.

2.8.1.2. Chemical pretreatment

To this group belong the pretreatments that are purely initiated by chemical reactions for disruption of biomass structure (P. Kumar et al., 2009).

Ozonolysis

Ozone can be used to degrade lignin and hemicellulose in many lignocellulosic materials such as wheat straw, bagasse, green hey, peanut, pine, cotton straw, and poplar sawdust. The degradation

was essentially limited to lignin and hemicellulose was slightly attacked, but cellulose was hardly affected (P. Kumar et al., 2009).

(Harmsen and Huijgen, 2010) investigated the pretreatment of lignocellulosic biomass using ozonolysis, advantages of ozonolysis is it effectively removes lignin, it does not produce toxic residue for the downstream processes, and the reactions are carried out at room temperature and pressure; however, a large amount of ozone is required, making the process expensive.

Liquid hot water

Liquid hot water (LHW) processes are biomass pretreatment with water at high temperature and pressure. Other terms are hydrothermolysis, hydrothermal pretreatment, aqueous fractionation, solvolysis or aquasolv (Limayem and Ricke, 2012). Solvolysis by hot compressed water contacts water with the biomass for up to 15 minutes at temperatures of 200-230⁰C; between 40% and 60% of the total biomass is dissolved in the process, with 4-22% of the cellulose, 35-60% of the lignin and all of the hemicellulose being removed. Over 90% of hemicellulose is recovered as monomeric sugars when acid were to hydrolyze the resulting liquid. In addition, acetic acid is formed during the treatment and acts as a catalyst for polysaccharide hydrolysis. This results in the formation of monomeric sugars that may further decompose in to furfural (inhibitor of fermentation) (Kuila and Sharma, 2016).

Room Temperature Ionic Liquids (RTIL)

Room temperature ionic liquids (RTIL) are salts that are in the liquid phase at temperature as low as room temperature. There is a vast variety of different RTIL; however, they share a common characteristic, which is that they are usually comprised of an inorganic anion and an organic cation of very heterogeneous molecular structure (Bensah and Mensah, 2013). The difference in the molecular structure of renders the bonding of the ions weak enough for the salt to appear as liquid at room temperature (Trajano and Wyman, 2013). As of yet, there is no industrial application employing RTIL; furthermore, very limited information exists in the literature to describe their action with lignocellulose. However, there is an indication that mainly due to their polarity and in general their unique properties, they can function as selective solvents of lignin or

cellulose. That would result in separation of lignin and increase of cellulose accessibility under ambient conditions and with no use of acid or alkaline solution. The formation of inhibitor compounds are also reduced, despite the potential this method appears to have, there are several uncertainties due to lack of experience. Among the most important ones are the ability to recover the RTIL used, the toxicity of the compounds, and the combination of water with RTIL (K. Appels et al., 2014).

Wet Oxidation

Wet oxidation operates with oxygen or air in combination with water at elevated temperature and pressure. It was presented as an alternative to steam explosion which had become the most widely used pretreatment method. Industrially, wet air oxidation processes have been used for the treatment of wastes with a high organic matter by oxidation of soluble or suspended materials by using oxygen in aqueous phase at high temperatures (140-350⁰C) and high pressure (5-20MPa) (Buffington, 2014).

Wet oxidation has been successfully applied for the treatment of lignocellulosic biomass of hardwood. In recent studies on alkaline wet oxidation of hardwood lignocellulosic biomass, the main degradation products found from lignin and hemicellulose were carboxylic acid, CO₂ and H₂O. Compared to other pretreatment processes, wet oxidation has been proven to be efficient for treating lignocellulosic materials because the crystalline structure of cellulose is opened during the process (Singh and Trivedi, 2013).

According to (Harmsen and Huijgen, 2010) about a 65% degree of delignification could be achieved with wet oxidation of hardwood lignocellulosic biomass. They reported that the disadvantage of wet oxidation process is the higher production of furfural and 5-hydroxymethylfurfural (HMF), which are the main inhibitors in the fermentation step.

Oxidative Delignification

Lignin biodegradation could be catalyzed by the peroxidase enzyme with the presence of H₂O₂, ozone, oxygen or air. The effectiveness in delignification can be attributed to the high reactivity of chemicals with the aromatic ring. The lignin ring will be converted to e.g. carboxylic acid.

Since these acid formed will act as an inhibitors in the fermentation step, they have to be neutralized or removed (Nidetzky et al., 2015).

(P. Kumar et al., 2009) in addition to an effect on lignin, oxidative treatment also affects the hemicellulose fraction of the lignocellulosic complex. A substantial portion of hemicellulose might be degraded and can no longer be used for sugar production.

2.8.1.3. Physic-chemical pretreatment

Steam explosion (Autohydrolysis)

Steam explosion is the most commonly used method for pretreatment lignocellulosic biomass. In this method, chipped biomass is treated with high-pressure saturated steam and then pressure is swiftly reduced, which makes the materials undergo an explosive decompression (P. Kumar et al., 2009). Steam explosion is typically initiated at a temperature of 150-260⁰C (corresponding pressure 0.69MPa to 4.83MPa) for several seconds to a few minutes before the material is exposed to atmospheric pressure. The process causes hemicellulose degradation and lignin transformation due to high temperature, thus increasing the potential for cellulose hydrolysis. 90% efficiency of enzymatic hydrolysis has been achieved in 24hr for poplar chips pretreated by steam explosion, compared to only 15% of hydrolysis of untreated chips (Wang and Liu, 2014). The factors that affect steam explosion are residence time, temperature, chip size and moisture content. Optimal hemicellulose solubilization and hydrolysis can be achieved by either high temperature and short residence time (270⁰C and 1min) or low temperature and longer residence time (190⁰C and 10min) (Olaoye and Kolawole, 2013).

Limitations of steam explosion include destruction of a portion of the xylan fraction, incomplete disruption of lignin-carbohydrate matrix, and generation of compounds that may be inhibitory to the growth of microorganisms used in the downstream processes (Zheng and Rehmann, 2014). Because of the formation of degradation products that are inhibitory to microbial growth, enzymatic hydrolysis, and fermentation, pretreated biomass needs to be washed by water to remove inhibitory materials along with water-soluble hemicellulose. The water wash decreases

overall saccharification yields due to the removal of soluble sugars, such as those generated by hydrolysis of hemicellulose (Meneses et al., 2017).

Ammonia fiber explosion (AFEX)

AFEX is another type of physico-chemical pretreatment in which lignocellulosic materials are exposed to liquid ammonia at high temperature and pressure for a period of time, and then the pressure is swiftly reduced. The concept of AFEX is similar to steam explosion, in a typical AFEX process, the dosage of liquid ammonia is 1-2kg ammonia/kg dry biomass, temperature 90°C and retention time of 30min (Li, 2010).

The AFEX pretreatment can significantly improve the saccharification rates of various herbaceous crops and grasses. It can be used for the pretreatment of many lignocellulosic materials including alfalfa, wheat straw, barely straw, corn stover, rice straw, municipal solid waste, softwood newspaper, switch grass, aspen chips and bagasse. The AFEX pretreatment does not significantly solubilize hemicellulose compared to acid pretreatment and acid-catalyzed steam explosion (Than, 2017).

To reduce the cost and protect the environment, ammonia must be recycled after pretreatment. In an ammonia recovery process, a superheated ammonia vapor with a temperature up to 200°C was used to vaporize and strip the residual ammonia in the pretreated biomass and the evaporated ammonia was then withdrawn from the system by a pressure controller for recovery (Kuila and Sharma, 2016).

CO₂ explosion

Similar to steam and ammonia explosion pretreatment, CO₂ explosion is also used for pretreatment of lignocellulosic materials. It was hypothesized that CO₂ would form carbonic acid and increase hydrolysis rate. The yields were relatively low compared to steam or ammonia explosion pretreatment, but high when compared to the enzymatic hydrolysis without pretreatment (A. A. K. Chandel et al., 2011).

Carbonic acid may offer the benefits of acid catalysts without the use of an acid like sulfuric acid. The pH of carbonic acid is determined by the partial pressure of CO₂ in water, and can be neutralized by releasing a reactor pressure. Studies indicate that combined capital and operating costs of the carbonic acid system are slightly higher than a sulfuric acid-based system and slightly sensitive to reactor pressure and solid concentration (Moreira et al., 2013).

An alternative use of CO₂ in pretreatment is extraction with supercritical CO₂. CO₂ becomes supercritical under relatively milder conditions ($T_c=304K$ and $P_c=73bar$). Supercritical CO₂ (SC-CO₂) has been widely used as an extraction solvent. SC-CO₂ extraction is being considered as possible pretreatment route for lignocellulosic material. A positive effect of SC-CO₂ was found for lignocellulosic material with high moisture content (>40%), but the pretreatment was not effective enough to compensate for the high capital costs for high pressure equipment and SC-CO₂ was considered not an effective tool for lignocellulosic treatment (Harmsen and Huijgen, 2010).

2.8.1.4. Biological pretreatment

In biological pretreatment processes, microorganisms such as brown-, white- and soft-rot fungi are used to degrade lignin and hemicellulose in waste materials. Brown rots mainly attack cellulose, while white and soft-rots attack both cellulose and lignin. White-rot fungi are the most effective basidiomycetes for biological pretreatment of lignocellulosic biomass (Nuno and Carvalho, 2009).

The white-rot fungus *P. chrysosporium* produces lignin-degrading enzymes, lignin peroxidases, during secondary metabolism in response to carbon or nitrogen limitation. Both enzymes have been found in the extracellular filtrates of many white-rot fungi for the degradation of wood cell walls. Other enzymes including polyphenol oxidases, laccases, H₂O₂ producing enzymes and quinone-reducing enzymes can also degrade lignin. The advantages of biological pretreatment include low energy requirement and mild environmental conditions; however, the rate of hydrolysis in most biological pretreatment processes is very low (Amezcuallieri et al., 2017).

2.8.2. Hydrolysis

Hydrolysis is the reaction between a biomass and water under the presence of catalyst (acid or enzyme) to produce a simple sugars (Bokulich and Bamforth, 2013). During this reaction, the released polymer sugars, cellulose and hemicellulose are hydrolyzed in to free monomer molecules readily available for fermentation conversion to bioethanol (Novy and Longus, 2015). Hydrolysis is categorized as one stage and two stages.

There are different types of hydrolysis; chemical, biological and enzymatic, steam explosion, ionic liquids and hot water hydrolysis of these methods, chemical and enzymatic are dominant (Tsoutsos and Bethanis, 2011). Chemical hydrolysis is classified as either alkaline or acid hydrolysis (Parsapour, 2012). Alkaline solutions like sodium hydroxide, lime and usually also ammonia can remove lignin and some part of hemicellulose (Dehnavi, 2009). Acid (H_2SO_4 , HCL, H_3PO_4 , HNO_3) pretreatment firstly developed in Germany in 1898 (Vigo-ourense and Lagoas, 2004). The acidic hydrolysis can be divided in to concentrated or dilute acid hydrolysis (Axelsson et al., 2012).

Concentrated acid hydrolysis is powerful agents to both hemicellulose and cellulose conversion to monosaccharide sugars, but is toxic to environment, corrosive and hazardous and requires reactors that resist corrosion (P. Kumar et al., 2009). Enzymatic hydrolysis uses enzymes that hydrolyze hemicellulose and cellulose to simple sugars. Biological hydrolysis uses microorganisms such as brown-, white-, and soft-rot fungi are used to degrade lignin and hemicellulose in waste materials, brown-rot fungi mainly attack hemicellulose, while white- and soft-rots fungi attack both cellulose and lignin (A. A. K. Chandel et al., 2011). This methods, enzymatic hydrolysis, has drawback over other methods in that it requires long time for conversion of lignocellulosic biomass to simple sugars, recovering enzymes is costly, low yield of fermentable sugar production and low ethanol yield (Novy et al., 2015). Consequently, for the improvement of the reaction productivity, it is essential the pretreatment of the raw material. Generally, three hydrolysis alternatives exist after pretreatment processes (Verardi et al., 2014):

- Acid hydrolysis (Concentrated and Dilute acid hydrolysis)
- Enzymatic hydrolysis
- Alkaline hydrolysis

Among these methods, dilute acid mediated hydrolysis has been found more effective and less costly in complete hemicellulose and cellulose hydrolysis in short reaction time (Dussán et al., 2014).

2.8.2.1. Acid Hydrolysis

Acid-catalyzed hydrolysis has been widely employed to break down cellulose and hemicellulose polymers in lignocellulosic biomass to form individual sugar molecules which can be subsequently fermented to ethanol. Sulfuric acid is the most investigated acid during hydrolysis although other mineral acids such as HCl, H₃PO₄, HNO₃ and other mineral acids are used. Acid hydrolysis can be categorized in to two: (A. A. K. Chandel et al., 2011).

Concentrated-acid hydrolysis and

Dilute-acid hydrolysis

Concentrated-acid hydrolysis

Hydrolysis of lignocelluloses by concentrated-acids is a relatively an old process. Concentrated-acid processes are generally reported to give higher sugar yield (e.g. 90% of theoretical glucose yield) and consequently higher ethanol yield, compared to dilute-acid processes. Furthermore, concentrated-acid processes can operate at low temperature (e.g. 40⁰C), which is a clear advantage compared to dilute-acid processes (Jose and Reinaldo, 2011). However, the concentration of acid is very high in this method (e.g. 30-70%), and dilution and heating of the concentrated acid during the hydrolysis process make it extremely corrosive. Therefore, the process requires either expensive alloys or specialized non-metallic constructions, such as ceramic or carbon-brick lining (Akanksha et al., 2014). The acid recovery is an energy-intensive process, in addition, when sulfuric acid is used; the neutralization process produces large amounts of gypsum. Furthermore, environmental impacts strongly limit the application of hydrochloric acid. The high investment and maintenance costs have greatly reduced the potential commercial interest of this process (A. K. Chandel et al., 2012).

Dilute-acid hydrolysis

The dilute acid hydrolysis of lignocellulosic materials is an attractive process due to several advantages it offers. There is no need for pretreatment as the acid is known to penetrate lignin components, the acid does not need to be recovered and corrosion problems in the equipment are reduced when compared with concentrated acid hydrolysis processes (Tsoutsos and Bethanis, 2011). A main drawback of dilute-acid hydrolysis processes, particularly in one stage, is degradation of the sugars in hydrolysis reactions and formation of undesirable by-products. In order to avoid degradation of monosaccharides at high temperatures and formation of inhibitors, dilute-acid hydrolysis is carried out in two-stages (Than, 2017).

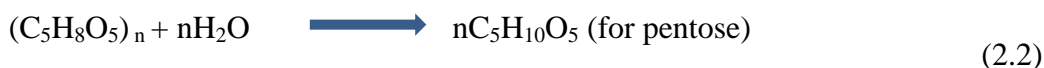
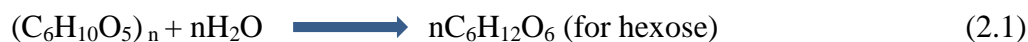
(Amezcuallieri and Aburto, 2017) investigated a two stage dilute acid hydrolysis of for a lignocellulosic feed, in the first stage, which should be carried out relatively under mild conditions, hemicellulose is converted to sugar monomers. In the second stage, the residual solid is hydrolyzed under more severe conditions, allowing cellulose to be hydrolyzed.

The two-stage hydrolysis process is usually preferred over one-stage dilute-acid hydrolysis because (A. K. Chandel et al., 2012):-

- The separate stages for hydrolysis of the hemicellulose and cellulose should result in higher sugar yield. Furthermore, a product with high hexose sugar can be obtained in the second-stage hydrolysis which can easily be fermented to ethanol. Mixtures of pentose and hexose are always problematic for fermentation, because of the difficulty in fermentation of pentose.
- The energy consumption should be minimized, since liquid is removed before the second-stage hydrolysis.
- The resulting sugar solution should be more concentrated.
- Less sugar degradation from the hydrolyzed materials in the first-stage leads to a higher overall yields of sugars.

During dilute-acid hydrolysis, the acid concentration is in a range of 2-4% and operating temperature is 130-160⁰C and retention time is 15-40 minutes. There are many mineral acids used during hydrolysis (Laopaiboon et al., 2013).

During the dilute acid hydrolysis of BSG, parameters such as temperature, reaction time, acid concentration, particle size of biomass and liquid to solid ratio play critical roles, from these parameters, acid concentration, reaction time and temperature are most significant factors in obtaining optimum sugar recovery and minimum generation of inhibitors (Roberto, 2005). The corresponding reaction is given below during the dilute acid as a catalyst (Arredondo et al., 2009).



2.8.2.2. Enzymatic hydrolysis

Enzymatic hydrolysis of cellulose is carried out by cellulase enzymes which are highly specific. In the hydrolysis reaction enzymes bind to the biomass to achieve the conversion. The organism responsible for producing cellulolytic enzymes was *Trichoderma reesei*, which today is used in the enzyme industry for producing wide range of commercial enzymes (Maache-rezzoug et al., 2009). The cellulases involved in the hydrolysis of lignocellulose include endoglucanases, which attack low-crystallinity regions of cellulose fiber and generate free chain-ends, and exoglucanases, which remove cellobiose from the free chain-ends.

(Forssell et al., 2012) investigated the advantages of enzymatic hydrolysis are high yields of glucose, due to the highly specific cellulose conversion, and that the reaction is performed at the mild conditions. The disadvantages of enzymatic hydrolysis are slow reaction rate of the enzymes, formation of degradation by-products, recovering of enzymes is difficult and requires additional cost and high price of enzymes and contamination of enzyme culture hinders this method from applying in large scale.

Ethanol production by enzymatic hydrolysis can be performed in a Separate Hydrolysis and Fermentation (SHF) mode or in a Simultaneous Saccharification and Fermentation (SSF) mode. In the SHF process, hydrolysis is performed separately from fermentation, which means that the optimal temperatures for both the enzymatic hydrolysis and fermentation can be applied. A drawback with SHF is that the generated cellobiose functions as cellulase inhibitor and it is also

a two-step process (Akanksha et al., 2014). To reduce enzyme inhibition and two-step process, SSF can be used. In SSF, hydrolysis and fermentation occur at the same time, which means that the glucose that is generated is immediately consumed by the fermenting microorganism and inhibition of α -glucosidase is therefore prevented. The disadvantages of SSF process is that the optimal temperatures for the cellulases and fermenting microorganism are not the same so the selected temperature is compromise, which means that neither hydrolysis nor fermentation will be performed under optimal conditions (Wilkinson and Cook, 2015).

2.8.2.3. Alkaline hydrolysis

Some bases such as NaOH, $\text{Ca}(\text{OH})_2$, KOH and NH_4OH can also be used for the pretreatment of lignocellulosic materials and the effect of alkaline hydrolysis depends on the lignin content of the material. The mechanism of alkaline hydrolysis is believed to be saponification of intermolecular ester bonds crosslinking xylan hemicelluloses and other components. The porosity of the lignocellulosic materials increases with the removal of crosslinks (Than, 2017). Dilute NaOH treatment of lignocellulosic materials causing swelling, leading to an increase in surface area, a decrease in the degree of polymerization, a decrease in crystallinity, separation of structural linkages between lignin and carbohydrates, and disruption of the lignin structure (A. K. Chandel et al., 2012).

2.8.3. Fermentation

After the BSG pretreatment and hydrolysis, the next step for bioethanol production is the sugars fermentation to ethanol (Mata et al., 2015). Bioethanol is produced mainly by three types of fermentation, such as, batch, fed-batch and continuous (Rojas-chamorro et al., 2017). In batch fermentation, feedstock is added to the fermentation vessel along with the microorganisms, nutrients and other ingredients at the beginning of the fermentation of whole batch followed by recovery of ethanol, while in fed-batch mode, one or more ingredients are added to the vessel as the fermentation is going on (Zabed et al., 2014). Continuous fermentation involves constant input of ingredients and removal of output from the fermentation vessel (Soupioni and Koutinas, 2013). Involvement of microorganisms in fermentation of sugars is a crucial part of bioethanol production (Zabed et al., 2014). In fuel ethanol production industry, the fermentation is a

biochemical process in which simple sugars (glucose, fructose, and sucrose) is metabolized in to ethanol by yeast *Saccharomyces cerevisiae* (Copa et al., 2013).

When the yeast is submitted to anaerobic conditions, its metabolic route is deviated to produce ethanol and carbon dioxide as shown in (2.3) below (Schisler et al., 2011).



A previous study does not address fermentation kinetics and thermodynamic analysis to have an optimum operating temperature and pH for the microorganism *Saccharomyces cerevisiae*.

Establishment of fermentation kinetics is important in describing microorganism and metabolic regulation with technical, economic and physiological implications, it would be a powerful instrument to predict and control fermentation problem and helpful in understanding fermentation process.

Factors affecting fermentation

Major factors that affect the performance of fermentation process were temperature, pH, alcohol tolerance, and inhibitor tolerance because microorganisms for fermentation of ethanol can best be described in terms of their performance parameters and other requirements such as compatibility with the existing products, processes and equipment. The major ones that affect fermentation process are: temperature, pH and sugar concentration (Maurice, 2011).

Temperature

Temperature has an important influence on the growth rate of microorganisms and the rate of ethanol production. Wine and beer fermentations are generally conducted below 20⁰C; whereas higher temperatures (30-38)⁰C are being examined for industrial alcohol production by yeast cultures (Wang and Liu, 2014). Too high temperatures kill yeast and low temperatures slow down yeast activity. All the recombinant strains are mesophilic organisms and function best at a temperature range of (30-38)⁰C (Kuila and Sharma, 2016).

pH

A very important factor for cellular growth is pH. Most alcoholic fermentations are conducted in a pH range of 4.5 to 5.5; yeast cultures can grow over a wide range of pH 3 to 8 with an optimum for growth generally acidic range. Shifts in pH can also affect the final ratio of organic waste products produced by yeast cultures (Sun and Cheng, 2002).

Sugar concentration

The concentration of sugar can affect the microbial ethanol fermentation in various ways. The amount of ethanol produced is proportional to the amount of sugar added; thus, high sugar concentrations are desired. However, too high sugar concentrations can inhibit metabolism due to increased osmotic pressure (Da Silva and Chandel, 2012). Very low levels of sugar, on the other, may limit the rate of ethanol production. Hence, each fermentation process will have an optimal glucose or equivalent sugar concentration of 3-20% is satisfactory and also other concentrations are used (Idrees et al., 2013).

2.8.4. Distillation

The fermentation broth (mash or beer) is a mixture of ethanol, water, cell mass, fusel oil, and other components available in the fermentation media such as residual sugars, nonfermentable sugars and hydrolysis by-products (Erdelji et al., 2007).

Distillation is a method for separating two or more liquid compounds on the basis of boiling-point differences. Distillation is a purification process wherein a substance is heated to its boiling point, the vapor produced upon boiling is allowed to flow away from the boiling liquid, and the vapor is cooled to condense it back to the liquid. The boiling point of a mixture is a function of vapor pressures of various components in the mixture (Thiago et al., 2014).

2.9. Benefits and Impacts of Cellulosic Biomass Conversion to EtOH

2.9.1. Greenhouse Gas Reduction

Perhaps the most unique and powerful attribute of converting cellulosic biomass to fuels and chemicals is very low net greenhouse gas emissions, particularly when compared to fossil fuels. For ethanol production in particular, non-fermentable and unconverted solids and wastes left after making targeted products can be burned to provide all the heat and electricity to run the process, and no fossil fuel is required to operate the conversion plant for mature technology (Ruiz and Teixeira, 2012). Similar results are expected for making many chemicals from biomass, provided process heat and power requirements are not excessive. Additionally, low levels of fertilizers and cultivation are needed for many lignocellulosic crops, thereby keeping energy inputs for growing biomass low (Saadavate et al., 2013).

2.9.2. Strategic benefits

Despite much political clamor to reduce petroleum use during several energy crises in which petroleum supplies were tightened and prices ballooned, petroleum imports have been grown, making petroleum importing nations vulnerable to supply disruptions and price hikes. Many chemicals are also derived from petroleum (Woiciechowski and Faraco, 2015). Today, an interruption in oil supplies or increase in petroleum costs would badly damage or even cripple transportation and organic chemical production. Although there is a controversy in estimating biomass availability, use of petroleum for making chemicals is far less than for fuels, and there is almost certainly more than enough cellulosic biomass to support the manufacturing of all the chemicals that could be derived from this resource (Trajano and Wyman, 2013). Many studies estimated that enough cellulosic biomass could be available from wastes and dedicated energy crops to make a significant dent in the huge amount of gasoline consumed in the United States (Zainab and Fakhra, 2014). Development of technology for recovery of animal feed quality protein from cellulosic biomass would allow land to be support both fuel and feed production, greatly enhancing fuel production. Use of cellulosic biomass has been called the “new petroleum” because of its tremendous, although still untapped, potential (Kang et al., 2014).

2.9.3. Solid waste disposal

Disposal of wastes is a mounting problem as the population continues to grow and we seek to maintain and improve the environment. For example, farmers must reduce the burning of rice straw after a harvest and less waste wood should be burned to improve air quality. Converting such waste biomass in to fuels and chemicals through hydrolysis of cellulose and hemicellulose would provide a valuable solution to these growing problems while also generating valuable products (Machado et al., 2016). However, solid waste disposal via hydrolysis to sugars for fermentation and reaction to valuable products is underappreciated and deserves far more attention. In addition, many chemicals that can be from biomass are biodegradable, reducing the accumulation of solid wastes and facilitating waste treatment for liquids and gases. Thus, production of such materials could provide an economically attractive path to solid waste reduction (Trajano and Wyman, 2013).

2.9.4. International Fuels Market

Energy demand is growing rapidly in developing countries, and increased mobility will become more important as well, driving up the demand for transportation fuels. Given that transportation is so dependent on petroleum now, meeting this growing demand will be challenging unless new fuel sources are developed. Producing fuels from domestic sources of biomass would also reduce trade deficit for both developed and developing countries with limited petroleum resources and help grow their economy (Acacio et al., 2014).

2.9.5. Sustainable Production of Organic Fuels and Chemicals

When one line-up all sustainable resources and compares them to human needs, biomass provides the only known routes to produce organic fuels and chemicals sustainably. Furthermore, liquid fuels provide many important attributes for transportation including ease of fueling and storage and relatively high energy density (Yohannan and Walker, 2008). Thus, fermenting of sugars released by hydrolysis of cellulose and hemicellulose to ethanol or other liquid fuels can provide a unique and powerful path to making fuels for transportation on an ongoing. It can also

help diversify a transportation sector that is almost totally dependent (>96%) on one source, petroleum, for energy. In addition, most organic chemicals also come from petroleum and other fossil resources and making these products from biomass would help stabilize the price and availability of organic chemicals. Although sugar and starch now supply fermentation sugars for manufacture of several products, hydrolysis of cellulosic biomass can provide abundant, low-cost sugars that could support even larger-scale uses, provided processing costs are reduced (Li, 2010).

2.9.6. Competition with Food

One of the major determining factors of long-term economic feasibility of bio-fuels, ethanol, is its competition with food. According to FAO's definition, food security exists when "all people, at all times, have physical, social, and economic access to sufficient, safe, and nutritious food which meets their dietary needs and food preferences for an active and healthy life" (Zabed et al., 2014). When feedstocks used for food are also used for bioethanol, the food price increases and also the availability of food will be limited by the biofuel supply so far they compete for the same resources such as land, fertilizers, water etc. Therefore, bioethanol's potential competition with food should be considered when investing in bioethanol this is being tackled by making use of second generation feedstocks. The definition considers four dimensions; food availability, food access, food use and food stability. These dimensions are appraised next with regard to bio-energy production expansion (Vieira and Tavarela, 2010).

2.10. Physical and Chemical characteristics of Ethanol

Ethanol is a clear colorless, flammable solvent with a boiling point of 78.5°C; also known as ethyl alcohol, grain spirits, or alcohol. Unlike other alcohols of similar molecular weight, ethanol is considered non-toxic or a drinking alcohol. Ethanol found in transportation fuels has been denatured, generally by the addition of up to 5 percent gasoline, rendering it unfit for drinking (Borzani, 2016).

It is a renewable fuel source that is produced by fermentation and distillation process. The most common source of ethanol in the United States in 2008 is corn. However, it can be produced

from other products such as sugar cane, saw grass, and other agro-industrial products that will be conducive to the fermentation and distillation process. Ethanol is a polar solvent that is water-soluble and has a 55°F flash point. Ethanol has a vapor density of 1.59, which indicates that it is heavier than air (R. Kumar and Horváth, 2016). Consequently, ethanol vapors do not rise, similar to vapors from gasoline which seeks lower altitudes (Sun and Cheng, 2002).

Ethanol's specific gravity is 0.79, which indicates it is lighter than water but since it is water-soluble it will thoroughly mix with water. Ethanol has an auto-ignition temperature of 793°F and a boiling point of 173°F. Ethanol is less toxic than gasoline or methanol. In a pure form, ethanol does not produce visible smoke and has a hard-to-see blue flame. Interestingly, ethanol and some ethanol blends can conduct electricity (Jaisil and Laopaiboon, 2013).

Physical and chemical property of ethanol is summarized in table: 2.4 below.

Table 2.4 Physical and Chemical property of Ethanol

| Property | Value |
|-----------------------------|---------------------------------|
| Flash Point | 55°F |
| Ignition Temperature | 793°F |
| Molecular formula | C ₂ H ₆ O |
| Molar mass | 46.069 $\frac{g}{mol}$ |
| Specific Gravity | 0.79 |
| Vapor Density | 1.49 |
| Kinematic viscosity at 25°C | 1.4912E-06 m ² /s |
| Vapor Pressure | 44 mmHg |
| Boiling Point | 173°F |
| Flammable Range (LEL–UEL) | 3.3%–19% |
| Conductivity | Yes |
| Smoke Character | Slight to none |
| Toxicity | Lower than methanol |
| Solubility | Higher |

Source: The National Institute for Occupational Safety and Health pocket guide to chemical hazard

Chapter Three

3. MATERIALS AND METHODS

3.1. Materials, Chemicals and Equipment

Materials

The material that was used in this work was, brewer`s spent grain. The material, brewer`s spent grain, was collected from Heineken brewing factory located at Addis Ababa, Ethiopia, and transported to AAiT, School of Chemical and Bio Engineering Laboratory.

Chemicals

The chemicals that were used in this work were: sulfuric acid (98%), phosphoric acid (98%), nitric acid (65%), NaOH pellet, dextrose, peptone, DNS, sodium potassium tartrate (40%), sodium sulphite, crystal phenol, yeast strain, and distilled water. All the experimental works were done in the laboratories of School of Chemical and Bio-Engineering, AAiT, AAU except FTIR analysis which was conducted at Arat kilo, Faculty of Science, AAU from January 10, 2017 to April 20, 2018. All the chemicals, except the distilled water, were purchased and delivered from Neway PLC import and export, Addis Ababa, Ethiopia.

Equipment

The equipment used during this thesis work were: plate dryer, beaker, rotary hammer mill, oven, furnace, autoclave, desiccator, burette, crucible, vacuum pump, vacuum filtration, fermenter, volumetric flasks, agitator incubator, water bath, simple distillation unit, conical flasks, stirred tank reactor, spectrophotometer/colorimeter, pH meter, Erlenmeyer flask, FTIR, analytic balance vibro-viscometer and refractive index.

3.2. Methods

3.2.1. Proximate analysis and mechanical pretreatment of BSG

Proximate analysis

Moisture content determination

Moisture content was determined by drying a sample in an oven (WTB Binder) at $105^{\circ}\text{C} \pm 5^{\circ}\text{C}$ for 2 hour followed by cooling in desiccator and weighing until constant weight was obtained (Ktenioudaki and Gallagher, 2012); ASTM E1209-67.

$$\text{Moisture Content} = \frac{m_1 - m_2}{m_1} \times 100 \quad (3.1)$$

Where, m_1 is the amount (g) sample collected

m_2 is the amount (g) after drying

Ash content determination

The ash content was determined using a furnace (Nabertherm B150) at $550^{\circ}\text{C} \pm 5^{\circ}\text{C}$ for 8 hour. ASTM A365-407.

$$\text{Ash Content} = \frac{m_2}{m_1} \times 100 \quad (3.2)$$

Where, m_1 is the mass of sample before burning, g

m_2 is the mass of ash after burning, g

Cellulose content determination

Cellulose content was determined by using a 75ml mixture of concentrated sulfuric acid in distilled water (with a ratio of 1:3 volume) which is refluxed with a gram of oven-dried sample of BSG for one hour at 120⁰C in autoclave. The specimen was filtered using vacuum filter and washed with a 200ml distilled water and oven dried for four hours at 105⁰C. The white residue after extraction is considered as a cellulose and its composition in the sample was determined as (Walker and Goran, 2015): ASTM D3175-04 and AOAC E124-345.

$$\text{Cellulose Content} = \frac{m_2}{m_1} \times 100 \quad (3.3)$$

Where: m_1 is the mass of oven-dried sample of BSG, g

m_2 is the mass of oven-dried residual after hydrolysis, g

Hemicellulose content determination

Hemicellulose content was determined using a beaker, by adding 200ml of NaOH solution 2% (w/v) to a 1.5gram of BSG sample and allowing it to boil at 120⁰C for four hour. After this time the material was filtered and washed with a distilled water of 200ml, and was placed in oven for three hour at 105⁰C. The hemicellulose content was determined by Walker and Goran, 2015: ASTM D3175-07.

$$\text{Hemicellulose Content} = \frac{m_2}{m_1} \times 100 \quad (3.4)$$

Where: m_1 is the mass of oven-dried sample before extraction, g

m_2 is the mass of oven-dried sample after extraction, g

Lignin content determination

Lignin content was determined using oven-dried sample at 105⁰C of 2.5 gram, beaker of capacity 200ml, and 15ml of 72% H₂SO₄ was be added slowly with magnetic stirrer. The reaction was preceded for one hour in a controlled environment at room temperature of 25⁰C. After one hour reaction the specimen was transferred to a 1000ml flask by washing with a 600ml of distilled water, diluting the concentration of H₂SO₄ to a 3% and refluxed for one hour in autoclave at 130⁰C. The flask was then removed from the autoclave and the black insoluble material was allowed for overnight to settle. The content of the flask was filtered using vacuum filtration. The residue was washed to free of acid with 500ml of hot tap water and then oven-dried at 105⁰C then cooled in desiccators and weighed until a constant weight (Muthusamy, 2014). ASTM B1135-47. The amount of lignin content of BSG was determined as:

$$\text{Lignin Content} = \frac{m_2}{m_1} \times 100 \quad (3.5)$$

Where: m_1 is the mass of oven-dried sample before hydrolysis, g

m_2 is the mass of oven-dried sample after hydrolysis, g

Mechanical pretreatment of BSG

The dried sample was grinded using a vibratory hammer mill to a size range of 2mm-1mm and the particle size classification was done using a mesh of sieves with different opening sizes and with respective vibrator. The mass of each sample collected was measured and stored using a polyethylene bag for hydrolysis stage.

3.2.2. Hydrolysis (first and second stages)

3.2.2.1. First stage hydrolysis

The chemical pretreatment was conducted at mild condition; it is basically used to hydrolyze hemicellulose using an autoclave. The dried biomass was homogenized by agitation. It was conducted at a temperature, retention time and phosphoric acid concentration of 130⁰C, 20 min, and 1%, respectively and liquid to solid ratio of 10g/g and particle with size of at 2mm-1mm is

held constant. After hydrolysis, the hydrolyzate was washed to remove maximum inhibitory from solid residue, cellulignin. (A. K. Chandel et al., 2012).

The interest in the use of H_3PO_4 acid is that after neutralization with NaOH, it would yield sodium phosphate which was remain in the hydrolysates and can subsequently be used as a nutrient by microorganisms in down-stream fermentation media. Therefore, centrifugation is not required with the consequent advantage of improving the economics of the process; and it is also friendly to the environment (the salt formed is not a waste). (Angela M.Orozco, 2011).

3.2.2.2. Second stage hydrolysis

After the first stage hydrolysis was done, the solution was washed to separate the maximum hemicellulosic inhibitors by using distilled water. The remaining solid was favored to an extreme condition in order to release fermentable sugar from cellulose using autoclave. The hydrolysis reaction was conducted at a temperature of range (140-150⁰C), retention time (20-30min), and acid concentration (2-3%) by holding liquid to solid ratio and particle size constant at 10%(v/w) and 2mm-1mm, respectively.

Factors and their respective operating ranges were given in table 3.1 below.

Table 3.1 Factors and respective operating values for second-stage hydrolysis

| Factors | Units | Level | | |
|--------------------|----------------|-------|--------------|------|
| | | Low | Center point | High |
| Temperature | ⁰ C | 140 | 145 | 150 |
| Retention time | min | 20 | 25 | 30 |
| Acid Concentration | M (%) | 2 | 2.5 | 3 |

Quantification of recovered sugar concentration and the yield Y (gram of total reduced sugar that can be obtained from g of BSG dry matter) was calculated using equation (3.6) and (3.7), respectively. The concentration of simple sugar in terms of total reduced sugar from absorbance was determined by using spectrophotometer method at a wave length of 540nm.

$$C = \frac{\text{Abs}-b}{m} \quad (3.6)$$

Where: C is concentration of total reduced sugar

Abs is absorbance of unknown sample, %

b is the intercept from standard curve, %

m is the slope from standard curve, ml/g

The yield of total reduced sugar was calculated from equation (3.7) as:

$$Y = C \times \frac{V}{M} \times 100 \quad (3.7)$$

Where: Y is the yield of total reduced sugar

V is the liquid volume and M is the amount of biomass

The concentration of simple sugar was determined by titration using 3, 5-DNS.

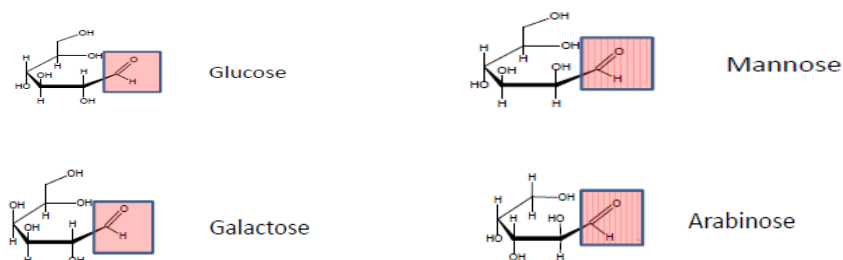
During the hydrolysis stage (both first and second), dilution of concentrated phosphoric acid was conducted using a mole balance equation (3.8) given below for the known volume of liquid solution.

$$C_1V_1=C_2V_2 \quad (3.8)$$

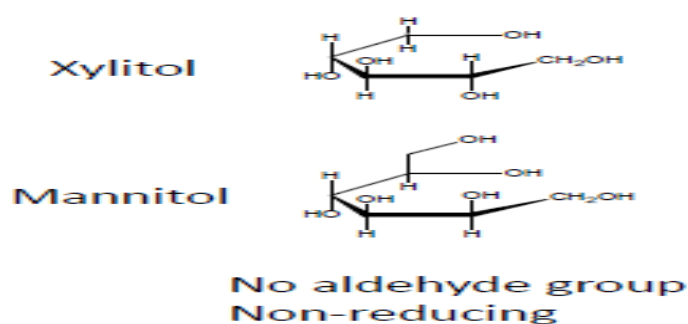
Where: C₁ and C₂ is the concentration of phosphoric acid (dilute and concentrated) respectively and V₁ is the volume of phosphoric acid to be added and V₂ is the volume of solution.

3.2.2.3. Characterizing reducing sugar using FTIR

Reducing sugars are monosaccharides that contain an aldehyde functional group in the open chain form as it was seen from figure 3.1 below and their respective spectra on FTIR explains the band stretching and transmittance to characterize reducing and non-reducing sugar in terms of aldehyde and ketone functional groups.



- a) Presence of aldehyde functional group showing a reduced sugar



- b) Absence of aldehyde functional group showing non-reducing sugar

Fig. 3.1 Sugar showing aldehyde functional group in open chain form

3.2.3. Preparation of yeast cultures for fermentation

For conversion of the sugars resulting from the dilute-acid hydrolysis into bioethanol, yeast strains were used: *Saccharomyces cerevisiae*. The inoculum of yeast biomass to be used in the fermentation trials was prepared using the culture medium Yeast Extract Peptone Dextrose. Liquid Yeast Extract Peptone Dextrose media was prepared for the cultures' growth (Borzani, 2006).

The Yeast Extract Peptone Dextrose liquid culture medium was prepared in 300ml conical flask by dissolving 10 g/l of yeast extract, 20 g/l peptone, Urea 5g/l, $MgSO_4 \cdot 7 H_2 O$ 5g/l and 20 g/l Dextrose in 100mL of water. The yeast cultures were grown in Yeast Extract Peptone Dextrose liquid and incubated at 25 °C for 3 days. The yeasts were maintained in test tubes in the Yeast Extract Peptone Dextrose solid at 3 °C of temperature. All the material used in the preparation of

the culture media and yeast cultures was sterilized by autoclaving at 121 °C for 20 min in order to denature any microorganisms. Developed yeast culture was shown in figure 3.3 below.

3.2.4. Filtration

Before fermentation and titration by using DNS method, the brewer`s spent grains hydrolyzates was vacuum filtered using glass fiber membranes and filter paper for removing the solids, lignin, and degraded cellulose and then the filtrate was then neutralized using a 2M NaOH solution to have a pH range for the microorganism, *Saccharomyces cerevisiae*. All the flasks and the filtrate were sterilized by autoclaving at 121 °C for 20 min before introduced in to fermentation unit in order to avoid any unnecessary microorganisms.

3.2.5. Design of experiment

The experimental design follows a general factorial design, two level factorial; factorial designs are the most efficient for experiments that involve two or more factors. By factorial design we mean that in each complete trial or replication of the experiment all possible combinations of the levels were investigated. The analysis of variance (ANOVA) was used as one of the primary tools for statistical data analysis using a design Expert software 6.0.8 (Montgomery, n.d.).

To determine the optimum conditions for a second stage hydrolysis, a 2^3 full factorial design with three replicates for three factors were generated. The optimum conditions were obtained from the Model graphs. These factors were; temperature (140-150⁰C), dilute phosphoric acid concentration (2-3%), and retention time of (20-30) min. Constant variables are the amount of biomass, liquid volume and mesh size. Total number of experiments was $2^3 \times 3 + 6$ (center point) 30 runs. Addition of center point allows to the two level factorial design provides protection against curvature as well as allow an independent estimate of error to be obtained.

The notation for the yield for the linear regression model having three factors was expressed in equation (3.9) below as:

$$Y = \beta_0 + \beta_1 \cdot x_1 + \beta_2 \cdot x_2 + \beta_3 \cdot x_3 + \beta_{12} \cdot x_1 x_2 + \beta_{13} \cdot x_1 x_3 + \beta_{23} \cdot x_2 x_3 + \beta_{123} \cdot x_1 x_2 x_3 + \epsilon \quad (3.9)$$

Where: β_0 is a mean coefficient and all other β^s are the regression coefficients for respective factors.

3.2.6. Fermentation

The fermentation process was done in a shaker incubator bath at 30-38⁰C with stirring at 175rpm for 72 hour period. The hydrolysate solution was adjusted to a pH of 4.5 to 5.5, which is a favorable range for an enzyme *saccharomyces cerevisae*. The fermentation reaction for the C6 was given in equation (3.10) and (3.11) below as:



The fermentation process was conducted at a five different temperatures (30, 32, 34, 36 and 38)⁰C and five pH (4.5, 5, 5.5, 4.8 and 5.2) ranges in order to obtain an optimum fermentation parameters by holding the substrate to yeast strain ratio, rotational speed, pressure and fermentation time constant at 10v/v, 175rpm 1atm, and 72 hours, respectively.

The thermodynamic and kinetic relationship for the above reaction was carried out as follows:

3.2.6.1. Thermodynamic Analysis:

From the first law of thermodynamics, energy was transformed in to work and heat, which was given by equation (3.12) (Ness, n.d.):

$$\Delta U = Q - W, dU = dQ - dW \quad (3.12)$$

From second law of thermodynamics, change in entropy, measure of the spontaneity of a reaction, was determined from equation (3.13) below as:

$$\Delta S^0_{rxn} = \sum nS^0_{pro} - \sum mS^0_{rec} \quad (3.13)$$

The enthalpy change of activation was determined using equation (3.14) below:

$$\Delta H = \Delta U + PV \quad (3.14)$$

By taking first derivative of both sides, and after rearranging, change in enthalpy was obtained from equation (3.15) below as:

$$dH = TdS + VdP \quad (3.15)$$

Enthalpy change of reaction was given in equation (3.16) and (3.17) below by:

For varying heat capacity and temperature change (3.16) was used

$$dH = \Delta H_{\text{rxn}}^{\circ} + C_p dT \quad (3.16)$$

At standard state equation (3.17) was used.

$$\Delta H_{\text{rxn}} = \sum nH_{\text{pro}} - \sum nH_{\text{rea}} \quad (3.17)$$

The relationship between Gibbs free energy and equilibrium constant for the reaction above was determined from (3.18).

$$\Delta G = \Delta H - T\Delta S = RT \ln K \quad (3.18)$$

Gibbs free energy change of reaction was calculated in equation (3.19) below as:

$$\Delta G_{\text{rxn}} = \Delta G_{\text{pro}} - \Delta G_{\text{rec}} \quad (3.19)$$

3.2.6.2. Kinetic Analysis of total reduced sugar to ethanol

To determine the kinetic parameters from reaction equations (3.10) and (3.11) above; the rate of disappearance of A), reactant from equation (3.11), was given in equation (3.20): for non-elementary reaction.

$$\frac{-dC_A}{dt} = kC_A^n \quad (3.20)$$

By taking the natural logarithm of equation (3.20) in both sides, the reaction rate constant and order were determined from equation (3.21) below.

$$\ln \left(\frac{-dC_A}{dt} \right) = \ln K + n \ln C_A \quad (3.21)$$

From Arrhenius Equation,

$$K = A \exp\left(-\frac{E_a}{RT}\right) \quad (3.22)$$

By taking the natural logarithm of equation (3.22) in both sides, after generating a plot of $\ln K$ versus $\frac{1}{T}$, we can determine A and E_a from equation (3.23) below.

$$\ln K = \ln A - \left(\frac{E_a}{R}\right) \times \frac{1}{T} \quad (3.23)$$

The reaction rate and order of reaction for the above reaction was determined from equation (3.21) by taking natural logarithm: assuming a power law for the reaction and batch reactor design equation holds, the concentration of reduced sugar in fermenter versus time data was generated and the corresponding plot was obtained in order to determine the reaction rate constant and order of the reaction for glucose to ethanol conversion.

3.2.7. Distillation of water-ethanol mixture

A distillation setup usually consists of a distilling flask, a distilling head, a thermometer condenser, and a receiving vessel (Erdelji, 2007). The volume of the distilling flask should be two to three times the volume of liquid to be distilled. If the flask was not full enough, separation was poor because a substantial fraction of the liquid was needed to vaporize for condensation to occur. If the flask is too full, the liquid was easily bumps over into the condenser and distillation will not occur. Steam was supplied from the water bath to the distillation column to raise the temperature of the feed mixture to its boiling point. Distillation was taken place at a temperature of 78⁰C for 4 hours. Due to the formation of an azeotrope the purity of ethanol was around 95% (A. Dávila, et al 2016).

3.2.8. Characterization of ethanol

Ethanol recovered from the distillation unit was characterized by its: density, kinematic viscosity and its functional groups by FTIR as it was elaborated as follows.

3.2.8.1. Determination of Density

Density of ethanol was measured by using a refractive index method by measuring the specific gravity of ethanol after injecting the sample in the density-meter by using a syringe.

$$\rho_{\text{ETOH}} = S.g \times \rho_{\text{water}} \quad (3.24)$$

3.2.8.2. Determination of kinematic viscosity

Vibro-viscometer was used to determine the viscosity of ethanol at room temperature. After maintaining the equilibrium temperature, the vibro viscometer tip was inserted in the sample and the reading was recorded from the controller. This was done in triplicate and the average dynamic viscosity was recorded. The kinematic viscosity was calculated as:

$$\text{Kinematic viscosity} = \frac{\text{dynamic viscosity}}{\text{density}} \quad (3.25)$$

3.2.8.3. Determination of functional groups in ethanol

After recovering the ethanol from the distillation column, the condensed liquid or distillate was analyzed by using prinks Elmer Spectrum 65 Fourier Transform Infrared (FT-IR), the IR spectrum was reported as % absorbance with the wave number region for the analysis was 4000cm^{-1} to 400cm^{-1} in order to identify the functional groups found in the ethanol (Rubio-arroyo et al., 2011). The FTIR analysis was conducted in Arat kilo campus, Faculty of Natural Science, Chemistry Department, AAU.

3.3. Process description, Processes flow diagram and Experimental setup of bioethanol production from BSG

3.3.1. Process description

The production of bioethanol from BSG as it is explained in the process flow diagram in figure 3.4, it involves the transportation of BSG to the storage and BSG was oven dried at a temperature of 105°C for 8 hour in order to reduce the moisture content to around 12%. The dried sample was then mechanically pretreated, grinded, using a hammer mill to reduce the crystallinity of cellulose and increase the surface area for the hydrolysis and screened using a mesh of sieves for appropriate size. After the BSG sample was mechanically pretreated, the sample was favored to a hydrolysis, first and second stage, dilute acid hydrolysis, by adding liquid solution which was made by addition of dilute phosphoric acid and distilled water with the grinded sample to a hydrolysis reactor with stirrer situated to a heating system. After the

completion of hydrolysis stage, the hydrolysate was sent to a filtration unit in order to separate the solid, lignin, from the total reduced sugar solution and the filtrate was sent to a neutralization tank in order to set the appropriate pH for fermentation process, *Saccharomyces cerevisiae*, in which the glucose solution with the inoculum to a fermenter. After the fermentation process, the water-ethanol mixture was separated using a distillation column, the top product, ethanol was collected in the receiving tank for distribution and the bottom product, water, was stored for treatment and further use. The process flow diagram for the production process described above was given in figure 3.4 below.

3.3.2. Processes flow diagram

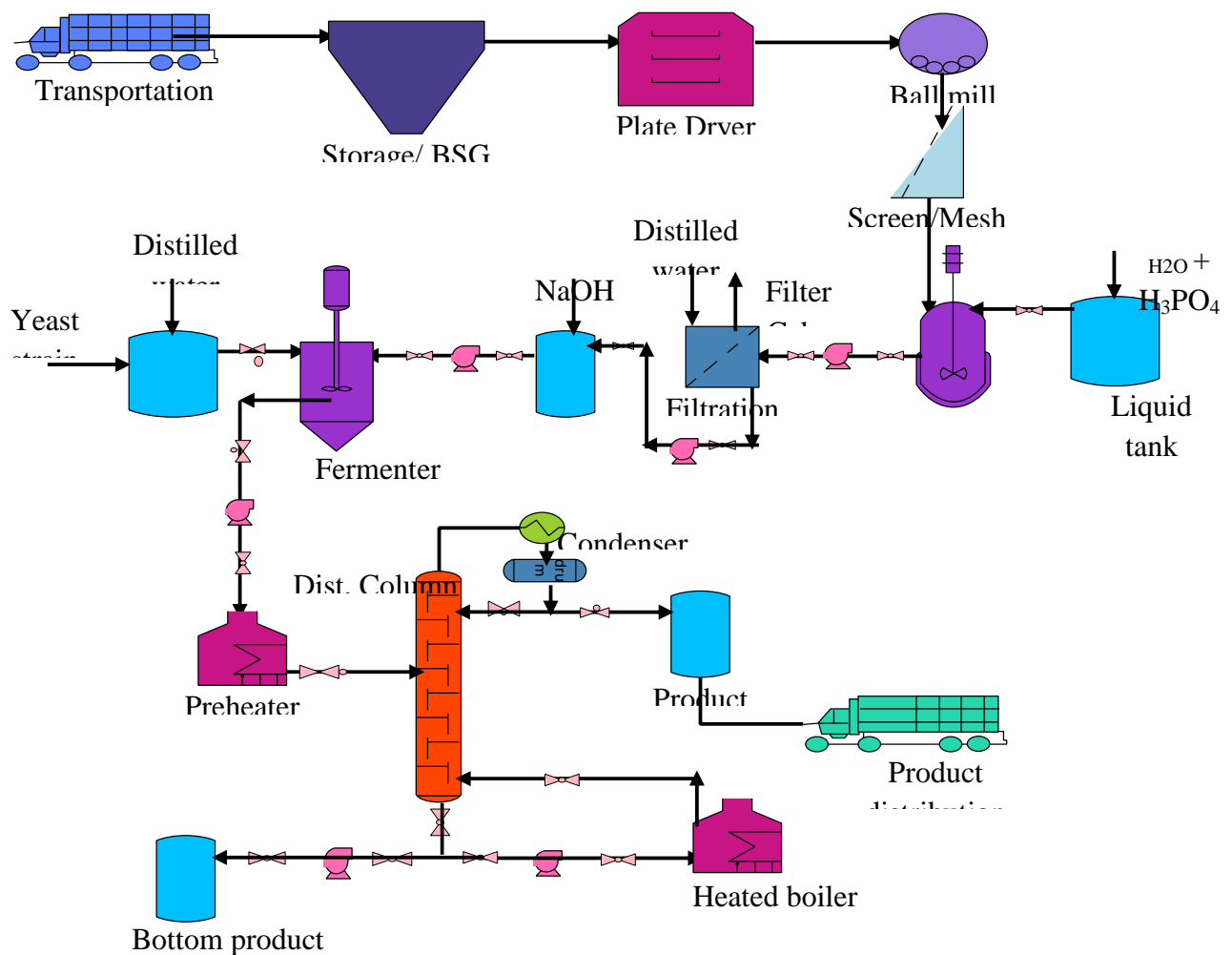


Fig. 3.2 Process flow diagram for production of bioethanol from Brewer's Spent Grain

3.3.3. Experimental Setup

The production and optimization of bioethanol from BSG was conducted in AAiT, school of Chemical and Bio engineering laboratory except the FTIR analysis, which was conducted in arat kilo, Faculty of Science, AAU. The raw material was first collected from Heineken Brewery and its moisture was removed by oven drying at 105⁰C for over 8 hours until it has a constant weight. The dried sample was then milled, after milling the sample was sieved by a mesh of sieves to have an appropriate size for pretreatment, the laboratory setup was shown in figure 3.5 below.

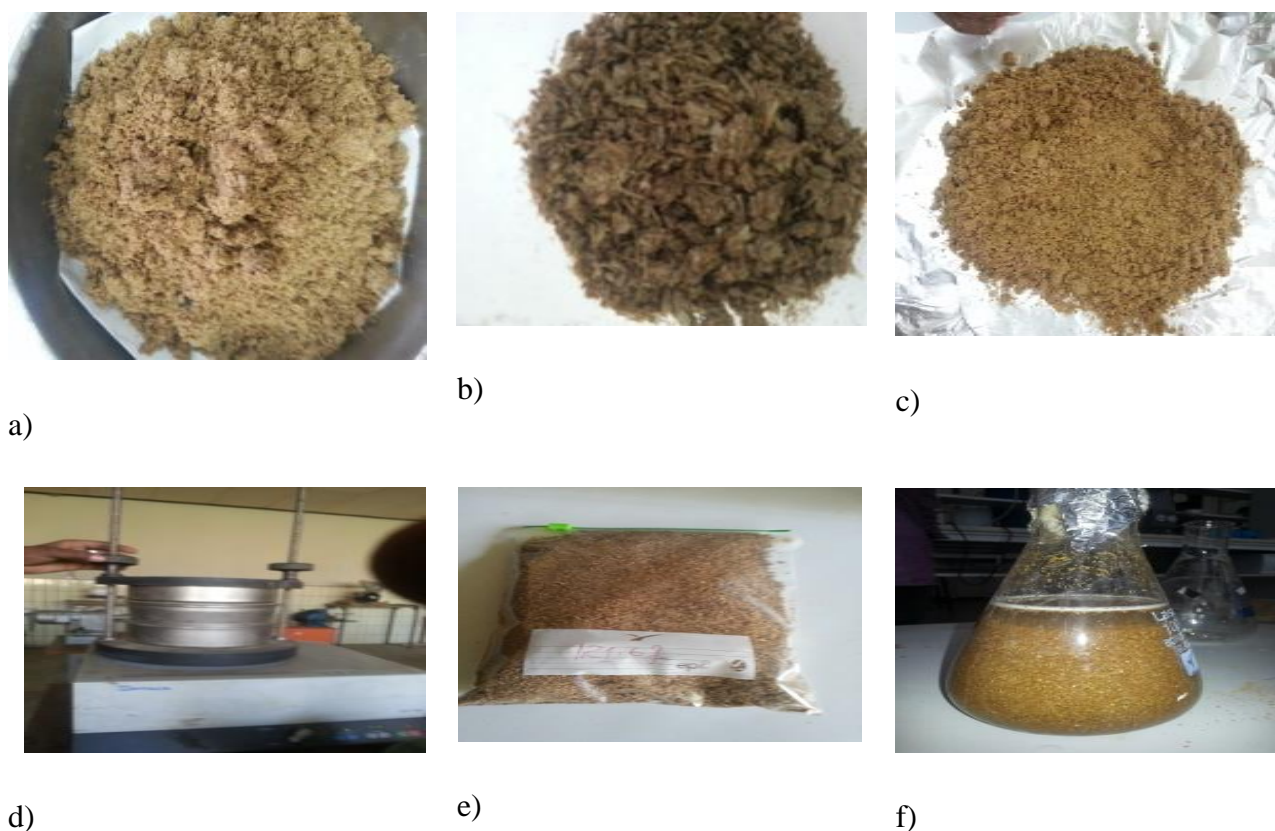


Fig.3.3 Preparation and pretreatment stage of BSG: a) raw BSG, b) dried BSG, c) size reduced BSG, d) rotating mesh of sieves, e) BSG of size range 2mm-1mm, f) sample ready for pretreatment

After pretreatment, the hydrolysis reaction was conducted using an autoclave then the hydrolysate was filtered using a vacuum filter, the filtrate was then titrated in order to determine the total reduced sugar as it was shown in figure 3.6 below.



g)



h)



i)



j)



k)



l)

Fig.3.4 Hydrolysis and Titration stage of BSG hydrolysate: g) sample in autoclave, h) sample ready for filtration, i) vacuum filtration unit, j) sample collected after filtration from hydrolysis run and DNS reagent, k) titrated hydrolysate in water bath before determining absorbance to observe color change and l) sample ready for measuring absorbance

The standard glucose solution was prepared and the standard curve was generated. The produced reduced sugar concentration was measured through measuring the absorbance by using Spectrophotometer at a wave length of 540nm, after calculating the concentration of total

reduced sugar, the concentration was converted in to yield in order to determine an optimum yield and an optimum operating range of the process parameters identified for the hydrolysis process, then total reduced sugar was fermented in order to produce the fermented liquor then the fermented liquor was sent to a distillation unit in to recover ethanol from water-ethanol mixture as the set up was shown in figure 3.7 below.



m)



n)



o)



p)



q)



r)

Fig.3.5 Fermentation and Distillation of water-ethanol mixture stage: m) absorbance measuring using Spectrophotometer, n) autoclave beakers and sample before fermentation, o) samples ready for fermentation, p) shaker incubator, fermenter with sample, q) simple distillation setup, r) final recovered ethanol after distillation of water-ethanol mixture

Chapter Four

4. RESULTS AND DISCUSSIONS

4.1. Proximate analysis of BSG

Moisture content of BSG

Moisture Content was determined by continuously putting the measured sample in oven at 105⁰C for a period of 2 hours until a constant weight was achieved.

Moisture content was determined using equation (3.1):

Crucible weight = 28.842g

Gross weight = 52.367g

Initial Mass of sample = 23.525g at zero time, after the sample was measured the experiment was replicated for three times in order to reduce error due to reproducibility and average result was filled in the table(4.1) using equation (3.1).

$$\text{Moisture content, \%} = \frac{m_1 - m_2}{m_1} \times 100$$

For example, the moisture content for sample one was calculated as follows and similar procedures were done for the rest of samples two and three:

$$\text{Moisture content, \%} = \frac{23.525 - 20.584}{23.525} \times 100 = 12.5\%$$

Table 4.1 Moisture Content of BSG at 105⁰C a triplicate sample, g

| Drying Time (hrs.) | 0 | 2 | 4 | 6 | 8 | Moisture content, % | Average moisture, % |
|--------------------|--------|---------|---------|--------|--------|---------------------|---------------------|
| Mass of Sample1,g | 23.525 | 22.8067 | 21.8704 | 20.586 | 20.584 | 12.50 | |
| Mass of Sample2,g | 23.525 | 22.235 | 21.921 | 20.464 | 20.817 | 11.51 | 12.08% |
| Mass of Sample3,g | 23.525 | 22.724 | 21.025 | 20.662 | 20.650 | 12.22 | |

The moisture content of BSG samples, 1, 2 and 3 in dry basis, which means after it lost the water used during mashing process by exposing it to sun light, were 12.5%, 11.51% and 12.22%, respectively. Thus the average moisture content of the three samples was 12.08%.

Ash content determination

The sample weight was measured and then put in to a furnace at a temperature of 550⁰C for 8 hours until the sample was turned in to ash using equation (3.2). The analysis was conducted in triplicate to reduce reproducibility error.

Total weight = 39.491g

Weight of crucible = 28.848g

Sample weight, $m_1 = 10.643\text{g}$

Weight of ash, $m_2 = 0.227\text{g}$,

$$\text{Ash content, \%} = \frac{m_2}{m_1} \times 100 = \frac{0.227\text{g}}{10.643\text{g}} \times 100 = 2.14\%$$

Cellulose content determination

Sample weight, $m_1 = 2.5\text{gm}$

Mass of filter paper = 0.7gm

Mass of oven dried sample, $m_2 = 1.565\text{gm} - 0.7\text{gm} = 1.032\text{gm}$; using equation (3.3)

$$\text{Cellulose content} = \frac{m_2}{m_1} \times 100 = \frac{0.865\text{g}}{2.5\text{g}} \times 100 = 34.62\%$$

Hemicellulose content determination

Sample weight, $m_1 = 1.5\text{gm}$, Mass of filter paper = 0.5gm

Mass of oven dried sample, $m_2 = 0.7825\text{gm} - 0.5\text{gm} = 0.2825\text{gm}$; using equation (3.4)

$$\text{Hemicellulose Content, \%} = \frac{m_2}{m_1} \times 100 = \frac{0.2826\text{g}}{1.5\text{g}} \times 100 = 18.84\%$$

Lignin content determination

Sample weight, $m_1 = 2.5\text{gm}$

Mass of filter paper = 0.7gm

Mass of oven dried sample, $m_2 = 0.9807\text{gm} - 0.7\text{gm} = 0.2807\text{gm}$; using equation (3.5)

$$\text{Lignin content, \%} = \frac{m_2}{m_1} \times 100 = \frac{0.2807\text{g}}{2.5\text{g}} \times 100 = 11.23\%$$

The proximate analysis of BSG was conducted and the summary in terms of percentage composition was shown in fig. 4.1 below. As it is shown in fig.4.1 the BSG has a moisture content of 12.08% which is in acceptable range for storage of BSG for later processing without exposed to spoilage by microorganisms. BSG has low ash content and extractive content, which makes BSG favorable for processing the raw material for different products since ashes are considered as impurity and BSG has low mineral and extractives content. Major desirability of BSG for bioethanol production lays on its composition of cellulose, 34.62%, and hemicellulose, 18.84% and relatively low composition of lignin, 11.23%. This experimental finding was approximately similar with the literature values studied by (Muthusamy et al , 2014). Relatively, BSG has a high content of cellulose which is a polysaccharide made of glucose unit. It implies BSG rich in cellulose is good for the production of cellulosic ethanol, bioethanol and other

value-added cellulosic products. Low content of lignin is advantageous in converting BSG in to ethanol through hydrolysis.

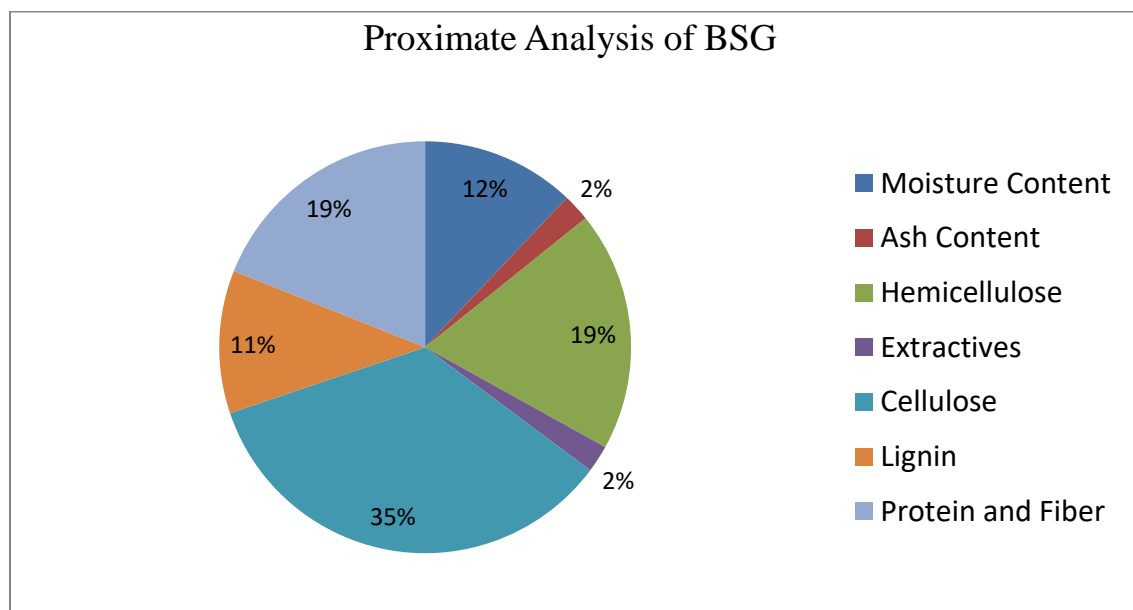


Fig. 4.1 Proximate analysis result of BSG composition

4.2. Hydrolysis

4.2.1. First-Stage hydrolysis

This stage is used to remove furan and hydroxymethyl furfural components, acetic acid and other fermentation inhibitory side products. It was done by using diluted phosphoric acid in order to remove hemicellulose at a temperature of 130⁰C, acid concentration of 1% H₃PO₄ and retention time of 15min. The solution of phosphoric acid and distilled water was made at a beaker of size 500ml to a level of 300ml. The solution was then mixed with a size reduced BSG of amount 30gm to a beaker of size 2000ml and then the mixture was inserted in the autoclave for 15min.

The mixture after hydrolysis was released and rigorously washed with distilled water to a pH of 7, which was neutral and filtered using a vacuum filtration unit. The solid was then sent to an oven dryer to remove moisture and then collected to conduct a second stage hydrolysis to release a maximum reduced sugar, mostly glucose, from cellulose by using distilled water and dilute phosphoric acid.

4.2.2. Titration using a DNS method

DNS Method was used for the analysis of reducing sugar by titration from hydrolysis and kinetic analysis. The total reducing sugar (TRS) was measured using 3, 5-dinitrosalicylic acid (DNS) method. When the alkaline solution of 3, 5-dinitrosalicylic acid reacts with reducing sugar (e.g., glucose), it is converted into 3-amino-5-nitrosalicylic acid with orange red color. Intensity of the color is an index of reducing sugar. This method tests for the presence of free carbonyl group (C=O), so called reducing sugars. This involves the oxidation of the aldehyde functional group present in glucose. Simultaneously, 3,5-dinitrosalicylic acid (DNS) is reduced to 3-amino-5-nitrosalicylic acid under alkaline conditions:

Oxidation

Aldehyde group \longrightarrow Carboxyl group

Reduction

3,5-dinitrosalicylic acid \longrightarrow 3-amino-5-nitrosalicylic acid

The above reaction scheme shows that one mole of sugar was reacted with one mole of 3,5-dinitrosalicylic acid .

Procedure for DNS method

Reducing sugar has the property to reduce many of the reagents. A reducing sugar is one that in a basic solution forms an aldehyde or ketone. The aldehyde group of glucose converts 3,5-dinitrosalicylic acid (DNS) to 3-amino-5-nitrosalicylic acid, which is the reduced form of DNS. Water is used up as a reactant and oxygen gas is released during the reaction. The formation of 3-amino-5-nitrosalicylic acid results in a change in the amount of light absorbed, at a wave length of 540nm.

A series of solution containing varying concentrations of reducing sugars were prepared in test tubes and a known quantity of DNS was added to each tubes. These test tubes were then heated on a water bath for five minutes (5min) and their absorbance was measured using a

spectrophotometer. A graph was then plotted with amount of glucose concentration on x-axis and the observed absorbance at y-axis. The plot thus obtained was called a standard glucose curve.

Standard stock solution of glucose

10% D-glucose was prepared by putting 50ml of distilled water in a 100ml volumetric flask with a stir bar. Placed 50ml of distilled water on stir and hot plate and turned on heat and start stirring. 50ml of distilled water was allowed to get warm, but not necessary to have boiled. Finally, it was added 10 g of glucose (dextrose) and filled the volumetric flask up to 100ml with distilled water.

Preparation of dinitrosalicylic acid (DNS) reagent

2.5g of 3,5-dinitrosalicylic acid, 500mg of crystalline phenol, and 125mg of sodium sulphite were simultaneously dissolved in 250ml of 1%NaOH solution by stirring. 40% of Rochelle salt solution (sodium-potassium tartrate solution) was prepared. The DNS solution was stored in dark glass bottle at temperature below 25⁰C.

Preparation of standard curve

Standard curve was prepared by taking a blank solution ,0 ml of glucose, to 1ml with increment of 0.1ml of the standard stock solution of glucose and the volume was made up to 2ml by adding distilled water. 2ml of DNS reagent was added and the mixture was heated for 5minutes in a boiling water bath. After the development of the color, 1ml of a 40% sodium-potassium tartrate solution was added before the mixture was cooled and mixed thoroughly to stabilize the color. After cooling the tubes, the absorbance was recorded at a wave length of 540nm using spectrophotometer double beam PC and scanning auto cell. Sugar reduces the organic DNS which absorbs maximally at yellow wave length, results in change in absorption spectrum from yellow to red or brown at 540nm; the amount of absorbance is directly related to amount of reducing sugar. A standard curve was plotted and the concentration of unknown sugar samples was determined from the standard curve. The above titration methods with DNS were adapted from ASTM: A223-247 and AOAC B124-345, Miller J.G., 2011).

Table 4.2 Concentration versus Absorbance for the Standard glucose solution

| Run | Standard Glucose solution ,g/ml | Absorbance, % |
|-----|---------------------------------|---------------|
| 1 | 0 | 0 |
| 2 | 0.002 | 0.014 |
| 3 | 0.004 | 0.08 |
| 4 | 0.006 | 0.316 |
| 5 | 0.008 | 0.508 |
| 6 | 0.01 | 0.745 |
| 7 | 0.012 | 0.965 |
| 8 | 0.014 | 1.195 |
| 9 | 0.016 | 1.397 |
| 10 | 0.018 | 1.559 |
| 11 | 0.02 | 1.661 |

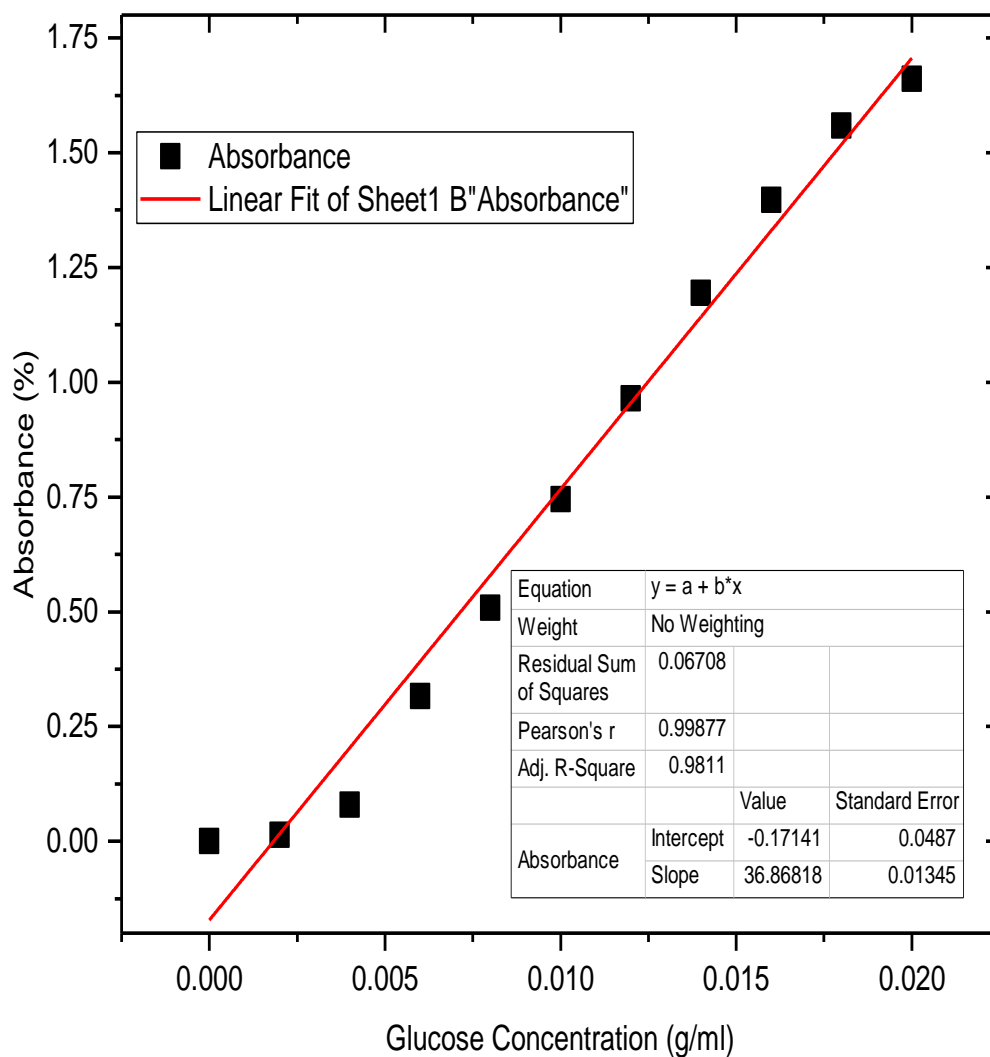


Fig 4.2 Standard curve for standard glucose solution

4.2.3. Second-stage hydrolysis

Sugars are members of the carbohydrate family. Examples include glucose, fructose, galactose, mannose and arabinose. Some sugars can act as a reducing agent and these sugars will contain an aldehyde and ketone functional group. This property can be used as a basis for the analysis of reducing sugar. Figure 3.2 above, which was conducted in Arat kilo campus, Science Faculty, AAU after extracting total reduced sugar from BSG, shows us the functional group of aldehyde and ketone with hydroxyl groups found in the total reduced sugar which tells that the produced sugar is reduced with the aldehyde and ketone functional groups shown in the band stretch from FTIR result.

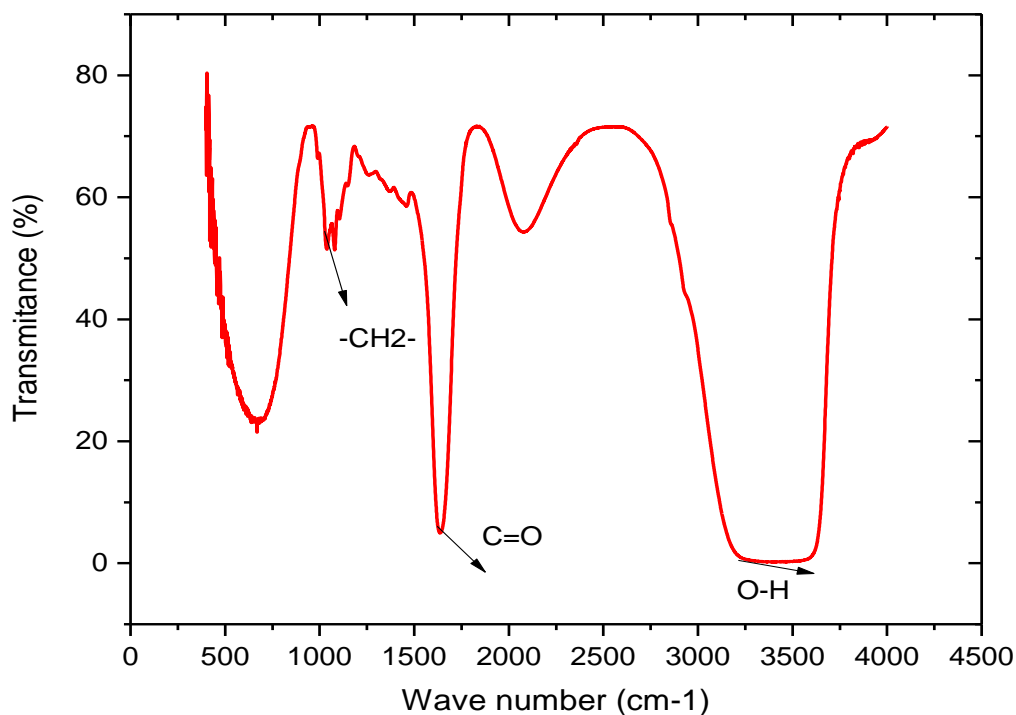


Fig. 4.3 FTIR result of hydrolysate for reducing sugar

Second stage hydrolysis was conducted in order to produce glucose or total reduced sugar from BSG and selected process parameters and their operating ranges were temperature, retention time, and acid concentration; 140-150⁰C, 20-30min and 2-3%, respectively and the concentration and corresponding yield of total reduced sugar was given in table 4.3 below.

The concentration of unknown sample from the standard curve and the absorbance values was determined by using equation (3.6). Now substituting numerical values, the concentration of unknown sample was determined. For example, Run 1, Abs = 0.525, b= -0.1714 and m=36.86818,

$$C = \frac{\text{Abs}-b}{m} ; C = \frac{0.525-(-0.1714)}{36.86818} = 0.01889\text{g/ml}$$

A similar procedure was followed for the rest of runs; and column for concentration was filled in the table 4.3 below under concentration column.

The yield of total reduced sugar was determined from equation (3.7), For example, Run 1,

$$Y, \% = \frac{C \times V}{M} \times 100; Y, \% = \frac{0.01889\text{g/ml} \times 300\text{ml}}{30\text{g}} \times 100 = 18.89\%$$

Similar procedures were followed in order to calculate the yield for the rest of Runs, and corresponding table 4.3 below under yield column was filled.

Table 4.3 Experimental analysis of total reduced sugar concentration and yield from absorbance.

| Std | Run | Blocks | A,Temp. (⁰ C) | B,Time (min) | C,Acid Conc.(%) | Absorbance (%) | Concentration (g/ml) | Yield (%) |
|-----|-----|---------|------------------------------|-----------------|--------------------|-------------------|-------------------------|--------------|
| 1 | 12 | Block 1 | 140 | 20 | 2 | 0.525 | 0.01889 | 18.89 |
| 2 | 23 | Block 1 | 140 | 20 | 2 | 0.547 | 0.01948 | 19.48 |
| 3 | 24 | Block 1 | 140 | 20 | 2 | 0.544 | 0.0194 | 19.4 |
| 4 | 6 | Block 1 | 150 | 20 | 2 | 1.154 | 0.0359 | 35.9 |
| 5 | 4 | Block 1 | 150 | 20 | 2 | 1.121 | 0.0350 | 35 |
| 6 | 27 | Block 1 | 150 | 20 | 2 | 1.133 | 0.03538 | 35.38 |
| 7 | 29 | Block 1 | 140 | 30 | 2 | 0.721 | 0.0242 | 24.2 |
| 8 | 8 | Block 1 | 140 | 30 | 2 | 0.743 | 0.0248 | 24.8 |
| 9 | 22 | Block 1 | 140 | 30 | 2 | 0.751 | 0.0250 | 25 |
| 10 | 11 | Block 1 | 150 | 30 | 2 | 1.623 | 0.04867 | 48.67 |
| 11 | 21 | Block 1 | 150 | 30 | 2 | 1.633 | 0.0489 | 48.9 |
| 12 | 7 | Block 1 | 150 | 30 | 2 | 1.641 | 0.0491 | 49.1 |
| 13 | 28 | Block 1 | 140 | 20 | 3 | 0.897 | 0.0289 | 28.9 |
| 14 | 10 | Block 1 | 140 | 20 | 3 | 0.886 | 0.0286 | 28.6 |
| 15 | 19 | Block 1 | 140 | 20 | 3 | 0.891 | 0.0288 | 28.8 |
| 16 | 17 | Block 1 | 150 | 20 | 3 | 1.921 | 0.0568 | 56.8 |
| 17 | 5 | Block 1 | 150 | 20 | 3 | 1.932 | 0.05705 | 57.05 |
| 18 | 3 | Block 1 | 150 | 20 | 3 | 1.962 | 0.0578 | 57.8 |
| 19 | 9 | Block 1 | 140 | 30 | 3 | 0.931 | 0.0299 | 29.9 |
| 20 | 14 | Block 1 | 140 | 30 | 3 | 0.944 | 0.03025 | 30.25 |
| 21 | 30 | Block 1 | 140 | 30 | 3 | 0.925 | 0.0297 | 29.7 |
| 22 | 13 | Block 1 | 150 | 30 | 3 | 1.841 | 0.05458 | 54.58 |
| 23 | 25 | Block 1 | 150 | 30 | 3 | 1.832 | 0.0543 | 54.3 |
| 24 | 1 | Block 1 | 150 | 30 | 3 | 1.824 | 0.0541 | 54.1 |

| Std | Run | Blocks | A,Temp. (⁰ C) | B,Time (min) | C,Acid Conc. (%) | Absorbance (%) | Concentration (g/ml) | Yield (%) |
|-----|-----|---------|------------------------------|-----------------|---------------------|-------------------|-------------------------|--------------|
| 25 | 26 | Block 1 | 145 | 25 | 2.5 | 1.652 | 0.0494 | 49.4 |
| 26 | 20 | Block 1 | 145 | 25 | 2.5 | 1.661 | 0.0497 | 49.7 |
| 27 | 15 | Block 1 | 145 | 25 | 2.5 | 1.592 | 0.0478 | 47.8 |
| 28 | 18 | Block 1 | 145 | 25 | 2.5 | 1.635 | 0.0489 | 48.9 |
| 29 | 2 | Block 1 | 145 | 25 | 2.5 | 1.622 | 0.0486 | 48.6 |
| 30 | 16 | Block 1 | 145 | 25 | 2.5 | 1.644 | 0.0492 | 49.2 |

The statistical analysis conducted during a second-stage hydrolysis was a two level three factor full factorial with three replications and six center point design with a total number of runs, 30, as it was explained in chapter three above and the yield and concentration of total reduced sugar calculate from the above equations was filled in table 4.3 above.

The response variable, total reduced sugar yield was filled in the Design Expert 6.0.8 and ANOVA result was analyzed. The effect of each factor on the yield was given in fig. 4.4 below.

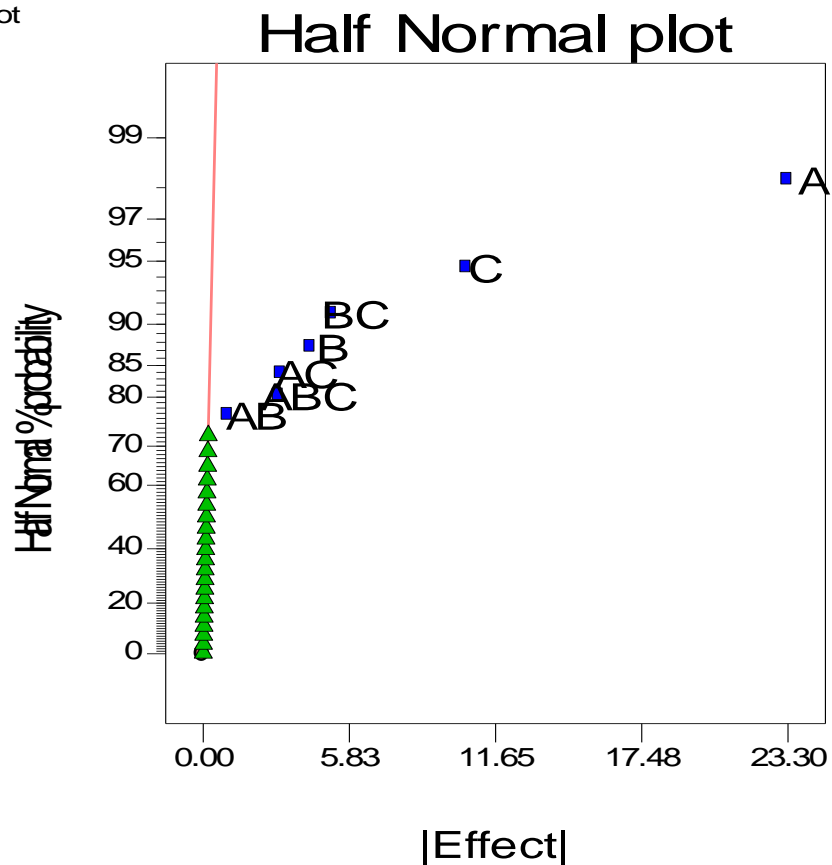
DESIGN-EXPERT Plot
YieldA: Temperature
B: Time
C: Acid Concentration

Fig. 4.4 Half Normal probability plot of design parameter effect on the yield

From figure 4.4 it was indicated that the effect each factor had on the yield of total reduced sugar was shown. As it is seen from the figure, factor A, temperature, has high studentized effect of 23.30 on the yield which accounts 65.68% percentage contribution, factor B, retention time, has low effect compared to factor A and factor C, which has studentized effect of 4.29 with a percentage contribution of 2.23% and factor C, phosphoric acid concentration, has more effect than factor B, retention time, but less effect than temperature on the yield of total reduced sugar which has a studentized effect of 10.5 and percentage contribution of 13.34%. The other important thing noted from the above figure is that their interaction effect of factors. The interaction between temperature and retention time is very low with studentized effect of 1.00 and percentage contribution of 0.12. The interaction between temperature and phosphoric acid concentration is also low. But the interaction between temperature and acid concentration and

retention time and acid concentration is significant. The ANOVA result was elaborated for the second stage hydrolysis in table 4.4 below.

Response: Yield of total reduced sugar

Table 4.4 ANOVA for Selected Factorial Model Analysis of variance table

| Source | Sum of Squares | DF | Mean Square | F Value | Prob < F | Remarks |
|------------|----------------|----|-------------|----------|----------|---------|
| Model | 4309.26 | 7 | 615.61 | 3088.83 | < 0.0001 | a* |
| A | 3258.74 | 1 | 3258.74 | 16350.79 | < 0.0001 | a* |
| B | 110.51 | 1 | 110.51 | 554.49 | 0.021 | b* |
| C | 662.13 | 1 | 662.13 | 3322.25 | 0.0001 | a* |
| AB | 5.94 | 1 | 5.94 | 29.80 | 0.031 | b* |
| AC | 57.97 | 1 | 57.97 | 290.87 | <0.0001 | a* |
| BC | 158.83 | 1 | 158.83 | 796.91 | 0.041 | b* |
| ABC | 55.15 | 1 | 55.15 | 276.70 | 0.0231 | b* |
| Curvature | 648.21 | 1 | 648.21 | 3252.41 | < 0.0001 | a* |
| Pure Error | 4.19 | 21 | 0.20 | | | |
| Cor Total | 4961.66 | 2 | | | | |

Key: a* and b*, highly significant and significant model parameters, respectively.

Where: A, B, and C stands for temperature, retention time and acid conc.repectively.

The Model F-value of 3088.83 implies the model is significant. There is only a 0.01% chance that a "Model F-Value" this large could occur due to noise. Values of "Prob > F" less than 0.0500 indicate model terms are significant. In this case A, B, C, AB, AC, BC, ABC are significant model terms.

Which implies that Temperature, Retention Time, Acid Concentration, interaction between Temperature and Retention Time, interaction between Temperature and Acid Concentration, interaction between Retention Time and Acid Concentration, interaction between Temperature, Retention Time and Acid Concentration are significant parameters for yield of total reduced sugar produced from BSG. Values greater than 0.1000 indicate the model terms are not significant. If there are many insignificant model terms (not counting those required to support hierarchy), model reduction may improve your model. In this case, no model reduction is suggested.

The "Curvature F-value" of 3252.41 implies there is significant curvature (as measured by difference between the average of the center points and the average of the factorial points) in the design space. There is only a 0.01% chance that a "Curvature F-value" this large could occur due to noise.

| | | | |
|-----------|-------|----------------|---------|
| Std. Dev. | 0.45 | R-Squared | 0.9990 |
| Mean | 39.64 | Adj R-Squared | 0.9980 |
| C.V. | 1.13 | Pred R-Squared | 0.9985 |
| PRESS | 7.58 | Adeq Precision | 155.242 |

PRESS is an acronym for Prediction Error Sum of Squares and it is defined as the sum of squares the differences between each observations y_i and the corresponding predicted value based on the model fit to the remaining $n-1$, say mean of y_i , used to evaluate competing regression models. Models that have small values of PRESS are preferred. So this implies that PRESS value of 7.58 is in an acceptable value for this model. C.V. is the coefficient of variation which measures the unexplained or residual variability in the data as a percentage of the mean of response variable. The "Pred R-Squared" of 0.9985 is in reasonable agreement with the "Adj R-Squared" of 0.998. "Adeq Precision" measures the signal to noise ratio. A ratio greater than 4 is desirable. Your ratio of 155.242 indicates an adequate signal. This model can be used to navigate the design space.

Table 4.5 shows that the regression coefficient of the factors for the determination of the yield in terms of both actual factors and coded factors with 95% confidence interval, which tells us that the range within which the true treatment effects is likely to lie. VIF is an abbreviation for

variance inflation factor, a value of 1.0 implies that the variance is constant with low error to designate the yield.

Table 4.5 The regression Coefficient estimate of the process variable and corresponding 95% CI Low and High.

| Factor | Coefficient | DF | Standard | 95% CI | | VIF |
|----------------------|-------------|----|----------|--------|-------|-----|
| | Estimate | | Error | Low | High | |
| Intercept | 37.31 | 1 | 0.0611 | 37.12 | 37.50 | 1.0 |
| A-Temperature | 11.65 | 1 | 0.0251 | 11.46 | 11.84 | 1.0 |
| B-Time | 2.15 | 1 | 0.0231 | 1.96 | 2.34 | 1.0 |
| C-Acid Concentration | 5.25 | 1 | 0.0521 | 5.06 | 5.44 | 1.0 |
| AB | 0.50 | 1 | 0.0131 | 0.31 | 0.69 | 1.0 |
| AC | 1.55 | 1 | 0.0451 | 1.36 | 1.74 | 1.0 |
| BC | -2.57 | 1 | 0.0591 | -2.76 | -2.38 | 1.0 |
| ABC | -1.52 | 1 | 0.0161 | -1.71 | -1.33 | 1.0 |
| Center Point | 11.62 | 1 | 0.0320 | 11.20 | 12.04 | 1.0 |

4.2.3.1. Development of regression Model Equation

The model equation that correlates the yield of total reduced sugar to the hydrolysis reaction parameters in terms of coded factors and actual factors were given below in equation (4.1) and (4.2), respectively.

Final Equation in Terms of Coded Factors:

$$\text{Yield} = +37.31 + 11.65 * A + 2.15 * B + 5.25 * C + 0.50 * A * B + 1.55 * A * C - 2.57 * B * C - 1.52 * A * B * C \quad (4.1)$$

Where: A is Temperature, B is Retention Time, C is acid concentration, A * B is Temperature * Time, A * C is Temperature * Acid Concentration, B * C is Time * Acid Concentration, A * B * C is Temperature * Time * Acid Concentration. The effect results due to B * C and A * B * C

decreases as the yield increases and vice versa, while A, B, C, A * B and A * C effect increases with the yield but relatively the effect of A * B, and relatively the effect B has little effect on the yield. The A and C has the dominant effect on the yield of total reduced sugar as shown in equation (4.1) above.

Final Equation in Terms of Actual Factors:

$$\begin{aligned} \text{Yield} = & +994.55667 - 7.30033 * \text{Temperature} - 43.84300 * \text{Time} - 493.50333 * \text{Acid} \\ & \text{Concentration} + 0.323 * \text{Temperature} * \text{Time} + 3.65333 * \text{Temperature} * \text{Acid Concentration} \\ & + 16.55467 * \text{Time} * \text{Acid Concentration} \\ & - 0.12127 * \text{Temperature} * \text{Time} * \text{Acid Concentration} \end{aligned} \quad (4.2)$$

4.2.3.2. Model Adequacy Checking

The importance of model adequacy checking is an alert for potential problems with normality assumption, unequal error variance by treatment or block-treatment interaction. The model was tested for adequacy by analysis of variance. The regression model was found to be highly significant with the correlation coefficient of determination of R-Squared, adjusted R-Squared and predicted R-Squared of 0.999, 0.998 and 0.9985, respectively.

The quality of the Model developed could be evaluated from their coefficients of determination. The value of R-Squared for the developed correlation is 0.999. It implies that 99.9% of total variation in the percentage of yield of total reduced sugar is attributed to the experimental variables studied. As it is seen from graph 4.6 below, normal probability plot versus the residuals results shows us that the regression model equation provided a very accurate description of experimental data, in which all the data points are very close to the line of perfect fit.

The adequacy of the Model was further checked with analysis of variance (ANOVA) as shown in table 4.4, based on 95% confidence interval, F-value is a test for comparing model variance with residual (error) variance. If the variances are close to the same, the ratio will be close to unity and it is likely that any factors have a insignificant effect on the response with the P-value greater than 0.05. It is calculated by model mean square divided by residual mean square. Here

the model F-value of 3088.83 implies that the model is significant. There is only 0.01% chance that a "Model F Vvalue" this large could occur due to personal error or noise.

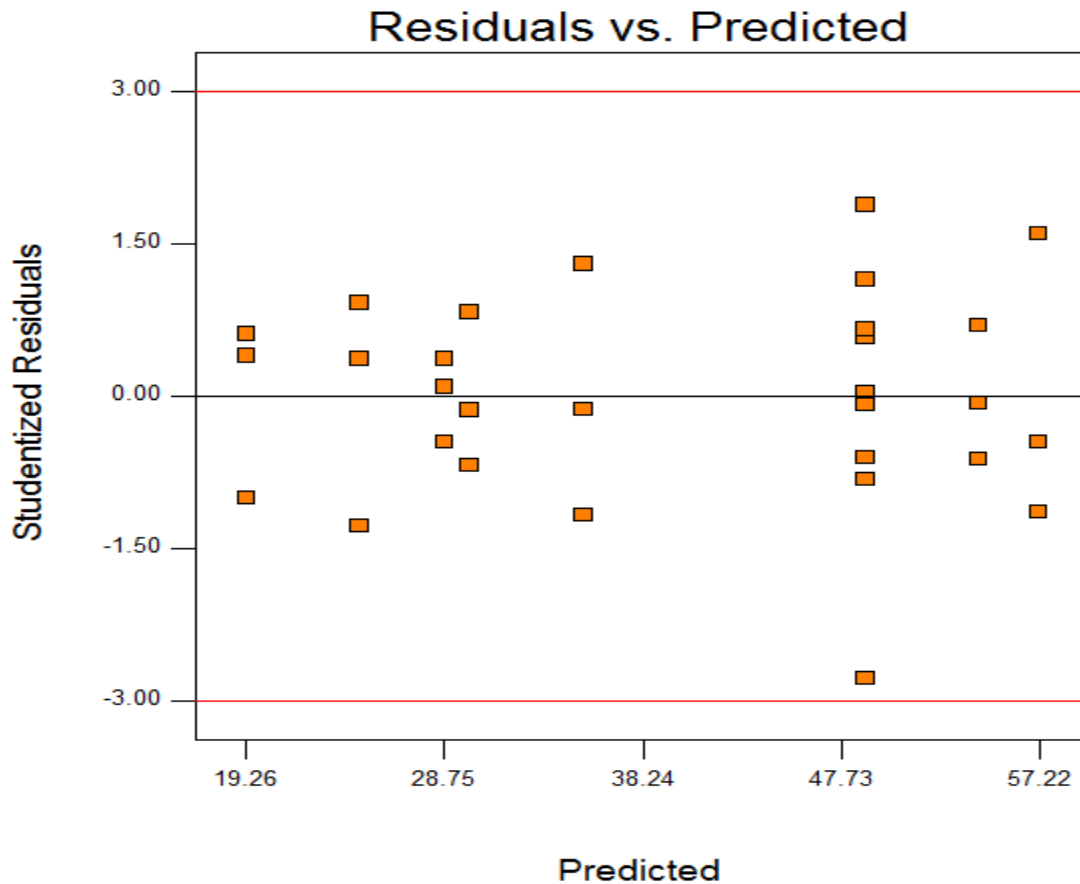


Fig. 4.5 Studentized Residuals versus Predicted Values of yield of total reduced sugar.

From figure 4.5 it was shown that the studentised residuals versus the predicted yield was structureless and scattered, implying that the experiment was conducted in the randomized design which build in protection against trends in response biasing the results, so that the conducted experimental model was correct. Design Expert 6.0.8 provides upper and lower red lines that are similar to 95% confidence interval limits on a run chart. In this case none of the points stands out. A plot of the studentized residuals versus rising predicted values from experiment tests assumption of constant variance. The plot also shows us the random scatter which justifies us no need for an alteration to minimize personal error.

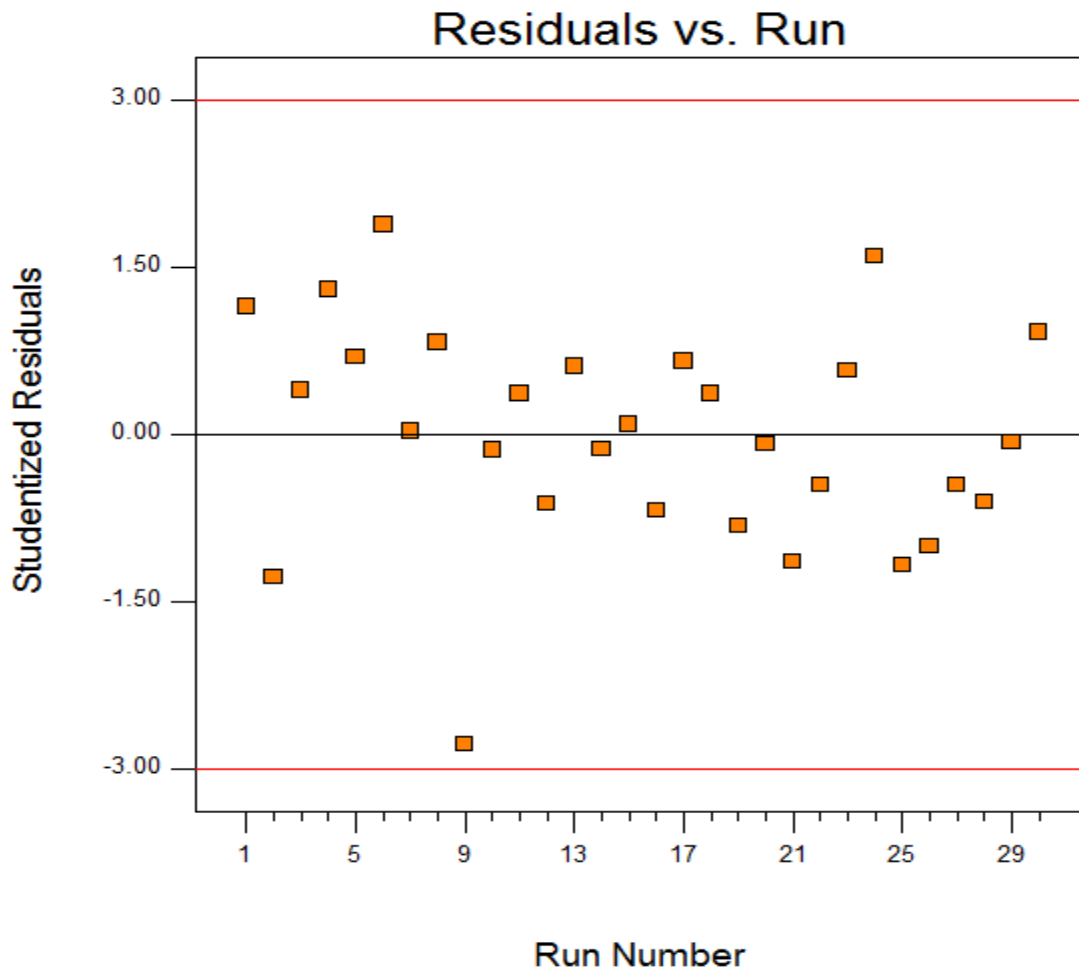


Fig. 4.6 Studentized Residuals versus Run numbers for yield of total reduced sugar

As it is seen from the figure 4.6 the studentized residuals versus the run numbers were not have a uniform structure which tells us that the experiment was conducted at a randomized design with random runs. So that the experiment conducted was not biased in terms of predicted yield and run number.

Figure 4.7 shows the normal%probability versus studentized residuals. As it is seen from the graph, the experimental data points in the plot shows that the variance is almost the same and approximately fits with the straight line, approving the linear equation for the yield by ignoring non significant terms interms of model coefficient esitmate from the model equation. The tendency of the normal probability plot to bend down slightly on the left side implies that the left tail of the error distribution is somewhat thinner than would be anticipated in normal distribution;

that is the negative residuals are not quite as large as expected. An error distribution that has considerably thicker or thinner tails than the normal is of more concern than a skewed distribution, because the F test is only slightly affected and we may say that the analysis of variance is robust to the normality assumption. This validates the model equation which fits the normal probability assumption.

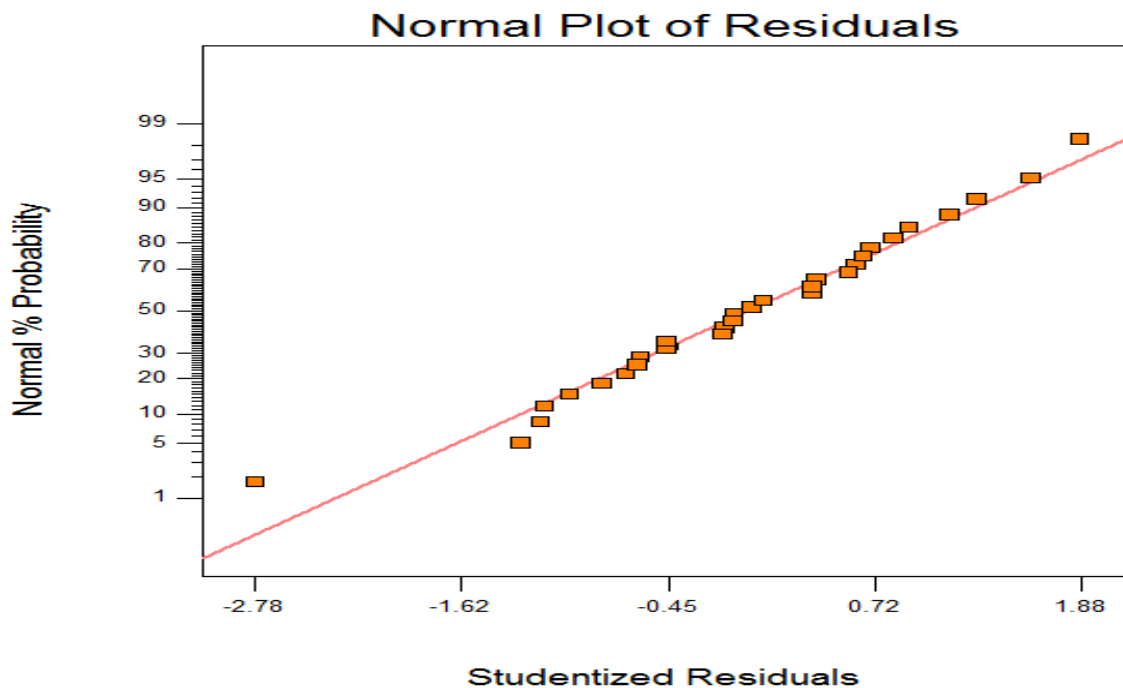


Fig. 4.7 Normal probability plot of residuals versus studentized residuals

4.2.4. Individual effect of process parameters on the yield of total reduced sugar

Figure 4.8 shows us the effect of temperature on the yield of total reduced sugar. As it is shown in figure 4.8 below, the yield of total reduced sugar from BSG strongly depends on the temperature. As temperature increases the yield also increases from 140°C to 145°C the yield of total reduced sugar changes from 20.35% to 26.57% until it reaches to its maximum point at 150°C. This implies that hydrolysis of cellulose resulted in producing higher reduced sugar yield at moderately higher temperature due to the recalcitrant nature of cellulose at lower temperature due to the glucosidic hydrogen bond. Which implies that cellulose decomposition into glucose directly dependent on the temperature.

According to (A. K. Chandel et al., 2012), the reaction temperature dominatly affects the the yield of total reduced sugar which is extracted from lignocellulosic biomass, specifically brewer`s spent grain.

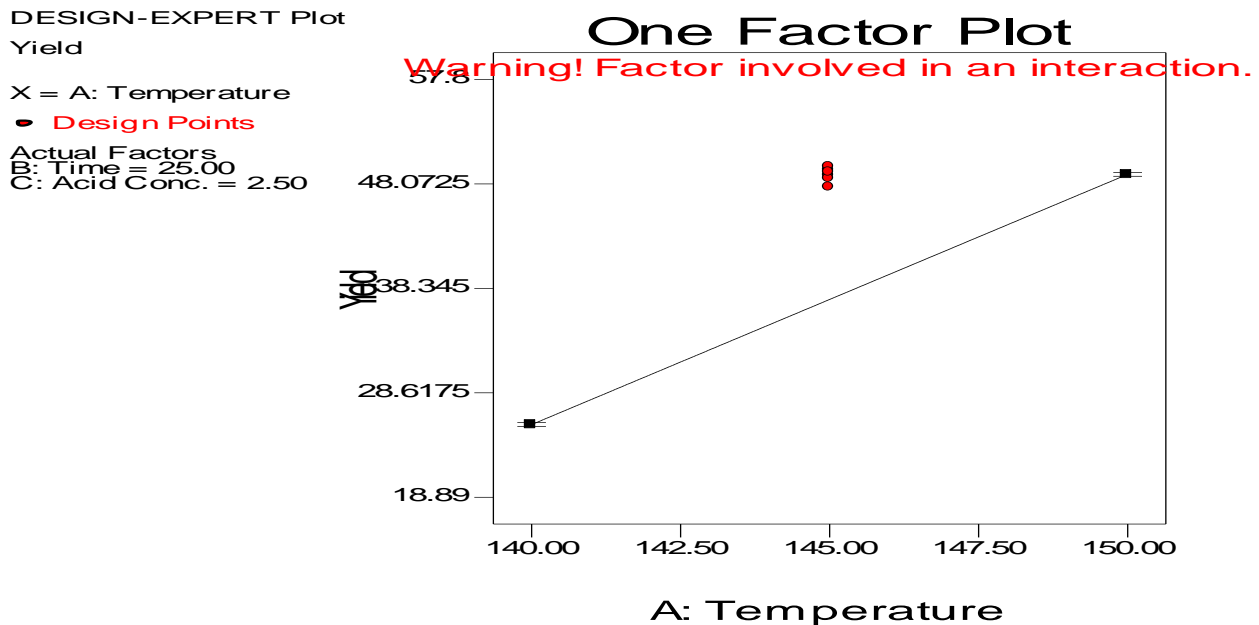


Fig. 4.8 Effect of temperature on the yield of total reduced sugar

Figure 4.9 shows that the effect of retention time on the yield of total reduced sugar. The retention time has little effect as it was shown in the figure 4.9. As retention time increases from 20 min to 25 min the yield of total reduced sugar 35.52% to 38.345% and remains there when time increases to 30min with slight increase but with no significant change this is due to as time increases cellulose will degrade to furan and acetic acid not to reduced sugar. But at lower retention time and high temperature, the total reduced yield is high, implying that the retention time is not a major factor during hydrolysis of cellulose to reduced sugar.

(Mata et al., 2015) conducted experiments on producing simple sugar from sugarcane bagasse and paper waste, cellulosic biomass, from their study they found that retention time has a little effect compared to temperature and acid concentration on the hydrolysis in producing reduced sugar due to the the conversion of cellulosic material to undesired side products like furan and acetic acid as the hydrolysis time was longer.

DESIGN-EXPERT Plot

Yield

X = B: Time

● Design Points

Actual Factors

A: Temperature = 145.00

C: Acid Conc. = 2.50

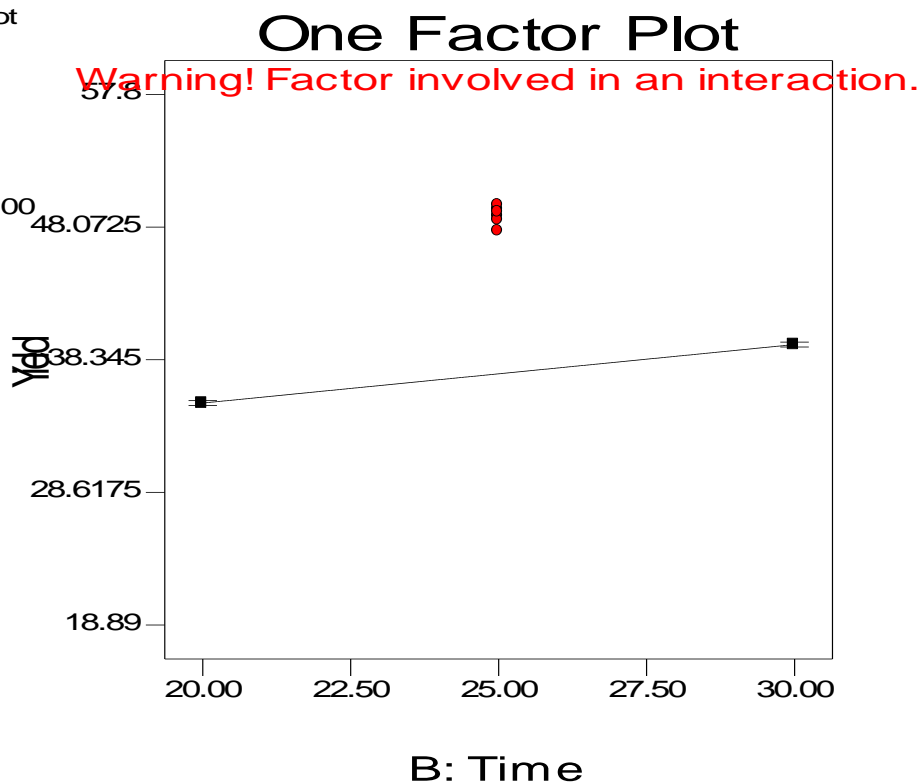


Fig. 4.9 Effect of retention time on the yield of total reduced sugar.

Figure 4.10 shows us the effect of phosphoric acid concentration on the yield of total reduced sugar. As it is shown in the figure 4.10, phosphoric acid concentration has an effect in cleaving the glycosidic bonds of cellulose and forming simple sugar. As the concentration of phosphoric acid increases from 2% to 2.5% the yield of total reduced sugar increases from 32.54% to 38.345% and with increasing yield as acid concentration increases; as acidic hydrolysis is strong in cleaving the glycosidic bond found in the cellulose forming reduced sugar than other products, furan and acetic acid or phenolics.

According to (A. K. Chandel et al., 2012), dilute acid concentration increase the yield of total reduced sugar from lignocellulosic biomass but it requires a moderate temperature (130-180)⁰C, which consumes energy but produces low side products relative to concentrated acid and enzymatic hydrolysis and environmentally less dangerous and it does not corrode the reactors and also the hydrolysis reaction takes lower time on average 25min.

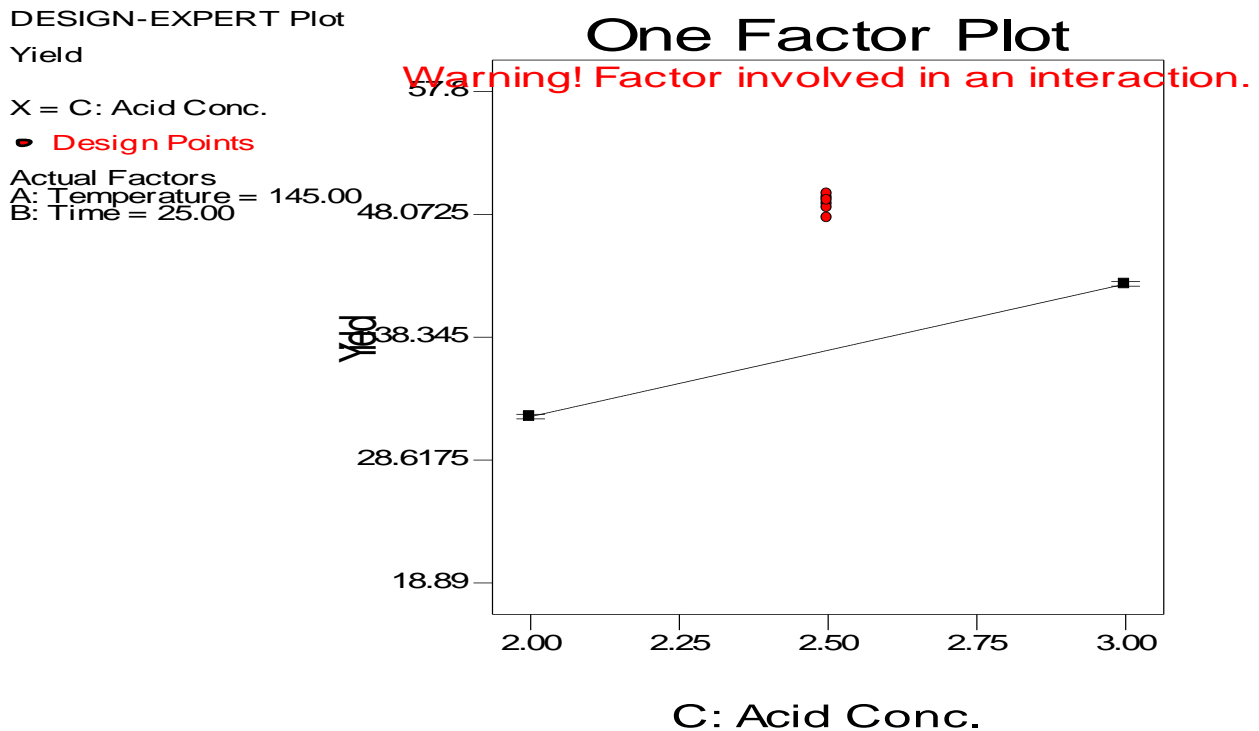


Fig. 4.10 Effect of phosphoric acid concentration on the yield of total reduced sugar.

4.2.5. The interaction effect of process parameters on the yield of total reduced sugar

Figure 4.11 shows us the interaction effect of temperature and retention time on the yield of total reduced sugar at a fixed acid concentration. As it was shown in the figure 4.11, as the interaction effect of temperature and retention time increases the yield of total reduced sugar also increases until it reaches its maximum design value. Unlike the individual effect, when temperature and retention time interact jointly during hydrolysis stage, the yield of total reduced sugar increases as the interaction of temperature and retention time increases, at high temperature and at lower retention time the reduced sugar yield is high. The yield does not vary at high retention time and lower retention time. Due to this operating at lower retention time and higher temperature with center point acid concentration is optimum.

DESIGN-EXPERT Plot

Yield

X = A: Temperature

Y = B: Time

● Design Points

■ B- 20.000

▲ B+ 30.000

Actual Factor

C: Acid Conc. = 2.50

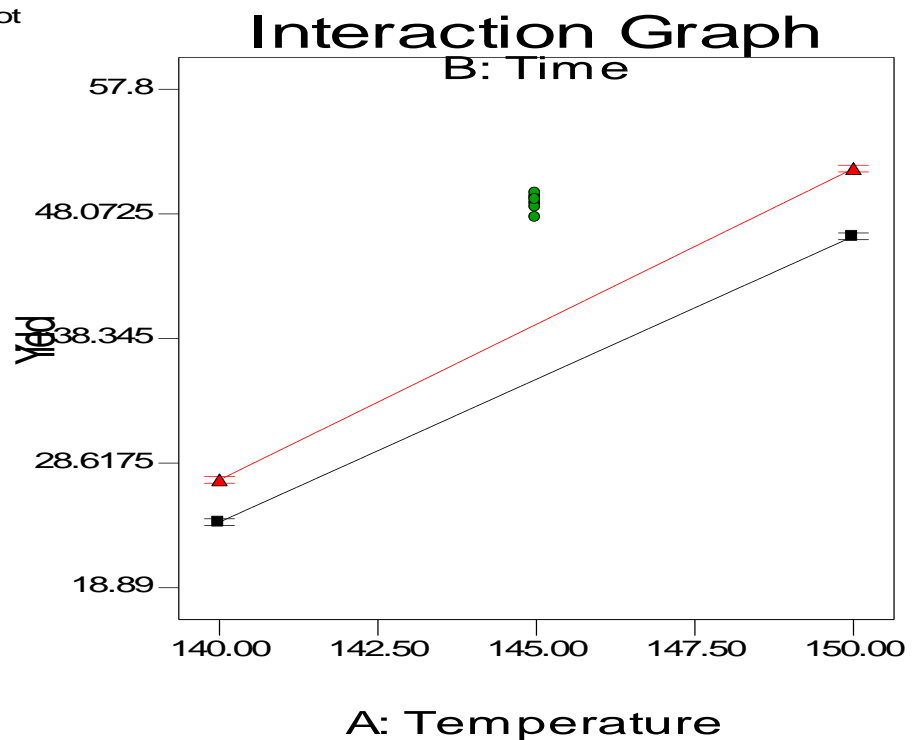


Fig. 4.11 Interaction of temperature and retention time on yield of total reduced sugar

Figure 4.12 shows us the interaction effect of temperature and phosphoric acid concentration on the yield of total reduced sugar at fixed retention time. As it was shown in the figure 4.12, the temperature and phosphoric acid concentration has a high effect on the yield of total reduced sugar. As the temperature and phosphoric acid jointly increases, the yield of total reduced sugar also linearly increases until it reaches to the maximum value of temperature and phosphoric acid concentration 150°C and 3%, respectively. Unlike individual effects, the interaction effect of temperature and phosphoric acid concentration on the yield of total reduced sugar has a linear effect, as the concentration of acid and temperature increases so does the yield of reduced sugar this is because as acids at higher temperature degrades the bonds of cellulose and converts cellulose to reduced sugar at center point retention time.

DESIGN-EXPERT Plot

Yield

X = A: Temperature

Y = C: Acid Conc.

● Design Points

■ C- 2.000

▲ C+ 3.000

Actual Factor

B: Time = 25.00

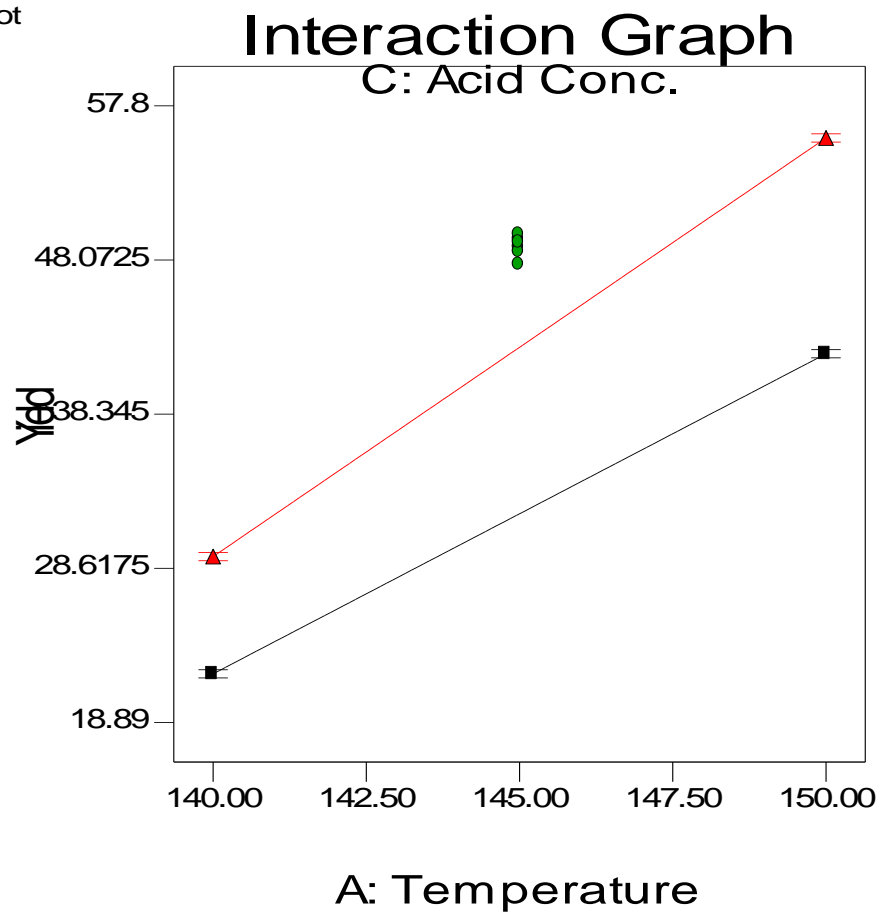


Fig.4.12 Interaction of temperature and acid concentration on the yield of total reduced sugar

Figure 4.13 shows us that the interaction effect of phosphoric acid concentration and retention time on the yield of total reduced sugar at fixed temperature. As it was shown in the figure 4.13 the interaction of phosphoric acid and retention time has effect on the yield of total reduced sugar at the lower level of factor combination but as the joint effect of concentration of acid and retention time increases the yield of total reduced sugar remains unchanged particularly for increase in acid concentration, but small change in yield of total reduced sugar was seen for increase in retention time. This is due to the fact that, the yield of total reduced sugar strongly depends on the temperature and acid concentration. This implies that operating at higher concentration of acid and lower retention time produces relatively high yield of reduced sugar but operating at lower

acid concentration and increasing retention time linearly produces a high yield of reduced sugar at center point temperature.

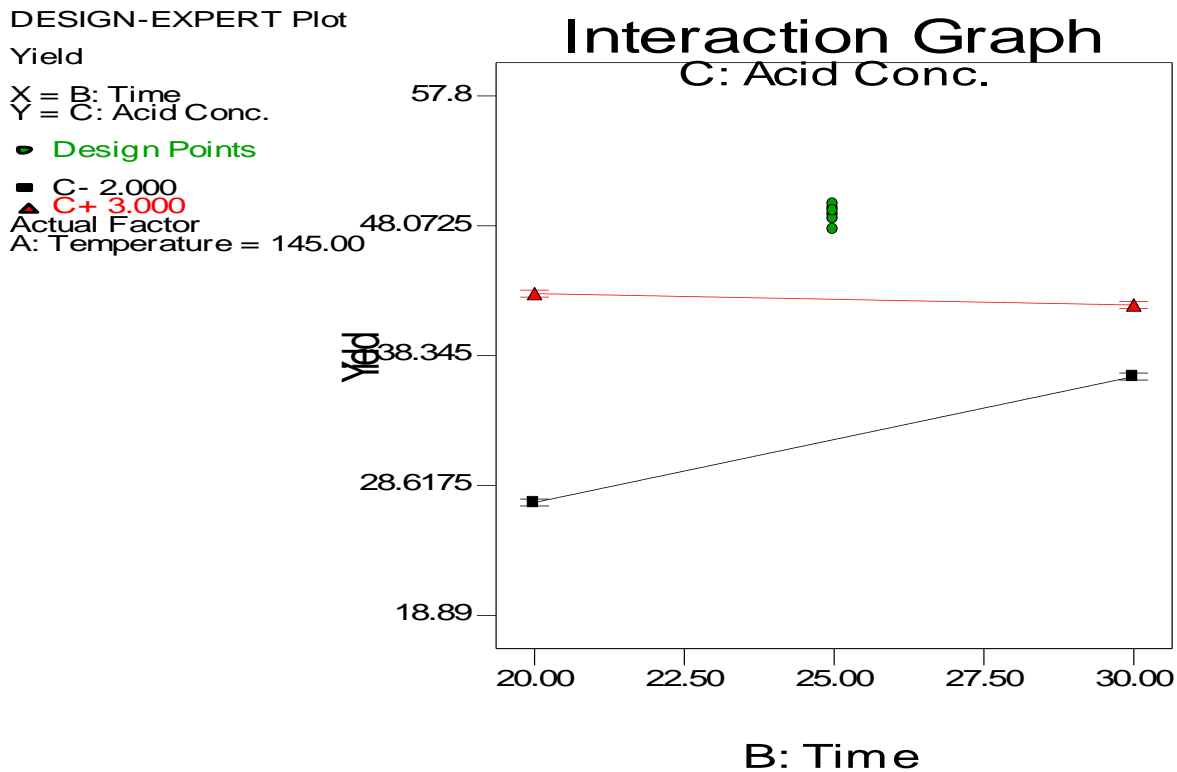


Fig. 4.13 Interaction of retention time and acid concentration on the yield of total reduced sugar

The response surface plot is another Model graph for 2^k full factorial design experiments. The response graph shown in figure 4.14 was the interaction between the reaction temperature and retention time on the yield of total reduced sugar.

The process variables have a significant interaction effect except the interaction between retention time and acid concentration on the yield of total reduced sugar. Figure 4.14 showing clearly, the interaction between temperature and retention time on the yield of total reduced sugar. Generally an increase in temperature resulted in higher yield. From the three interaction effects shown in the figure, at lower range of retention time, higher level of temperature and

center point of acid concentration the yield was higher. But operating at the center point temperature is economical in terms of energy saving.

In summary for the figure 4.14, operating at a center point temperature, lower range retention time and center point dilute acid concentration leads to the optimum yield of total reduced sugar.

DESIGN-EXPERT Plot

Yield

◇ = A: Temperature

◇ = B: Time

Actual Factor

C: Acid Conc. = 2.50

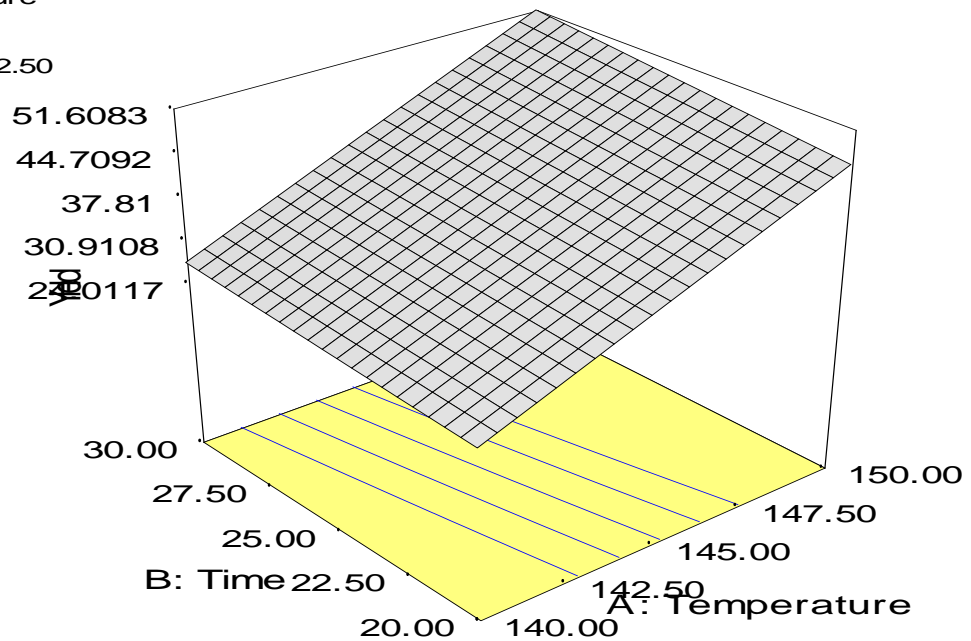


Fig. 4.14 Response surface plot of the interaction effect of temperature and retention time on yield of the total reduced sugar

The response surface plot is another Model graph for 2^k full factorial design experiments. The response graph shown in figure 4.15 was the interaction between the temperature and acid concentration on the yield of total reduced sugar. The process variables have a significant interaction effect except the interaction between retention time and acid concentration on the yield of total reduced sugar. Figure 4.15 shows us, the interaction between temperature and acid concentration on the yield of total reduced sugar. The maximum yield of total reduced sugar was obtained at a higher acid concentration and higher temperature by holding retention time at a center point. As it was shown from the effect list of factors in **figure 4.4** above, temperature and

acid concentration has a higher effect and high percentage contribution on the yield of total reduced sugar. Generally an increase in reaction temperature resulted in higher yield. From the three interaction effects shown in the figure 4.15, at higher range of acid concentration, higher level of temperature and center point of retention time the yield was higher. But operating at the center point temperature is economic in terms of energy saving.

Concluding from the figure 4.15, operating at a center point temperature, lower range of retention time and center point dilute acid concentration leads to the optimum yield of total reduced sugar.

DESIGN-EXPERT Plot

Yield
X = A: Temperature
Y = C: Acid Conc.

Actual Factor
B: Time = 25.00

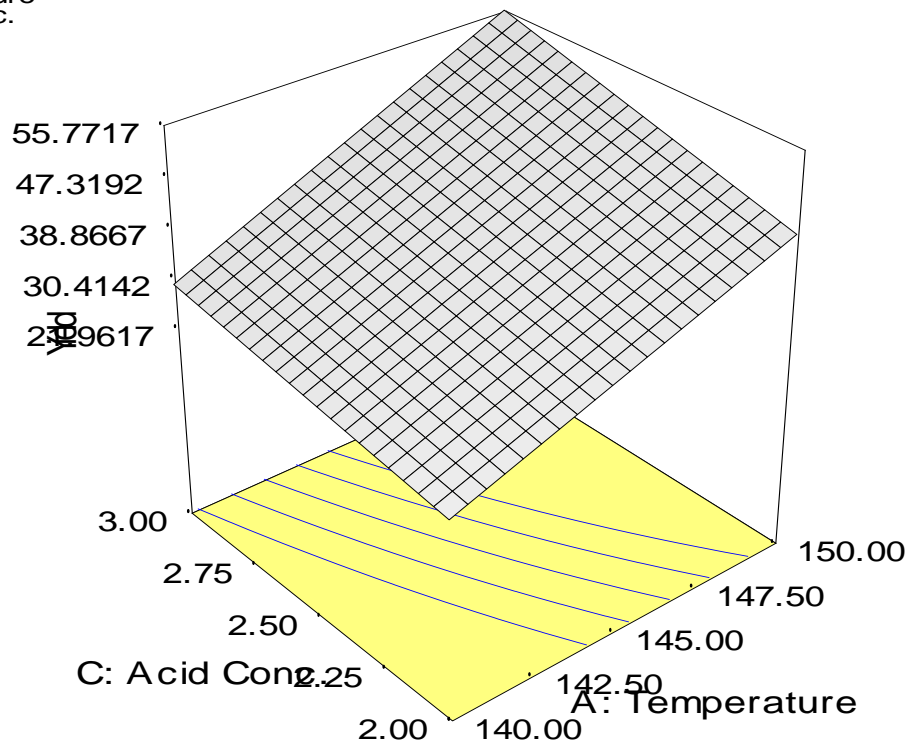


Fig. 4.15 Response surface plot of the interaction effect of acid concentration and temperature on the yield of total reduced sugar

Figure 4.16 shows that the cube graph of combination of process parameters, temperature, acid concentration and retention time on the yield of total reduced sugar. As it was seen from the cube graph, the levels and their interaction effects of process parameters on the yield of total reduced

sugar implies that the three factors; reaction temperature, retention time and dilute phosphoric acid concentration have an effect on the yield and the highest yield was obtained at lower retention time, higher temperature and high dilute phosphoric acid concentration which was at A+, B-, and C+ with a value of 57.22%. Cube graph is important for showing all the combination of process parameters and their levels for operating and running the process under consideration.

DESIGN-EXPERT Plot
 Yield
 X = A: Temperature
 Y = B: Time
 Z = C: Acid Concentration

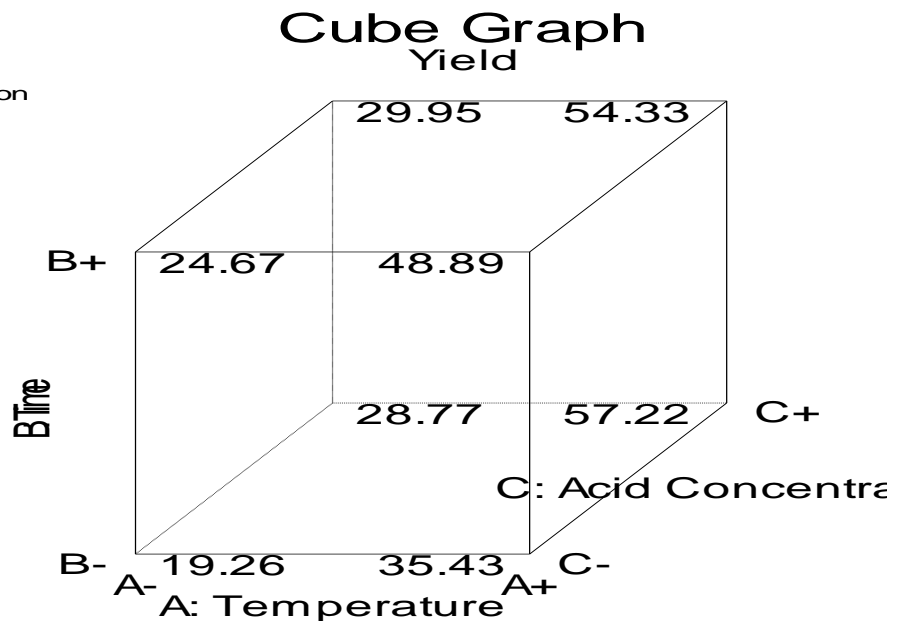


Fig. 4.16 A cube graph of yield of total reduced sugar with the three factor combination

4.2.6. Optimization

The above results show us that the process variables and their interaction effect has on the yield of total reduced sugar. Therefore, the next step is to optimize the process variable in order to obtain the highest (optimum) yield having all the constraints using the Model regression developed.

(Mata et al., 2015) reported that the maximum yield of total reduced sugar obtained from lignocellulosic biomass, BSG, was 51.86% with the liquid to solid ratio of 8%(v/w), size of particle 3mm, temperature 155⁰C, retention time of 18min and sulpheric acid concentration of

2.7%. It was recommended that phosphoric acid instead of sulphuric acid and reducing the particle size increases the yield of total reduced sugar up to 56% to 59%.

From the design expert 6.0.8 results, the maximum yield of total reduced sugar was obtained at a temperature of 150⁰C, retention time of 20 min, and phosphoric acid concentration of 3% which is 57.8%, and the minimum yield of total reduced sugar was obtained at temperature of 140⁰C, retention time 20min and phosphoric acid concentration 2% by holding liquid to solid ratio of 10% (v/w) and particle size at 2mm-1mm constant. This implies that the optimum reaction temperature, retention time, and dilute phosphoric acid concentration were, 150⁰C, 20min and 3%, respectively, which fits with the optimization result obtained from the Design Expert 6.0.8. maximum yield of 57.2098%, which agrees with the ANOVA result with negligible error of 1.02% with desirability of 0.989 as it was shown in table 4.6 below.

Table 4.6 Solution output from categorical optimization for maximum yield of total reduced sugar.

| Number | Temperature | Time | Acid concentration | Yield | Desirability | Remark |
|--------|---------------|-----------|--------------------|----------------|--------------|-----------------|
| 1 | <u>150.00</u> | <u>20</u> | <u>3.00</u> | <u>57.2098</u> | <u>0.989</u> | <u>Selected</u> |
| 2 | 149.85 | 20.26 | 2.89 | 57.1419 | 0.983 | |
| 3 | 148.63 | 23.13 | 2.95 | 56.312 | 0.962 | |
| 4 | 140.45 | 24.91 | 2.45 | 55.7965 | 0.949 | |
| 5 | 149.20 | 27.5 | 2.69 | 55.0487 | 0.929 | |
| 6 | 140.00 | 28.05 | 2.35 | 54.8906 | 0.925 | |
| 7 | 142.65 | 28.22 | 2.26 | 54.8412 | 0.924 | |
| 8 | 144.89 | 29.80 | 2.18 | 54.3842 | 0.912 | |
| 9 | 148.70 | 30.00 | 2.12 | 51.5265 | 0.839 | |

4.3. Fermentation

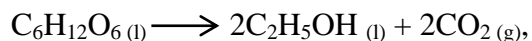
Before carrying out fermentation process the yeast culture, which was used as a fermentation media, was developed as shown in figure 4.17 below.



Fig. 4.17 Developed yeast culture

Fermentation kinetics and thermodynamics analysis were conducted as elaborated below.

Assuming that all TRS in the hydrolyzate was glucose and the fermentation reaction was given equation (3.10) below.



4.3.1. Thermodynamic analysis

Thermodynamic summary table 4.7 below was given which shows the thermodynamic quantity analysis from appendix A for the fermentation stage. With equilibrium conversion at 25⁰C and 32⁰C was $K_{\text{eq}, 298\text{k}} = 6.433 \cdot 10^{39}$ and $K_{\text{eq}, 305\text{k}} = 5.06 \cdot 10^{39}$, respectively.

Table 4.7 Summary of thermodynamic analysis from Appendix A

| Thermodynamic quantity | Units | Formula | Value |
|------------------------|-------|---|---------|
| Enthalpy | KJ | $\Delta H_{\text{rxn}} = \Delta H_{298\text{K}}^0 + \int_{T_0}^T \Delta C_P dT$ | -66.665 |
| Entropy | J/K | $\Delta S_{\text{rxn}} = \Delta S_{298\text{K}}^0 + \int_{T_0}^T \frac{\Delta C_P}{T} dT$ | 541.658 |
| Gibbs free energy | KJ | $\Delta G = \Delta H - T\Delta S$ | -231.84 |

Remarks noted from **table 4.7** above: the negative value of enthalpy implies that the fermentation reaction is exothermic and releases **66.665 KJ** of energy. From calculation it was noted that positive entropy of **541.658 J/K**, shows us that the reaction is spontaneous and the combined effect of enthalpy and entropy, Gibbs free energy, negative Gibbs free energy of **231.84KJ** tells us that the reaction is thermodynamically favorable and spontaneous to proceed in forward direction.

4.3.2. Kinetics of ethanol formation from total reduced sugar

Different values of absorbance for each run at an average of 12 hour were recorded from Spectrophotometer, which was converted in to concentration by using a standard curve from standard glucose solution, concentration versus time data were collected. After generating logarithmic data from the change in concentration versus concentration of TRS, K and n were determined and filled in the tables below (4.8-4.12), which were reaction rate constant and order of reaction, respectively; through equation (3.20) to (3.23).

$$\left(\frac{-dC_A}{dt}\right) = KC_A^n$$

$$\ln\left(\frac{-dC_A}{dt}\right) = \ln K + n \ln C_A$$

Arrhenius equation,

$$K = A \exp\left(\frac{-E_a}{RT}\right)$$

By taking the natural logarithm of the above equation

$$\ln K = \ln A - \left(\frac{-E_a}{R}\right) \times \frac{1}{T}$$

The fermentation kinetics was conducted at temperatures and pH of 30⁰C, 32⁰C, 34⁰C, 36⁰C, and 38⁰C and 4.5, 5, 5.5, 4.8, and 5.2, respectively. The fermentation was conducted for the change in both temperature and pH at the same time by keeping substrate to yeast ratio, rpm, time and pressure constant and the fermentation temperature was varied at an increment of 2⁰C, but pH was arbitrarily varied as per designers' interest.

N.B: The absorbance in fermentation stage for each run filled in tables (table 4.8-table 4.12) was determined using a DNS titration method.

At 30⁰C and pH of 4.5, concentration of unknown sample was determined using the equation (3.6).

For b= -0.17141 and m=36.86818

$C = \frac{\text{Abs}-b}{m}$, for example $C = \frac{1.962-(-0.17141)}{36.86818} = 0.0578$ g/ml, at t=0 sec similar procedures were followed and filled the table 4.8 below for the corresponding runs.

Table 4.8 Generated concentration at a fermentation temperature of 30⁰C and pH of 4.5.

| Run | Time (hr) | Absorbance (%) | C _A (g/ml) | $\frac{dC_A}{dt}$ | $\ln\left(\frac{dC_A}{dt}\right)$ | $\ln C_A$ |
|-----|--------------|-------------------|--------------------------|-------------------|-----------------------------------|-----------|
| 1 | 0 | 1.962 | 0.0578 | 0.0002667 | -8.23 | -5.74 |
| 2 | 12 | 1.798 | 0.0546 | 0.000184 | -8.6 | -6.11 |
| 3 | 24 | 1.696 | 0.0524 | 0.000921 | -6.99 | -4.51 |
| 4 | 36 | 1.565 | 0.0404 | 0.000850 | -7.07 | -4.585 |
| 5 | 48 | 1.442 | 0.0302 | 0.001367 | -6.595 | -4.11 |
| 6 | 60 | 1.121 | 0.0138 | 0.000489 | -7.622 | -5.138 |
| 7 | 72 | 0.962 | 0.0114 | | | |

From table 4.8 above, the linear plot in the Origin Lab Pro was plotted after feeding the data for $\ln\left(\frac{dC_A}{dt}\right)$ and $\ln C_A$ in order to find the slope and intercept from the graph. The Origin Lab Pro result with summary of linear fit was given in figure below.

From the plot, figure 4.18, the small table inside the plot is a summary table which tells us the slope, intercept, R^2 , coefficient of determination for the linear fit of the data, and corresponding error conducted during the generation of equation and the plot.

$\ln\left(\frac{dC_A}{dt}\right) = \ln K + n \ln C_A$, Slope which is the order of reaction, n , and intercept $\ln K$ were known with the coefficient of determination, $R^2 = 0.862$, from inside table in figure 4.18.

So, $n = 0.87$ and $\ln K = -3.412$

Therefore, $\ln K = -3.412$ and order of reaction, $n = 0.87$, the order of reaction and rate constant were 0.87 and 0.0329 hr^{-1} , which was obtained at temperature of 30°C and pH of 4.5.

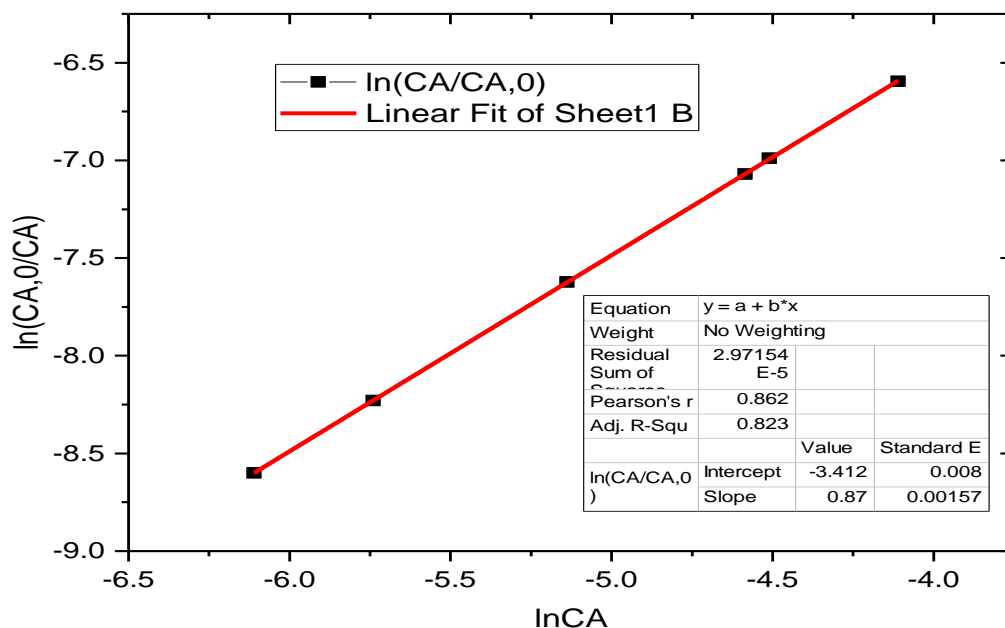


Fig. 4.18 $\ln\left(\frac{dC_A}{dt}\right)$ versus $\ln C_A$ at a temperature of 30°C and pH of 4.5

At 32⁰C and pH of 5, concentration of TRS sample was determined using the equation (3.6)

For $b = -0.17141$ and $m = 36.86818$

$C = \frac{\text{Abs}-b}{m}$, for example $C = \frac{1.932 - (-0.17141)}{36.86818} = 0.05705$ g/ml, at $t=0$ sec similar procedures

were followed and filled the table 4.9 below for the corresponding runs.

Table 4.9 Generated concentration at a fermentation temperature of 32⁰C and pH of 5.

| Run | Time (hr) | Absorbance (%) | C_A (g/ml) | $\frac{dC_A}{dt}$ | $\ln\left(\frac{dC_A}{dt}\right)$ | $\ln C_A$ |
|-----|---------------|-------------------|-----------------|-------------------|-----------------------------------|-----------|
| 1 | 0 | 1.932 | 0.05705 | 0.0003626 | -7.922 | -5.434 |
| 2 | 12 | 1.772 | 0.0527 | 0.0003334 | -8.006 | -5.521 |
| 3 | 24 | 1.624 | 0.0487 | 0.000217 | -8.437 | -5.952 |
| 4 | 36 | 1.521 | 0.0461 | 0.000655 | -7.33 | -4.853 |
| 5 | 48 | 1.241 | 0.0383 | 0.0003168 | -8.057 | -5.572 |
| 6 | 60 | 1.02 | 0.0345 | 0.0006162 | -7.392 | -4.906 |
| 7 | 72 | 0.891 | 0.0271 | | | |

From table 4.9 above, the linear plot in the Origin Lab Pro was plotted after feeding the data for $\ln\left(\frac{dC_A}{dt}\right)$ and $\ln C_A$ in order to find the slope and intercept from the graph. The Origin Lab Pro result with summary of linear fit was given in figure 4.19.

From the plot, figure 4.19, the small table inside the plot is a summary table which tells us the slope, intercept, R^2 , coefficient of determination for the linear fit of the data, and corresponding error conducted during the generation of equation and the plot.

$\ln\left(\frac{dC_A}{dt}\right) = \ln K + n \ln C_A$, Slope which is the order of reaction, n , and intercept $\ln K$ were known

So, $n = 1.0043$ and $\ln K = -4.402$ and $R^2 = 0.9989$, from the inside table in figure 4.19 below.

Therefore, $\ln K = -4.402$ and order of reaction, $n = 1.0043$.

This implies that the reaction order and rate constant of 1.0043 and 0.0122 hr^{-1} , which was obtained at temperature of 32°C and pH of 5 and with 99.89% of the experimental analysis was represented by this equation.

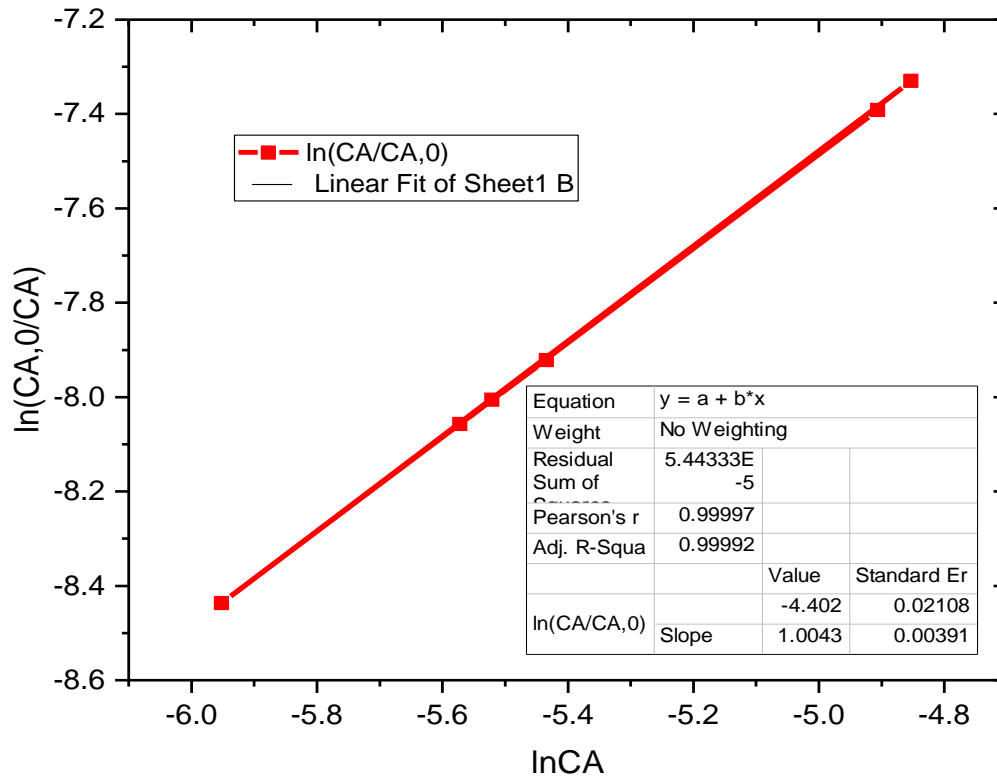


Fig. 4.19 $\ln\left(\frac{dCA}{dt}\right)$ versus $\ln C_A$ at a temperature of 32°C and pH of 5

At 34°C and pH of 5.5, concentration of TRS sample was determined using the equation (3.6)

For $b = -0.17141$ and $m = 36.86818$

$$C = \frac{\text{Abs}-b}{m}, \text{ for example } C = \frac{1.936 - (-0.17141)}{36.86818} = 0.0572 \text{ g/ml, at } t=0 \text{ sec similar procedures were}$$

followed and filled the tables below for the corresponding runs.

Table 4.10 Generated concentration at a fermentation temperature of 34⁰C and pH of 5.5

| Run | Time (hr) | Absorbance (%) | C _A (g/ml) | $\frac{dC_A}{dt}$ | $\ln\left(\frac{dC_A}{dt}\right)$ | $\ln C_A$ |
|-----|--------------|-------------------|--------------------------|-------------------|-----------------------------------|-----------|
| 1 | 0 | 1.936 | 0.0572 | 0.000366 | -7.911 | -5.426 |
| 2 | 12 | 1.789 | 0.0532 | 0.000233 | -8.363 | -5.878 |
| 3 | 24 | 1.569 | 0.0472 | 0.000286 | -8.168 | -5.684 |
| 4 | 36 | 1.323 | 0.0405 | 0.000342 | -7.982 | -5.496 |
| 5 | 48 | 1.102 | 0.0345 | 0.000672 | -7.305 | -4.815 |
| 6 | 60 | 0.867 | 0.0281 | 0.000358 | -7.934 | -5.449 |
| 7 | 72 | 0.825 | 0.027 | | | |

From table 4.10 above, the linear plot in the Origin Lab Pro was plotted after feeding the data for $\ln\left(\frac{dC_A}{dt}\right)$ and $\ln C_A$ in order to find the slope and intercept from the graph. The Origin Lab Pro result with summary of linear fit was given in figure below.

From the plot, figure 4.20, the small table inside the plot is a summary table which tells us the slope, intercept, R^2 , coefficient of determination for the linear fit of the data, and corresponding error conducted during the generation of equation and the plot.

$\ln\left(\frac{dC_A}{dt}\right) = \ln K + n \ln C_A$, Slope which is the order of reaction, n , and intercept $\ln K$ were known with the coefficient of determination, $R^2 = 0.973$

So, $n = 0.941$ and $\ln K = -4.569$

Therefore, $\ln K = -4.569$ and order of reaction, $n = 0.941$

Therefore, the order of reaction and rate constant were 0.941 and 0.0103 hr⁻¹, which was obtained at temperature of 34⁰C and pH of 5.5.

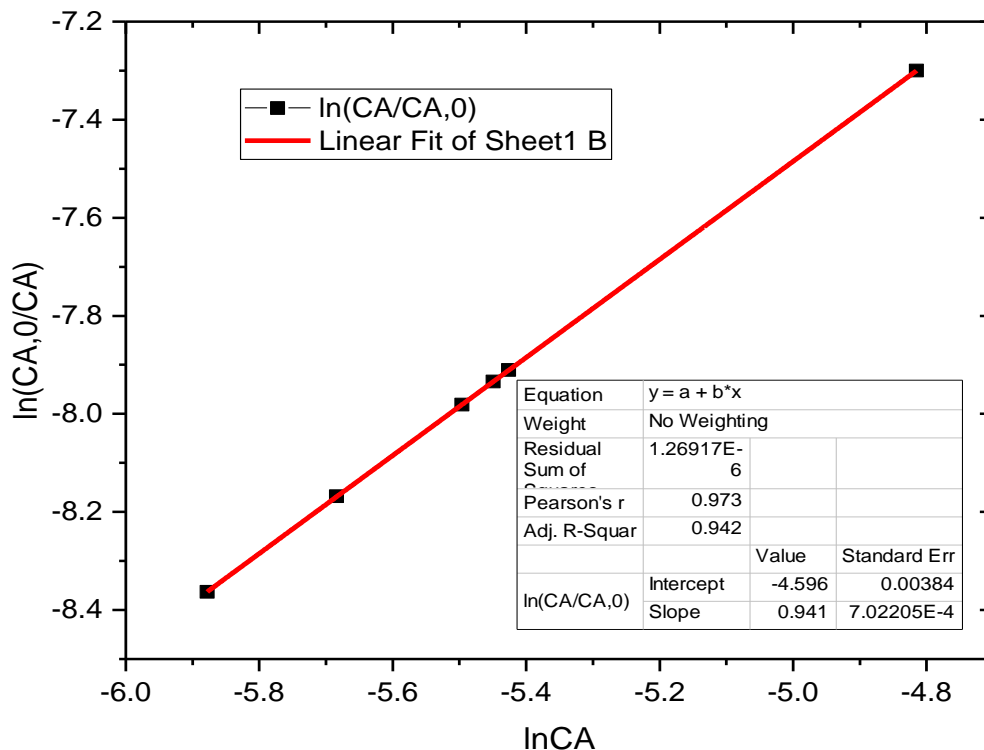


Fig. 4.20 $\ln\left(\frac{dCA}{dt}\right)$ versus $\ln C_A$ at a temperature of 34°C and pH of 5.5

At 36°C and pH of 4.8, concentration of TRS sample was determined using the equation (3.6).

For $b = -0.17141$ and $m = 36.86818$

$$C = \frac{\text{Abs}-b}{m}, \text{ for example } C = \frac{1.937 - (-0.17141)}{36.86818} = 0.0572 \text{ g/ml, at } t=0 \text{ sec similar procedures were}$$

followed and filled the tables below for the corresponding runs.

Table 4.11 Generated concentration at a fermentation temperature of 36⁰C and pH of 4.8

| Run | Time (hr) | Absorbance (%) | C _A (g/ml) | $\frac{dC_A}{dt}$ | $\ln\left(\frac{dC_A}{dt}\right)$ | $\ln C_A$ |
|-----|--------------|-------------------|--------------------------|-------------------|-----------------------------------|-----------|
| 1 | 0 | 1.937 | 0.0572 | 0.000319 | -8.05 | -5.572 |
| 2 | 12 | 1.787 | 0.05314 | 0.000525 | -7.552 | -5.067 |
| 3 | 24 | 1.565 | 0.0471 | 0.00055 | -7.505 | -5.02 |
| 4 | 36 | 1.321 | 0.0405 | 0.0005 | -7.6 | -5.116 |
| 5 | 48 | 1.101 | 0.0345 | 0.0005287 | -7.545 | -5.06 |
| 6 | 60 | 0.8668 | 0.0282 | 0.00008836 | -9.334 | -6.849 |
| 7 | 72 | 0.833 | 0.0271 | | | |

From table 11 above, the linear plot in the Origin Lab Pro was plotted after feeding the data for $\ln\left(\frac{dC_A}{dt}\right)$ and $\ln C_A$ in order to find the slope and intercept from the graph. The Origin Lab Pro result with summary of linear fit was given in figure below.

From the plot, figure 4.21, the small table inside the plot is a summary table which tells us the slope, intercept, R^2 , coefficient of determination for the linear fit of the data, and corresponding error conducted during the generation of equation and the plot.

$\ln\left(\frac{dC_A}{dt}\right) = \ln K + n \ln C_A$, Slope which is the order of reaction, n , and intercept $\ln K$ were known from figure 4.21 with the coefficient of determination, $R^2 = 0.822$

So, $n = 0.892$ and $\ln K = -4.665$

Therefore, $\ln K = -4.665$ and order of reaction, $n = 0.892$, which was obtained at temperature of 36⁰C and pH of 5.5, with the reaction rate constant, $K = 0.00942 \text{hr}^{-1}$ and reaction order, $n = 0.892$.

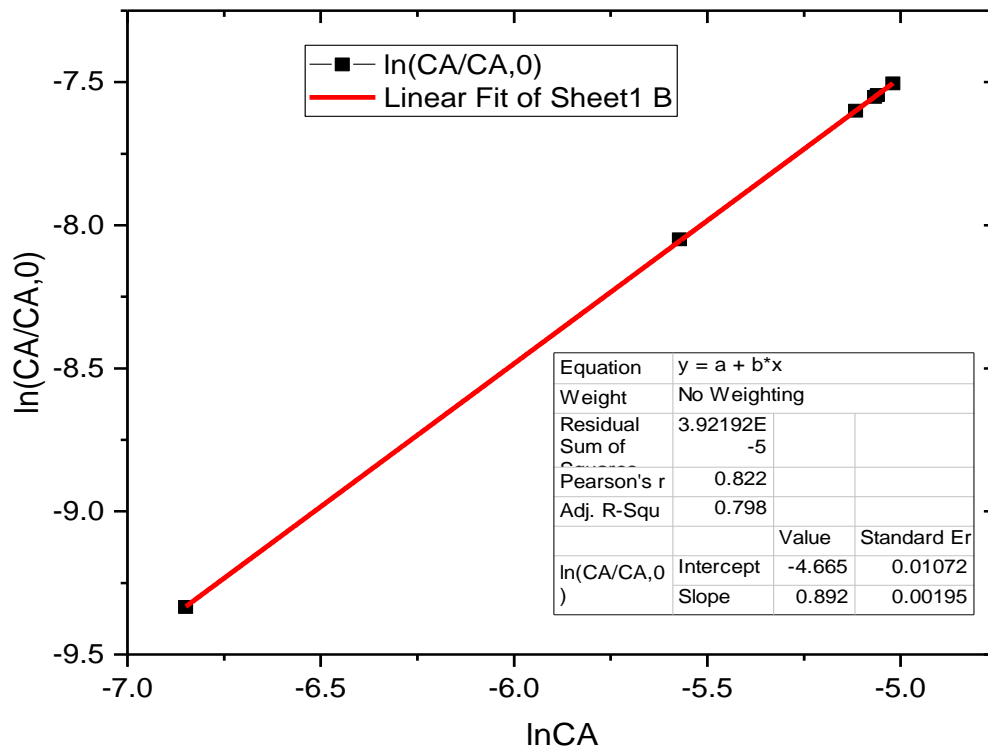


Fig. 4.21 $\ln\left(\frac{dCA}{dt}\right)$ versus $\ln C_A$ at a temperature of 36°C and pH of 4.8

At 38°C and pH of 5.2, concentration of TRS sample was determined using the equation (3.6).

For $b = -0.17141$ and $m = 36.86818$

$C = \frac{\text{Abs}-b}{m}$, for example $C = \frac{1.922 - (-0.17141)}{36.86818} = 0.0568 \text{ g/ml}$, at $t=0$ sec similar procedures were

followed and filled the tables below for the corresponding runs.

Table 4.12 Generated concentration at a fermentation temperature of 38°C and pH of 5.2

| Run | Time (hr) | Absorbance, (%) | C _A (g/ml) | $\frac{dC_A}{dt}$ | $\ln\left(\frac{dC_A}{dt}\right)$ | $\ln C_A$ |
|-----|-----------|-----------------|-----------------------|-------------------|-----------------------------------|-----------|
| 1 | 0 | 1.922 | 0.0568 | 0.0003 | -8.11 | -5.626 |
| 2 | 12 | 1.79 | 0.0532 | 0.000316 | -8.06 | -5.572 |
| 3 | 24 | 1.648 | 0.0494 | 0.000495 | -7.61 | -5.116 |
| 4 | 36 | 1.428 | 0.0434 | 0.000266 | -8.23 | -5.744 |
| 5 | 48 | 1.311 | 0.0402 | 0.000233 | -8.363 | -5.878 |
| 6 | 60 | 1.207 | 0.0374 | 0.000508 | -7.584 | -5.099 |
| 7 | 72 | 0.982 | 0.0313 | | | |

From table 12 above, the linear plot in the OriginLab Pro was plotted after feeding the data for $\ln\left(\frac{dC_A}{dt}\right)$ and $\ln C_A$ in order to find the slope and intercept from the graph. The OriginLab Pro result with summary of linear fit was given in figure 4.20 below.

From the plot, figure 4.22, the small table inside the plot is a summary table which tells us the slope, intercept, R^2 , coefficient of determination for the linear fit of the data, and corresponding error conducted during the generation of equation and the plot.

$\ln\left(\frac{dC_A}{dt}\right) = \ln K + n \ln C_A$, Slope which is the order of reaction, n , and intercept $\ln K$ were known from the plot with the coefficient of determination, $R^2 = 0.895$

So, $n = 0.712$ and $\ln K = -4.786$

Therefore, $\ln K = -4.786$ and order of reaction, $n = 0.712$, which was obtained at temperature of 38°C and pH of 4.8, the reaction rate constant $K = 0.00834 \text{hr}^{-1}$ and order of reaction, $n = 0.712$.

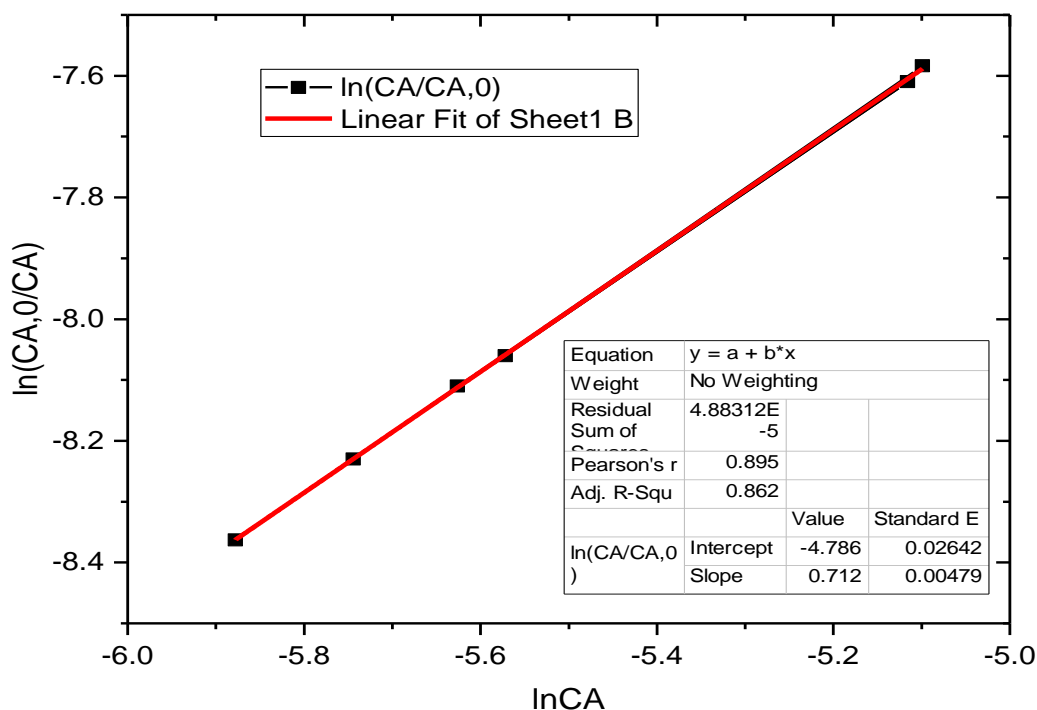


Fig. 4.22 $\ln\left(\frac{dC_A}{dt}\right)$ versus $\ln C_A$ at a temperature of 38°C and pH of 5.2

The kinetic summary for fermentation process was given in table 4.13 below.

Table 4.13 Kinetic summary for decomposition of glucose in to ethanol and carbon dioxide

| Run | T (K) | pH | $\frac{1}{T}$ (K^{-1}) | lnK | K (hr^{-1}) | Order, n | R^2 | Remarks |
|-----|----------|-----|--------------------------------------|--------|---------------------------|-------------|--------|----------|
| 1 | 303 | 4.5 | 0.0033 | -3.412 | 0.03298 | 0.87 | 0.862 | |
| 2 | 305 | 5 | 0.00327 | -4.402 | 0.01225 | 1.0043 | 0.9989 | Selected |
| 3 | 307 | 5.5 | 0.00325 | -4.596 | 0.01009 | 0.941 | 0.973 | |
| 4 | 309 | 4.8 | 0.00323 | -4.665 | 0.00942 | 0.892 | 0.822 | |
| 5 | 311 | 5.2 | 0.00321 | -4.786 | 0.00834 | 0.712 | 0.895 | |

By using the generated $\ln K$ values at different temperature from above tables, the values of A and E_a were determined from the plots/graph of $\ln K$ versus $\frac{1}{T}$ shown in figure 4.23 and the summary for above reaction data were given in table 4.13 below showing optimum temperature and pH for the fermentation kinetics of ethanol production from total reduced sugar.

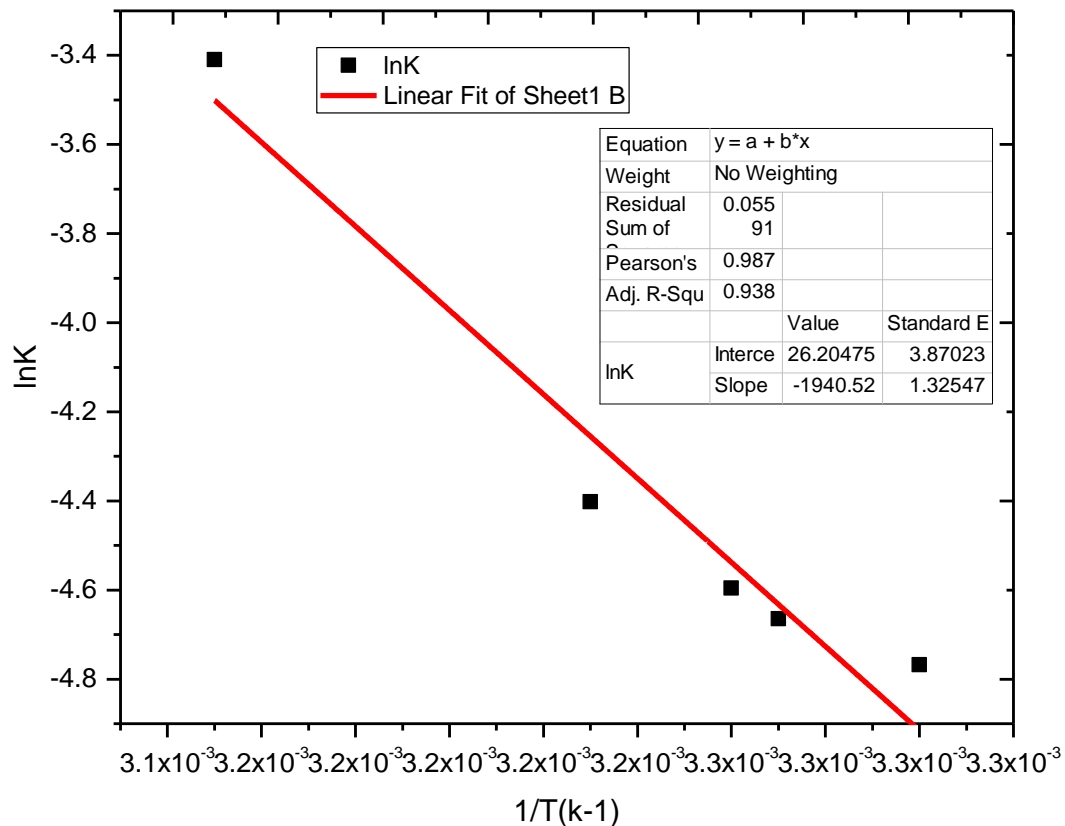


Fig. 4.23 $\ln K$ versus $\frac{1}{T}$ plot

From figure 4.21, the values of pre-exponential factor, A , and activation energy from Arrhenius equation (3.21) were determined. $\ln K = \ln A - \left(\frac{E_a}{R}\right) \times \frac{1}{T}$, slope, $m = -1940.52 \text{ gmol.K}$ and intercept, $b = 26.20467$: Intercept = $\ln A$ and slope = $-\frac{E_a}{R}$; $A = \exp(\text{intercept})$

$$A = \exp(26.20467) = 2.4 \times 10^{11}$$

Assuming 1gmol of glucose was feed to the fermenter. Slope = -1940.52 gmol.K,

$$E_a = -R \times \text{slope} = -(-1940.52 \text{ gmol.K} \times 8.314 \frac{\text{J}}{\text{gmol.K}}) = 16133.48 \text{ J}$$

$$E_a = 16.133 \text{ KJ}$$

From the above plot of $\ln K$ versus $\frac{1}{T}$, the frequency factor and activation energy of the reaction was determined as 2.4×10^{11} and 16.133 KJ, respectively. This shows us that the fermentation process requires activation energy of 16.133 KJ, at an optimum temperature and pH of 32°C and 5, respectively.

Now the rate constant, K, from Arrhenius equation was written as:

$$K = 2.4 \times 10^{11} e^{\frac{1940.46}{T}} \quad \text{at } 32^\circ\text{C} = 305\text{K}, K = 1.4 \times 10^{14} \text{ and order of reaction is } 1.0043.$$

This shows that the rate constant and order of reaction were 1.4×10^{14} and 1.0043, respectively.

The rate equation for the fermentation process was expressed in general from equation (3.20):

$$\frac{dC_A}{dt} = K (C_A)^n$$

$$\frac{dC_A}{dt} = 2.4 \times 10^{11} e^{\frac{1940.46}{T}} (C_A)^{1.0043}$$

4.4. Distillation of water-ethanol mixture

The distillation of water-ethanol mixture was conducted at a temperature of 78⁰C, due to the formation of azeotrope, a condition in which both the vapor and liquid phase has the same composition at a particular temperature, the purity of ethanol recovered was around 95%, the distillation setup was shown below in figure 4.24.



Fig. 4.24 Simple distillation setup to recovery ethanol from water-ethanol mixture

4.5. Characterization of recovered ethanol

Ethanol after recovery in distillation unit was characterized for its physic-chemical properties as identified below.

4.5.1. Density of ethanol

The density of ethanol after recovery was determined using equation (3.26) below as: $s.g = 0.812$; obtained on average basis by taking triplicates from refractive index after injecting the sample in the syringe and putting in to the density meter; $\rho_{\text{water}} = 1 \frac{\text{g}}{\text{cm}^3}$ at 25⁰C.

$$\rho_{\text{EtOH}} = s.g \times \rho_{\text{water}}; \rho_{\text{EtOH}} = 0.812 \times 1 \frac{\text{g}}{\text{cm}^3} = 0.812 \frac{\text{g}}{\text{cm}^3}$$

The deviation of the value of specific gravity from literature, 0.79 to 0.812, was due to the presence of water approximately 5% was found in the recovered ethanol due to the formation of an azeotrope, a condition by which the vapor and liquid phase of a mixture are at the same composition at specific temperature, at 78⁰C. In order to increase the concentration of recovered ethanol to 99.9%, molecular sieves should be used for dehydration.

4.5.2. Determination of kinematic viscosity

Dynamic viscosity, from vibro-viscometer reading, was = 1.235mPa.s. which was measured in triplicate and the average value was taken. The kinematic viscosity was determined using equation (3.27) below.

$$\text{Kinematic viscosity} = \frac{\text{dynamic viscosity}}{\text{density}}, \nu = \frac{\mu}{\rho}; \nu = \frac{0.001235 \text{kg.m}^{-1}.\text{s}^{-1}}{812 \text{kg/m}^3}$$

$$\nu = 1.52\text{E-}06 \text{ m}^2/\text{s}.$$

The kinematic viscosity at room temperature was found as 1.52E-06 m²/s which closer to the literature value found 1.4912E-06 m²/s. The small deviation in the value happened due to personal and experimental errors.

4.5.3. FT-IR result of bioethanol produced from BSG

Alcohols have a characteristic IR absorptions associated with the O-H, C-O, and C-H stretching vibrations. When run as liquid film the region 3000-3600 cm⁻¹ with a very intense and broad band indicates the O-H stretch of alcohols, while the region 1050-1280 cm⁻¹ confirms the C-O stretch. The bands at around 1500-2200 cm⁻¹ were assigned as the symmetric stretching modes of -CH₂ and -CH₃ groups respectively (Paul Held, 2012).

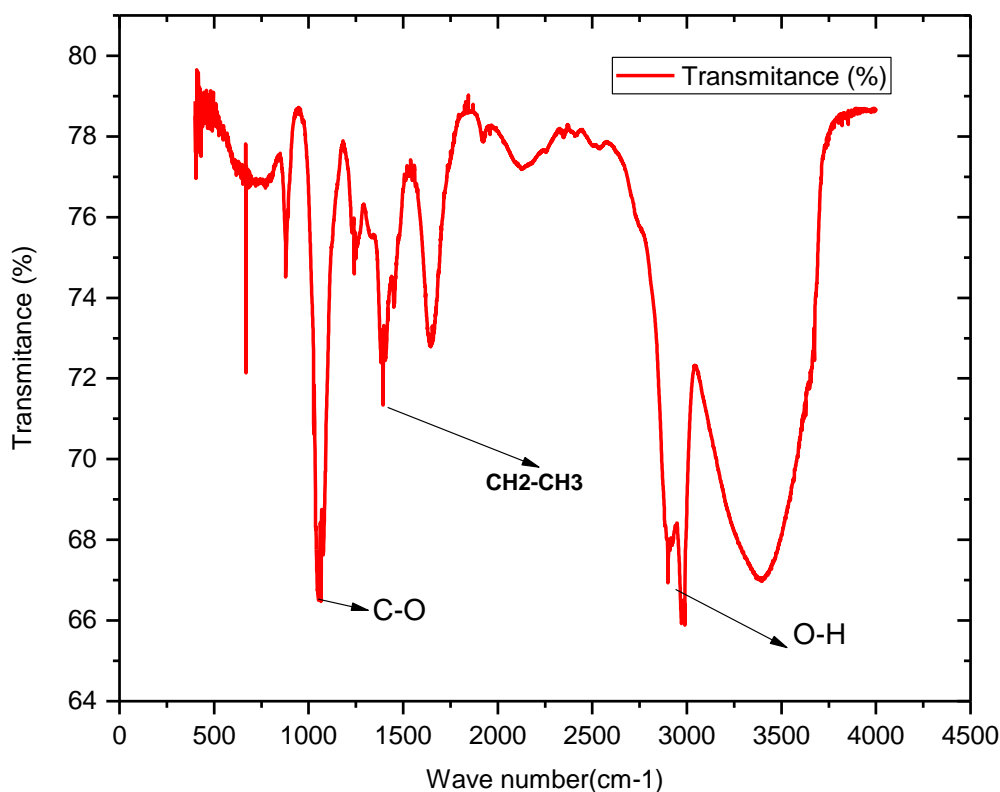


Fig. 4.25 Fourier Transform Infrared spectra of ethanol produced from BSG

The FTIR spectrum of alcohol was obtained using Perkins Elmer Spectrum 65 FT-IR spectrometer in Addis Ababa University, Faculty of Science, Chemistry department and functional groups was determined with the help of IR correlation charts. The result was obtained with %transmittance to wave number range from (4000-400) cm^{-1} .

This assures that the product obtained from BSG contains as shown in figure 4.25 above, with stretching band with wave number correlation and corresponding functional groups, is exactly fits with the stretching bands from literature and therefore, the product obtained fits exactly stretching bands and functional groups found in the ethanol by using FTIR.

Chapter Five

5. CONCLUSION AND RECOMMENDATION

5.1. CONCLUSION

Bioethanol, currently produced from sugar cane and starchy sources is directly interfering with the food consumption. Lignocellulosic feedstocks, agro-industrial wastes, are the most renewable feedstocks for the sustainable production of ethanol. Currently, ethanol is used as fuel blended or pure for the transportation sector. As there is diversifying brewing companies locally and globally, that show a direction for exploiting the waste or low value by-product from breweries, BSG, for value added product production, bioethanol.

The main aim of this thesis work is to produce ethanol from BSG. The production stages were pretreatment, hydrolysis, fermentation and distillation of water-ethanol mixture to recover ethanol. The proximate analysis was conducted and found that the cellulose and hemicellulose compositions were higher in BSG which accounts 34.62% and 18.84%, respectively. The pretreatment was used to reduce the crystallinity of cellulose during hydrolysis and in order to remove inhibitory products which affect in fermentation stage. The hydrolysis stage was conducted in two-stage, first-stage (pretreatment) and second-stage, to produce fermentable sugar, the hydrolysis process was designed using randomized run two factor full factorial three factor conducted in three replicate and hydrolysis stage parameters were identified as reaction temperature, retention time and dilute acid concentration and the optimum operating condition to have a maximum total reduced sugar yield was analyzed using ANOVA and found at a temperature, retention time and phosphoric acid concentration of 150⁰C, 20min and 3% as 57.8%, showing that the biomass, BSG, is rich in fermentable sugar. The individual and interaction effect of the process parameters for the hydrolysis stage was carried out using model graphs and response surface plots from design expert 6.0.8. Temperature, interaction between temperature and dilute phosphoric acid concentration, dilute phosphoric acid concentration, interaction between temperature and retention time had major effect on the yield of total reduced sugar from BSG. After obtaining the optimum operating condition for the hydrolysis stage,

fermentation was conducted in order to produce bioethanol, ethanol from total fermentable sugar which was produced during hydrolysis of pretreated BSG in the autoclave. Fermentation was conducted at different at temperature of (30, 32, 34, 36 and 38) °C and pH of (4.5, 5, 5.5, 4.8 and 5.2) these were an operating ranges for the microorganism *Saccharomyces cerevisiae* in order to have an optimum operating condition.

The thermodynamic and kinetic analysis on fermentation stage was conducted and fermentation commenced for 72 hours and on average each 12 hour, from each fermenting bottle sample was taken and the absorbance of sample was measured at wavelength of 540nm and converted to a concentration using a standard glucose curve for temperature-pH combination. After determining the concentration from absorbance values, the rate constant and order of reaction was determined from the assumption that power law holds for fermentation. Different values of rate constant at different temperature were generated and plotted in order to determine the activation energy and frequency factor from Arrhenius equation. The water-ethanol mixture was separated using a simple distillation unit and ethanol was recovered in the vapor phase and water and other heavy components were remained in the bottom of distilling flask after recovery, ethanol was characterized in order to fulfill its physic-chemical property.

5.2. RECOMMENDATIONS

The following recommendations were drawn from this thesis work for future work as:

- Further research on BSG harness to release fermentable sugar as it is produced in high amount as there are diversifying brewing company all across the globe in general and in Ethiopia in particular, as well it is rich source of cellulose and hemicellulose, it needs stake holders and policy makers to take in to consideration this low-value lignocellulose for the value-added product, bioethanol, since energy needs to be renewable in the future as the fossil fuel is degrading and prices are increasing.
- Detailed economic and feasibility study in the production processes for rational commercialization is suggested.
- Further research on fuel property of ethanol from BSG in relation to blending with gasoline and the efficiency of engine that operates using ethanol as fuel is recommended.
- Binary distillation of water-ethanol mixture needs to be optimized in order to design a distillation column and to obtain an optimum operating parameters: maximum ethanol yield, low heat duty and feed conditions. After recovery of ethanol from distillation unit, molecular sieves should be used in order to concentrate final product to a yield of 99.99%.
- In this paper dilute acid hydrolysis was conducted and diluting and working in acidic environment is not safe so that this needs a way to work on safe environment showing a direction to develop an enzyme which would be used for the hydrolysis of lignocellulose (hemicellulose and cellulose) at low cost that produces a high yield of total reduced sugar in short period without polluting the environment is recommended.

REFERENCES

- A. Dávila, J., Rosenberg, M., & A. Cardona, C. (2016). A biorefinery approach for the production of xylitol, ethanol and polyhydroxybutyrate from brewer's spent grain. *AIMS Agriculture and Food*, 1(1), 52–66. <https://doi.org/10.3934/agrfood.2016.1.52>
- Aboltins, A., & Palabinskis, J. (2015). Research in brewer's spent grain drying process, 230–235.
- Acacio, K., Apyan, A., Araiza, R. M., Chiem, E., Kapaldo, J., Kim, P., ... Marshall, T. (2014). Introduction to brewers' spent grain, 43(2006), 2006.
- Akanksha, K., Prasad, A., Sukumaran, R. K., K, M. N., & Pandey, A. (2014). Dilute acid pretreatment and enzymatic hydrolysis of sorghum biomass for sugar recovery — A statistical approach, 52(November), 1082–1089.
- Aliyu, S., & Bala, M. (2013). Brewer's spent grain: A review of its potentials and applications. *African Journal of Biotechnology*, 10(3), 324–331. <https://doi.org/10.4314/ajb.v10i3>.
- Amezcuca-allieri, M. A., Durán, T. S., & Aburto, J. (2017). Study of Chemical and Enzymatic Hydrolysis of Cellulosic Material to Obtain Fermentable Sugars, 2017.
- A.O.A.C.(2003) Official method of analysis of association of official analytical chemists International In :Walker and Harwitz, W.(Ed.),17th ed. AOAC Press, Arlington, VA, USA.
- Arredondo, V., A, R. C. A., & Junior, O. (2009). Ethanol Production from Banana Fruit and its Lignocellulosic Residues : Exergy and Renewability Analysis *, 12(3), 155–162.
- Awolu, O. O., & Ibileke, I. O. (2011). Bioethanol production from brewer's spent grain, bread wastes and corn fiber. *African Journal of Food Science*, 5(3), 148–155. Retrieved from <http://www.academicjournals.org/ajfs>
- Axelsson, L., Franzén, M., Ostwald, M., Berndes, G., Lakshmi, G., & Ravindranath, N. H. (2012). Perspective: Jatropha cultivation in southern India: Assessing farmers' experiences. *Biofuels, Bioproducts and Biorefining*, 6(3), 246–256. <https://doi.org/10.1002/bbb>
- Bensah, E. C., & Mensah, M. (2013). Chemical Pretreatment Methods for the Production of Cellulosic Ethanol : Technologies and Innovations, 2013.
- Bokulich, N. A., & Bamforth, C. W. (2013). The Microbiology of Malting and Brewing. *Microbiology and Molecular Biology Reviews*, 77(2), 157–172. <https://doi.org/10.1128/MMBR.00060-12>

- Borzani, W. (2006). batch ethanol fermentation: the correlation between the fermentation efficiency and the biomass initial concentration depends on what is considered as produced ethanol, 87–89.
- Buffington, J. (2014). The Economic Potential of Brewer's Spent Grain (BSG) as a Biomass Feedstock. *Advances in Chemical Engineering and Science*, (July), 308–318. <https://doi.org/10.4236/aces.2014.43034>
- Caetano, N. S., Moura, R. F., Meireles, S., Mendes, A. M., & Mata, T. M. (2013). Bioethanol from Brewer's Spent Grains: Acid Pretreatment Optimization, 35, 1021–1026. <https://doi.org/10.3303/CET1335170>
- Ccopa, E., Yamakawa, C. K., Herrera, M., Geraldo, C., Rossell, C. E. V, Maciel, R., & Bonomi, A. (2013). A Procedure for Estimation of Fermentation Kinetic Parameters in Fed-Batch Bioethanol Production Process with Cell Recycle, 32, 1369–1374.
- Chan-u-tit, P., Laopaiboon, L., Jaisil, P., & Laopaiboon, P. (2013). High Level Ethanol Production by Nitrogen and Osmoprotectant Supplementation under Very High Gravity Fermentation Conditions, 884–899. <https://doi.org/10.3390/en6020884>
- Chandel, A. A. K., Silva, S. da, Singh, O. V. O., Silvério, S., & Singh, O. V. O. (2011). Detoxification of lignocellulosic hydrolysates for improved bioethanol production. *Biofuel Production-Recent ...*, 2012, 989572. <https://doi.org/10.1155/2012/989572>
- Chandel, A. K., Antunes, F. A. F., Arruda, P. V. De, Milessi, T. S. S., Silva, S. S., & De, M. G. (2012). Dilute Acid Hydrolysis of Agro-Residues for the Depolymerization of Hemicellulose: State-of-the-Art. <https://doi.org/10.1007/978-3-642-31887-0>
- Chow, P. S., & Landhäusser, S. M. (2004). A method for routine measurements of total sugar and starch content in woody plant tissues. *Tree Physiology*, 24(Ashwell 1957), 1129–1136. <https://doi.org/10.1093/treephys/24.10.1129>
- Coman, G., Andreea, N., Ȃlăţ, S. P., Constan, E. L. U., & Bahrin, G. (2015). Original Research Paper Bioethanol Production By Solid State Fermentation From Cheese Whey Mixed With Brewer's Spent Grains, 39, 49–57.
- Da Silva, S. S., & Chandel, A. K. (2012). D-Xylitol: Fermentative production, application and commercialization. *D-Xylitol: Fermentative Production, Application and Commercialization*, 1–345. <https://doi.org/10.1007/978-3-642-31887-0>
- Dehnavi, G. Z. (2009). fractionation of the main components of barley spent grains from, (5), 1–

23.

Dussán, K. J., Silva, D. D. V, Moraes, E. J. C., Arruda, P. V, & Felipe, M. G. A. (2014). Dilute acid Hydrolysis of Cellulose to Glucose from Sugarcane Bagasse. *Chemical Engineering Transactions*, 38, 433–438. <https://doi.org/10.3303/CET1438073>

Elements of Chenzicn 1 Reaction Engineering. (n.d.).

Erdelji, V. (2007). *Bioethanol from Brewer's and Distiller's Spent Grains*, 7.

Fărcaș, A., Tofană, M., Socaci, S., Mudura, E., Scrob, S., Salanță, L., & Mureșan, V. (2014). *Brewers' spent grain – A new potential ingredient for functional foods*.

Ferreira, I. M. P. L. V. O., Pinho, O., Vieira, E., & Tavarela, J. G. (2010). Brewer's *Saccharomyces* yeast biomass: characteristics and potential applications. *Trends in Food Science and Technology*, 21(2), 77–84. <https://doi.org/10.1016/j.tifs.2009.10.008>

Forsell, P., Kontkanen, H., Schols, H. A., Hinz, S., Vincent, G. H., Treimo, J., ... Brew, J. I. (n.d.). *Hydrolysis of Brewers' Spent Grain by Carbohydrate Degrading Enzymes*.

Gencheva, P., Dimitrov, D., & Dobrev, G. (2012). *Hydrolysates from malt spent grain with potential application in the bioethanol production*, 1(Table 1), 135–141.

Harmsen, P., & Huijgen, W. (2010). *Literature Review of Physical and Chemical Pretreatment Processes for Lignocellulosic Biomass*, (September), 1–49.

Idrees, M., Adnan, A., Sheikh, S., Qureshi, F. A., Road, K., Control, D., ... Road, P. (2013). *Original article : optimization of dilute acid pretreatment of water hyacinth biomass for enzymatic hydrolysis and ethanol production*, 30–40.

Isaacs, S. H. (1984). *Ethanol Production by Enzymatic Hydrolysis Parametric Analysis of a Base-Case Process*.

Jose, D., Utfpr, H., Reinaldo, R., & Utfpr, P. (2011). *analysis of hydrolysis yields by using different acids for bioethanol production from brazilian woods*.

Kang, Q., Appels, L., Tan, T., & Dewil, R. (2014). *Bioethanol from Lignocellulosic Biomass : Current Findings Determine Research Priorities*, 2014(Ci).

Ktenioudaki, A., Chaurin, V., Reis, S. F., & Gallagher, E. (2012). *Brewer's spent grain as a functional ingredient for breadsticks*. *International Journal of Food Science and Technology*, 47(8), 1765–1771. <https://doi.org/10.1111/j.1365-2621.2012.03032.x>

Kuila, A., & Sharma, V. (2016). *iMedPub Journals Enzymatic Hydrolysis and Fermentation of Lignocellulosic Biomass for Bioethanol Production*, 21767. <https://doi.org/10.21767/2572->

5475.100

- Kumar, P., Barrett, D. M., Delwiche, M. J., Stroeve, P., Kumar, P., Barrett, D. M., ... Stroeve, P. (2009). Methods for Pretreatment of Lignocellulosic Biomass for Efficient Hydrolysis and Biofuel Production Methods for Pretreatment of Lignocellulosic Biomass for Efficient Hydrolysis and Biofuel Production. <https://doi.org/10.1021/ie801542g>
- Kumar, R., Tabatabaei, M., Karimi, K., & Horváth, I. S. (2016). Recent updates on lignocellulosic biomass derived ethanol - A review, 9, 347–356. <https://doi.org/10.18331/BRJ2016.3.1.4>
- Lenihan, P., Orozco, A., Neill, E. O., Ahmad, M. N. M., Rooney, D. W., Mangwandi, C., & Walker, G. M. (n.d.). Kinetic Modelling of Dilute Acid Hydrolysis of Lignocellulosic Biomass.
- Li, X. (2010). Bioethanol production from lignocellulosic feedstock using aqueous ammonia pretreatment and simultaneous saccharification and fermentation (SSF): process development and optimization.
- Liguori, R., Soccol, C. R., de Souza Vandenberghe, L. P., Woiciechowski, A. L., & Faraco, V. (2015). Second generation ethanol production from brewers' spent grain. *Energies*, 8(4), 2575–2586. <https://doi.org/10.3390/en8042575>
- Limayem, A., & Ricke, S. C. (2012). Lignocellulosic biomass for bioethanol production: Current perspectives, potential issues and future prospects. *Progress in Energy and Combustion Science*, 38(4), 449–467. <https://doi.org/10.1016/j.pecs.2012.03.002>
- Long-term Bioethanol Shift and Transport Fuel Substitution in Ethiopia Yacob Gebreyohannes Hiben Transport Fuel Substitution in Ethiopia. (2013).
- Maache-rezzoug, Z., Maugard, T., Goude, R., Maache-rezzoug, Z., Maugard, T., Goude, R., ... Improving, F. O. R. (2009). a thermomechanical process for improving enzymatic hydrolysis of brewer's spent grain.
- Machado, G., Leon, S., Santos, F., Lourega, R., Dullius, J., Mollmann, M. E., & Eichler, P. (2016). Literature Review on Furfural Production from Lignocellulosic Biomass, 115–129.
- Mata, T. M., Tavares, T. F., Meireles, S., & Caetano, N. S. (2015). Bioethanol from Brewers' Spent Grain: Pentose Fermentation. *Chemical Engineering Transactions*, 43, 241–246. <https://doi.org/10.3303/CET1543041>
- Maurice, M. L. (2011). Factors Effecting Ethanol Fermentation Via Simultaneous

Saccharification and Fermentation.

- Meneses, L. R., Raud, M., Orupöld, K., & Kikas, T. (2017). Second-generation bioethanol production : A review of strategies for waste valorisation, 15(3), 830–847.
- Miller, G.L., Use of dinitrosalicylic acid reagent for determination of reducing sugar, *Anal. Chem.*, **31**, 426, 1959.
- Montgomery, D. C. (n.d.). design and analysis of fifth edition.
- Moreira, M. M., Morais, S., Carvalho, D. O., Barros, A. A., & Guido, L. F. (2013). Brewer's spent grain from different types of malt : Evaluation of the antioxidant activity and identification of the major phenolic compounds. *FRIN*, 54(1), 382–388. <https://doi.org/10.1016/j.foodres.2013.07.023>
- Muigai, C. (2012). a Study of Thermal Energy Use At a Brewing Plant With Emphasis, (May).
- Muthusamy, N. (2014). Chemical Composition of Brewers Spent Grain – a Review. *International Journal of Science, Environment and Technology*, 3(6), 2109–2112.
- Ness, V. (n.d.). INTRODUCTION TO Sixth Edition in SI Units.
- Nigam, P. S. (2017). An overview: Recycling of solid barley waste generated as a by-product in distillery and brewery. *Waste Management*, 62, 255–261. <https://doi.org/10.1016/j.wasman.2017.02.018>
- Novy, V., Longus, K., & Nidetzky, B. (2015). From wheat straw to bioethanol : integrative analysis of a separate hydrolysis and co-fermentation process with implemented enzyme production, 1–12. <https://doi.org/10.1186/s13068-015-0232-0>
- Nuno, R., & Carvalho, L. De. (2009). Dilute acid and enzymatic hydrolysis of sugarcane bagasse for biogas production *Engenharia Biológica Dilute acid and enzymatic hydrolysis of sugarcane bagasse for biogas production Engenharia Biológica.*
- Olaoye, O. S., & Kolawole, O. S. (2013). Modeling of the kinetics of ethanol formation from glucose biomass in batch culture with a non structured model. *International Journal of Engineering Research and Application (IJERA)*, 3(4), 562–565.
- Orji, F. A., Dike, E. N., Lawal, A. K., Sadiq, A. O., Suberu, Y., Famotemi, A. C., ... Elemo, G. N. (2016). Properties of Bacillus species Cellulase Produced Using Cellulose from Brewers Spent Grain (BSG) as Substrate, (March), 142–148.
- Parsapour, A. (2012). Biogas Production System as an “ Upcyclers ” Biogas Production System

as an “ Upcycler .”

Paul Held. (2012). Chemical and Biochemical Means to Detect Alcohol Determination of Ethanol Concentration in Fermented Beer Samples and Distilled Products. *Biotek*, 1–6. Retrieved from www.biotek.com

Pejin, J. (2016). challenges in bioethanol production: utilization of, *22(4)*, 375–390. <https://doi.org/10.2298/CICEQ151030001N>

Pires, E. J., Ruiz, A., & Teixeira, J. A. (2012). A New Approach on Brewer`s Spent Grains Treatment and Potential Use as Lignocellulosic Yeast Cells Carriers.

Raposo, S., Pardão, J. M., Díaz, I., & Lima-costa, M. E. (2009). Kinetic modelling of bioethanol production using agro-industrial by-products, *3(1)*, 1–8.

Roberto, C. (2005). Acid hydrolysis and fermentation of brewer`s spent grain to produce xylitol, *2460(July 2004)*, 2453–2460. <https://doi.org/10.1002/jsfa.2276>

Rojas-chamorro, J. A., Romero, I., Ruiz, E., & Cara, C. (2017). Comparison of Fermentation Strategies for Ethanol Production from Pretreated Brewers Spent Grain, *61*, 637–642. <https://doi.org/10.3303/CET1761104>

Rubio-arroyo, M. F., Vivanco-loyo, P., Juárez, M., & Poisot, M. (2011). Bio-ethanol Obtained by Fermentation Process with Continuous Feeding of Yeast, *55(4)*, 242–245.

Sa, J. (n.d.). This paper contains a lot of good information on ethanol production from both sugar sources (grain , sugar cane , etc .) and cellulosic material . Please use only the information pertaining to cellulosic sources as we will cover sugar ethanol earlier in . <https://doi.org/10.1016/j.biortech.2007.11.013>

Saadavate, L. B., & Thesis, A. (2013). characteristics of bioethanol fuel obtained from lignocellulose biomass in internal combustion reciprocating engines with spark- and compression- ignition.

Schisler, D., Ruocco, J., & Mabee, M. (1982). Wort trub content and its effects on fermentation and beer flavor. *Journal of the American Society Chemests*, 57–61. Retrieved from <http://agris.fao.org/agris-search/search/display.do?f=2012/OV/OV201203131003131.xml;US19830907144>

Singh, D. P., & Trivedi, R. K. (2013). Acid And Alkaline Pretreatment Of Lignocellulosic Biomass To Produce Ethanol As Biofuel, *5(2)*, 727–734.

Soupioni, M., Golfinopoulos, A., Kanellaki, M., & Koutinas, A. A. (2013). Study of whey

- fermentation by kefir immobilized on low cost supports using ¹⁴C-labelled lactose. *Bioresource Technology*, 145, 326–330. <https://doi.org/10.1016/j.biortech.2012.12.131>
- Sun, Y., & Cheng, J. (2002). Hydrolysis of lignocellulosic materials for ethanol production : a review q, 83, 1–11.
- Than, S. S. (2017). Optimisation of Acid Hydrolysis of Grasses using Response Surface Methodology for the Preparation of Bioethanol, 56, 1615–1620. <https://doi.org/10.3303/CET1756270>
- Thiago, R. dos S. M., Pedro, P. M. de M., & Eliana, F. C. S. (2014). Solid wastes in brewing process: A review. *Journal of Brewing and Distilling*, 5(1), 1–9. <https://doi.org/10.5897/JBD2014.0043>
- Trajano, H. L., & Wyman, C. E. (2013). Fundamentals of Biomass Pretreatment at Low pH.
- Tsoutsos, T., & Bethanis, D. (2011). Optimization of the Dilute Acid Hydrolyzator for Cellulose-to-Bioethanol Saccharification, 1601–1623. <https://doi.org/10.3390/en4101601>
- Verardi, A., Bari, I. De, Ricca, E., & Calabrò, V. (n.d.). Hydrolysis of Lignocellulosic Biomass : Current Status of Processes and Technologies and Future Perspectives.
- Vigo-ourense, U. De, & Lagoas, A. (2004). Comparison of Two Posthydrolysis Processes of Brewery ' s Spent Grain Autohydrolysis Liquor to Produce a Pentose-Containing Culture Medium †, 113.
- Vince, A. K. (2010). bio-ethanol production from brewers spent grain : comparing pretreatment methods . bio-ethanol production from brewers spent grain : comparing pretreatment methods .
- Walker, R. W., & Goran, M. I. (2015). Laboratory Determined Sugar Content and Composition of Commercial Infant Formulas, Baby Foods and Common Grocery Items Targeted to Children, 5850–5867. <https://doi.org/10.3390/nu7075254>
- Wang, Y., & Liu, S. (2014). Kinetic modeling of ethanol batch fermentation by *escherichia coli* FBWHR using hot-water sugar maple wood extract hydrolyzate as substrate. *Energies*, 7(12), 8411–8426. <https://doi.org/10.3390/en7128411>
- White, J. S., Yohannan, B. K., & Walker, G. M. (2008). Bioconversion of brewer's spent grains to bioethanol. *FEMS Yeast Research*, 8(7), 1175–1184. <https://doi.org/10.1111/j.1567-1364.2008.00390.x>
- Wilkinson, S., Smart, K. A., & Cook, D. J. (2015). Optimising the (Microwave) Hydrothermal

- Pretreatment of Brewers Spent Grains for Bioethanol Production, 2015.
- Wilkinson, S., Smart, K. A., James, S., & Cook, D. J. (2017). Bioethanol Production from Brewers Spent Grains Using a Fungal Consolidated Bioprocessing (CBP) Approach. *Bioenergy Research*, 10(1), 146–157. <https://doi.org/10.1007/s12155-016-9782-7>
- World Energy Resources Bioenergy | 2016. (2016).
- Zabed, H., Faruq, G., Sahu, J. N., Azirun, M. S., Hashim, R., & Boyce, A. N. (2014). Bioethanol Production from Fermentable Sugar Juice, 2014.
- Zainab, B., & Fakhra, A. (2014). Production of Ethanol by fermentation process by using Yeast *Saccharomyces cerevisiae*, 3(7), 24–32.
- Zheng, J., & Rehmann, L. (2014). Extrusion Pretreatment of Lignocellulosic Biomass: A Review, 18967–18984. <https://doi.org/10.3390/ijms151018967>

APPENDICES

Appendix A: Thermodynamic Analysis for the fermentation stage

A1: Standard Gibbs free energy calculation

Assumptions: constant heat capacity, 1gmol of glucose is fed to fermenter, all TRS is glucose

Standard Gibbs free energy was calculated as follows at 25⁰C and 1 atm

$$\Delta G^0 = -RT \ln K_{eq}$$

$$\Delta G^0 = \Delta H^0 - \Delta S^0 T = RT \ln K$$

For a chemical reaction the Gibbs energy was calculated as follows:

$$\Delta G^0 = \sum(\Delta G)_{pro} - \sum(\Delta G)_{rec};$$

$$\Delta G^0_{,298} = v_i \Delta G^0_{,C_2H_6O} + v_i \Delta G^0_{,CO_2} - v_i \Delta G^0_{,C_6H_{12}O_6} = 2\Delta G^0_{,C_2H_6O} + 2\Delta G^0_{,CO_2} - \Delta G^0_{,C_6H_{12}O_6}$$

$$\Delta G^0_{,298} = 2*(-394.4KJ/mol) + 2*(-174.4KJ/mol) - (-910.5KJ/mol)$$

$$\Delta G^0_{,298} = -227.1KJ/mol, R = 8.314J/mol.K$$

Now the equilibrium constant at 25⁰C and 1 atm was determined from

$$\Delta G^0 = -RT \ln K_{eq}, R = 8.314J/mol.K \text{ and } T = 298K$$

$$-227.1KJ/mol * 1000J/KJ = -8.314J/mol.K * 298K * \ln K_{eq}$$

$$\frac{227100}{2477.572} = \ln K_{eq} = 91.66; K_{eq} = e^{91.66} = 6.433 * 10^{39}; K_{eq,298} = 6.433 * 10^{39}$$

A2: Enthalpy and equilibrium constant calculation at 32⁰C.

Now the temperature of interest was 32⁰C and 1 atm, so the following correlation was used in order to determine the equilibrium conversion at 32⁰C.

$$\frac{d \ln k}{dT} = \frac{-\Delta H_{rxn}^0}{RT^2}, \text{ integrating both sides}$$

$\ln \frac{k_2}{k_1} = -\left(\frac{-\Delta H_{rxn}^0}{R}\right)\left(\frac{1}{T_2} - \frac{1}{298}\right)$, assuming a constant enthalpy of reaction for constant specific heat capacity at 25°C and 32°C,

$$\Delta H_{rxn}^0 = v_i(\Delta H_{C_2H_6O}) + v_i(\Delta H_{CO_2}) - v_i(\Delta H_{C_6H_{12}O_6})$$

$$\Delta H_{rxn}^0 = 2*(-393.5\text{KJ/mol}) + 2*(-277.02\text{KJ/mol}) - (-1273.1\text{KJ/mol}) = -67.94\text{KJ/mol}$$

$$\Delta H_{rxn} = \Delta H_{298\text{K}}^0 + \int_{T_{ref}}^T \Delta C_P dT$$

$$\Delta C_P = (V_i C_P)_{pro} - (V_i C_P)_{rec} = 2* C_{P_{C_2H_5OH}} + 2* C_{P_{CO_2}} - C_{P_{C_6H_{12}O_6}}$$

$$\Delta C_P = 2*111.46\text{J/K} + 2*37.11\text{J/K} - 115\text{J/K} = 297.14\text{J/K} - 115\text{J/K} = 182.14\text{J/K}$$

$$\Delta H_{rxn} = \Delta H_{298\text{K}}^0 + \int_{T_{ref}}^T \Delta C_P dT = -67.94\text{KJ} + \int_{298\text{K}}^{305\text{K}} \Delta C_P dT$$

Assuming constant heat capacity for temperature difference less than 10K.

$$\Delta H_{rxn} = -67.94\text{KJ} + \int_{298\text{K}}^{305\text{K}} \Delta C_P dT = -67.94\text{KJ} + 182.14\text{J/K} * 7\text{K} = -67940\text{J} + 1274.98\text{J} = -66.665\text{KJ}$$

In a chemical reaction, the enthalpy change during the reaction indicates whether the reaction releases energy or consumes energy.

If $\Delta H_{rxn} < 0$, the reaction releases heat and it is EXOTHERMIC.

If $\Delta H_{rxn} > 0$, the reaction absorbs heat and is ENDOTHERMIC.

As it is known from literature that a fermentation of simple sugar, glucose, into ethanol is an exothermic reaction. The enthalpy obtained at an optimum temperature of 32°C or 305K was $\Delta H_{rxn} = -66.665\text{KJ}$, $\Delta H_{rxn} < 0$, therefore, the reaction is exothermic.

$$\text{Now, } \ln \frac{k_2}{k_1} = -\frac{\Delta H}{R} \left(\frac{1}{T_2} - \frac{1}{298} \right)$$

$\ln \frac{k_2}{k_1} = -\left(-\frac{66665.02}{8.314}\right)\left(\frac{1}{305} - \frac{1}{298}\right) = -0.24055$; $k_1 = K_{eq,298k} = 6.433 \times 10^{39}$, taking natural exponential to both sides.

$$k_2 = k_1 \cdot \exp(-0.24055) = 3.428 \times 10^{39}; k_{eq,305k} = 5.06 \times 10^{39}$$

The large value of equilibrium constant, 5.06×10^{39} , at 305K implies that the equilibrium lies far to the right (products).

A3: Entropy Determination

Entropy is a measure of randomness or disorder. A chemical reaction is said to be spontaneous if the entropy of the reaction system is positive.

$$\Delta S^0_{,298} = \sum(\Delta S)_{\text{pro}} - \sum(\Delta S)_{\text{rec}}; \Delta S^0_{,298} = \nu_i \Delta S^0_{,C_2H_6O} + \nu_i \Delta S^0_{,CO_2} - \nu_i \Delta S^0_{,C_6H_{12}O_6}$$

$$\Delta S^0_{,298} = 2 \cdot (161 \text{ J/mol.K}) + 2 \cdot (213.67 \text{ J/mol.K}) - (212 \text{ J/mol.K}) = 537.34 \text{ J/mol.K}$$

$$\Delta S^0_{,298} = 537.34 \text{ J/mol.K}$$

$$\Delta S_{\text{rxn}} = \Delta S^0_{,298} + \int_{T_0}^T \frac{\Delta C_P}{T} dT = 537.34 \text{ J/mol.K} + 182.14 \text{ J/K} \cdot \ln\left(\frac{T}{T_0}\right) = 537.34 \text{ J/mol.K} + 4.2289 \text{ J/K}$$

$$\Delta S_{\text{rxn}} = 541.568 \text{ J/K}$$

$\Delta S_{\text{rxn}} > 0$, the reaction is spontaneous.

Gibbs free energy calculation, $T = 32^\circ\text{C} = 305\text{K}$

$$\Delta G = \Delta H - T\Delta S = -66.665 \text{ KJ} \times 1000 \text{ J/KJ} - 305 \text{ K} \times 541.568 \text{ J/K}$$

$\Delta G = -66665 \text{ J} - 165178.24 \text{ J} = -231.84 \text{ KJ}$, implies that the reaction is thermodynamically favorable and possible to proceed in forward direction.

Appendix B: Thermodynamic property table for selected substance at 25⁰C and 1atm

| Substance | Formula | H _f ⁰ (KJ) | G _f ⁰ (KJ) | S _f ⁰ (J/K) |
|-------------------|---|-------------------------------------|-------------------------------------|--------------------------------------|
| Carbon | C (s) | 0 | 0 | 5.74 |
| Hydrogen | H ₂ (g) | 0 | 0 | 130.68 |
| Oxygen | O ₂ (g) | 0 | 0 | 205.04 |
| Carbon monoxide | CO(g) | -110.53 | -137.15 | 197.65 |
| Carbon dioxide | CO ₂ (g) | -393.52 | -394.36 | 213.8 |
| Water vapor | H ₂ O(g) | -241.82 | -228.6 | 188.83 |
| Water | H ₂ O(l) | -285.83 | -237.18 | 69.92 |
| Hydrogen peroxide | H ₂ O ₂ (g) | -136.31 | -105.6 | 232.63 |
| Ammonia | NH ₃ (g) | -46.19 | -16.59 | 192.33 |
| Methane | CH ₄ (g) | -74.85 | -50.79 | 186.16 |
| Acetylene | C ₂ H ₂ (g) | 226.73 | 209.17 | 200.85 |
| Ethylene | C ₂ H ₄ (g) | 52.28 | 68.12 | 219.83 |
| Ethane | C ₂ H ₆ (g) | -84.68 | -32.89 | 229.49 |
| Propylene | C ₃ H ₆ (g) | 20.41 | 62.72 | 266.94 |
| Propane | C ₃ H ₈ (g) | -103.85 | -23.49 | 269.91 |
| n-Butane | C ₄ H ₁₀ (g) | -126.15 | -15.71 | 310.12 |
| n-Octane | C ₈ H ₁₈ (g) | -208.45 | 16.53 | 466.73 |
| n-Octane | C ₈ H ₁₈ (l) | -249.95 | 6.610 | 360.79 |
| n-Dodecane | C ₁₂ H ₂₆ (g) | -291.01 | 50.15 | 622.83 |
| Benzene | C ₆ H ₆ (g) | 82.93 | 129.66 | 269.2 |
| Ethyl alcohol | C ₂ H ₆ O(g) | -235.31 | -168.57 | 282.59 |
| Ethyl alcohol | C ₂ H ₆ O(l) | -277.69 | -174.89 | 160.7 |
| Methyl alcohol | CH ₃ O(g) | -200.67 | -162 | 239.2 |
| Glucose | C ₆ H ₁₂ O ₆ (l) | -1273.1 | -910.5 | 212. |
| Hydroxyl | OH(g) | 39.46 | 34.28 | 183.7 |

(Source: Perry`s, “Chemical Engineers` Handbook”, 7th Edition, 1999.)

Appendix C: Infrared Spectroscopy Table with respective wavelength range for Functional Group Analysis

Simplified Infrared Correlation Chart

| Type of Vibration | | Wave number (cm^{-1}) | Intensity |
|-------------------|---|-------------------------------------|-----------|
| C-H | Alkanes (stretch) | 3000-2850 | s |
| | -CH ₃ (bend) | 1450 and 1375 | m |
| | -CH ₂ - (bend) | 1465 | m |
| | Alkenes (stretch) | 3100-3000 | m |
| | (out-of-plane bend) | 1000-650 | s |
| | Aromatics (stretch) | 3150-3050 | s |
| | (out-of-plane bend) | 900-690 | s |
| | Alkyne (stretch) | ~3300 | s |
| | Aldehyde | 2900-2800 | w |
| | | 2800-2700 | w |
| C-C | Alkane | not interpretatively useful | |
| C=C | Alkene | 1680-1600 | m |
| | Aromatic | 1600 and 1475 | m |
| C≡C | Alkyne | 2250-2100 | m |
| C=O | Aldehyde | 1740-1720 | s |
| | Ketone | 1725-1705 | s |
| | Carboxylic acid | 1725-1700 | s |
| | Ester | 1750-1730 | s |
| | Amide | 1670-1640 | s |
| | Anhydride | 1810 and 1760 | s |
| | Acid chloride | 1800 | s |
| C-O | Alcohols, Ethers, Esters, Carboxylic Acid, anhydrides | 1300-1000 | s |

Continued table from Appendix C

| | | | |
|-------|--|---------------|-----|
| O-H | Alcohols, Phenols | | |
| | Free | 3650-3600 | m |
| | H-bonded | | |
| | | 3500-3000 | m |
| | Carboxylic Acids | 3400-3200 | m |
| N-H | Primary and Secondary Amines and Amides | | |
| | (stretch) | 3500-3100 | m |
| | (bend) | 1640-1550 | m |
| C-N | Amines | 1350-1000 | m |
| C=N | Imines and Oximes | 1690-1640 | w |
| C≡N | Nitriles | 2260-2240 | m |
| X=C=Y | Allenes, ketenes, Isocyanates, Isothiocyanates | 2270-1950 | m |
| N=O | Nitro (R-NO ₂) | 1550 and 1350 | s |
| S-H | Mercaptans | 2550 | w |
| S=O | Sulfoxides | 1050 | s |
| | Sulfones, Sulfonyl Chlorides, Sulfates, Sulfonamides | 1375-1300 | and |
| | | 1200-1140 | |

(Source: http://en.wikipedia.org/wiki/Infrared_spectroscopy_correlation_table)

Appendix D: Diagnostics Case Statistics from Design Expert 6.0.8

| Standard Order | Actual Value | Predicted Value | Residual | Leverage | Student Residual | Cook's Distance | Outlier t | Run Order |
|----------------|--------------|-----------------|------------|----------|------------------|-----------------|-----------|-----------|
| 1 | 18.89 | 19.26 | -0.37 | 0.333 | -1.006 | 0.056 | -1.006 | 26 |
| 2 | 19.48 | 19.26 | 0.22 | 0.333 | 0.613 | 0.021 | 0.603 | 13 |
| 3 | 19.40 | 19.26 | 0.14 | 0.333 | 0.393 | 0.009 | 0.385 | 3 |
| 4 | 35.90 | 35.43 | 0.47 | 0.333 | 1.299 | 0.094 | 1.321 | 4 |
| 5 | 35.00 | 35.43 | -0.43 | 0.333 | -1.171 | 0.076 | -1.182 | 25 |
| 6 | 35.38 | 35.43 | -0.047 | 0.333 | -0.128 | 0.001 | -0.125 | 14 |
| 7 | 24.20 | 24.67 | -0.47 | 0.333 | -1.280 | 0.091 | -1.301 | 2 |
| 8 | 24.80 | 24.67 | 0.13 | 0.333 | 0.366 | 0.007 | 0.358 | 11 |
| 9 | 25.00 | 24.67 | 0.33 | 0.333 | 0.914 | 0.046 | 0.911 | 30 |
| 10 | 48.67 | 48.89 | -0.22 | 0.333 | -0.604 | 0.020 | -0.594 | 28 |
| 11 | 48.90 | 48.89 | 1.000E-002 | 0.333 | 0.027 | 0.000 | 0.027 | 7 |
| 12 | 49.10 | 48.89 | 0.21 | 0.333 | 0.576 | 0.018 | 0.567 | 23 |
| 13 | 28.90 | 28.77 | 0.13 | 0.333 | 0.366 | 0.007 | 0.358 | 18 |
| 14 | 28.60 | 28.77 | -0.17 | 0.333 | -0.457 | 0.012 | -0.448 | 22 |
| 15 | 28.80 | 28.77 | 0.033 | 0.333 | 0.091 | 0.000 | 0.089 | 15 |
| 16 | 56.80 | 57.22 | -0.42 | 0.333 | -1.143 | 0.073 | -1.152 | 21 |
| 17 | 57.05 | 57.22 | -0.17 | 0.333 | -0.457 | 0.012 | -0.448 | 27 |
| 18 | 57.80 | 57.22 | 0.58 | 0.333 | 1.600 | 0.142 | 1.667 | 24 |
| 19 | 29.90 | 29.95 | -0.050 | 0.333 | -0.137 | 0.001 | -0.134 | 10 |
| 20 | 30.25 | 29.95 | 0.30 | 0.333 | 0.823 | 0.038 | 0.816 | 8 |
| 21 | 29.70 | 29.95 | -0.25 | 0.333 | -0.686 | 0.026 | -0.677 | 16 |
| 22 | 54.58 | 54.33 | 0.25 | 0.333 | 0.695 | 0.027 | 0.686 | 5 |
| 23 | 54.30 | 54.33 | -0.027 | 0.333 | -0.073 | 0.000 | -0.071 | 29 |
| 24 | 54.10 | 54.33 | -0.23 | 0.333 | -0.622 | 0.021 | -0.613 | 12 |
| 25 | 49.40 | 48.93 | 0.47 | 0.167 | 1.145 | 0.029 | 1.154 | 1 |
| 26 | 49.70 | 48.93 | 0.77 | 0.167 | 1.881 | 0.079 | 2.013 | 6 |

Continued table from Appendix D

| | | | | | | | | |
|----|-------|-------|--------|-------|--------|-------|--------|----|
| 27 | 47.80 | 48.93 | -1.13 | 0.167 | -2.781 | 0.172 | -3.415 | 9 |
| 28 | 48.90 | 48.93 | -0.033 | 0.167 | -0.082 | 0.000 | -0.080 | 20 |
| 29 | 48.60 | 48.93 | -0.33 | 0.167 | -0.818 | 0.015 | -0.811 | 19 |
| 30 | 49.20 | 48.93 | 0.27 | 0.167 | 0.654 | 0.010 | 0.645 | 17 |

Appendix E: Laboratory Equipment and Experimental samples



D1: Autoclave



D2: Vacuum filtration unit



D3: Hydrolysate sample



D4: Sample in water bath



D5: Spectrophotometer absorbance



D6: Autoclave for sterilization



D7: Shaker incubator for fermentation



D8: Simple distillation set up



D9: FTIR instrument

